

**A STUDY OF GERMANIUM HYDRIDES, ANIONS  
AND RELATED SPECIES**

A STUDY OF GERMANIUM HYDRIDES, ANIONS  
AND RELATED SPECIES

by

IAN DRUMMOND, M.A.

A Thesis

Submitted to the Faculty of Graduate Studies

in Partial Fulfilment of the Requirements

for the Degree

Doctor of Philosophy

McMaster University

December 1970

DOCTOR OF PHILOSOPHY  
(Chemistry)

McMASTER UNIVERSITY  
Hamilton, Ontario.

TITLE: A Study of Germanium Hydrides, Anions and Related Species

AUTHOR: Ian Drummond, M.A. (Cambridge)

SUPERVISOR: Professor T. Birchall

NUMBER OF PAGES: (viii), 106.

SCOPE AND CONTENTS:

The relative acidities of some aryl germanes have been measured in liquid ammonia.

The NMR spectra of phenyl silane and phenyl germane have been completely analysed and the chemical shifts shown to arise from the presence of an electric dipole in the molecule. The NMR spectrum of phenyl germyl anion was unambiguously assigned and partially analysed. The results are consistent with little delocalization of the negative charge from the Ge onto the ring.

The vibrational spectra of the germyl anion have been observed and the geometry of the molecule estimated from a normal coordinate analysis of the data.

The Raman spectrum of liquid ammonia-D<sub>3</sub> has been measured and two bands in the Raman spectrum of liquid ammonia have been reassigned.

## ACKNOWLEDGEMENTS

The author wishes to thank Dr. T. Birchall for advice and encouragement. Thanks are also due to Mr. B. Sayer and Mrs. B. Spiers for the excellent NMR and Raman spectra and Dr. J. Bacon for assistance with computer programming. The advice (helpful and otherwise) and the friendship of the many people in the Chemistry Department and the members of the Climbing and Caving Club has been much appreciated.

McMaster University and the Department of University Affairs, Ontario, are thanked for financial assistance.

## TABLE OF CONTENTS

CHAPTER 1	<u>Introduction</u> .....	1
CHAPTER 2	<u>Experimental</u>	
	Preparation of Materials.....	13
	NMR Measurements.....	20
	Vibrational Spectra.....	25
	Dipole Moments.....	28
CHAPTER 3	<u>Acidity Measurements</u>	
	Acidity of Aryl Germanes.....	32
	Acidity of Silanes.....	46
CHAPTER 4	<u>NMR Measurements</u>	
	Phenyl Silane and Phenyl Germane.....	48
	Phenyl Germyl Anion.....	57
	Silyl Ion.....	61
	Fluorenyl Anion.....	62
	Variation of Coupling Constants with Temperature.....	65
CHAPTER 5	<u>Vibrational Spectra</u>	
	Vibrations of a Pyramidal $MH_3$ Molecule.....	70
	The Germyl Ion.....	74
	Polymeric Germanium Hydride.....	81
	Silyl Ion and Polymeric Silicon Hydride.....	82
	Liquid Ammonia and Ammonia- $D_3$ .....	86
	Force Constants of Group IV and V Hydride and Hydride Ions.....	93
CHAPTER 6	<u>General Conclusions</u> .....	96
APPENDIX I	Symmetry-allowed NMR Transition of a Phenyl Group.....	98
APPENDIX II	Calculation of Bond Angles from NMR Coupling Constants.....	101
REFERENCES.....		102

LIST OF TABLES

	Page
1. Some Physical Properties of Ammonia, Dimethoxyethane and Hexamethylphosphoramide.....	10
2. The NMR Parameters of Ammonia, Dimethoxyethane and Hexamethylphosphoramide.....	21
3. Data for Calculation of Dipole Moments of Phenyl Silane and Phenyl Germane.....	30
4. NMR Parameters of Acids and Anions used in Acidity Measurements.....	36
5. Comparative Acidity Measurements of the Germanes.....	39
6. The Chemical Shift of the Germyl Ion in Liquid Ammonia.....	42
7. Thermodynamic Data for Ionization of Substituted Benzoic Acids.....	44
8. NMR Parameters of Phenyl Silane and Phenyl Germane.....	52
9. NMR Parameters of Some Monophenyl Derivatives of Group IV Elements.....	54
10. NMR Parameters of Sodium Phenyl Germyl and Benzyl Lithium.....	60
11. NMR Parameters of Potassium Silyl.....	62
12. NMR Parameters of Sodium Fluorenyl.....	65
13. Variation of J(P-H) in Phosphine with Temperature.....	67
14. Vibrational Frequencies of the Germyl Ion.....	80
15. Vibrational Frequencies of Liquid Ammonia and Liquid Ammonia-D <sub>3</sub> .....	87
16. Calculated Frequencies for Liquid Ammonia and Liquid Ammonia-D <sub>3</sub> .....	92
17. Force Constants of Hydrides and Hydride Ions of Groups IV and V.....	94

## LIST OF FIGURES

	Page
1. The Mass Spectrum of Phenyl Germane in Molecular Ion Region.....	15
2. The NMR Spectrum of Bis Diphenylene Methyl Germanium Hydride.....	18
3. The Apparatus for Preparation of Solutions of Anions in Liquid Ammonia for NMR Spectroscopy.....	22
4. The Apparatus for Preparation of Solutions of Anions for Laser Raman Spectroscopy.....	26
5. A Full-scale Diagram of the High Pressure Infrared Cell.....	27
6. The Evaluation of the Differentials for Calculation of the Dipole Moments of Phenyl Silane and Phenyl Germane.....	31
7. The NMR Spectrum Comparing the Acidities of Phenyl Germane and Fluorene. The splitting of the solvent protons by the nitrogen nuclei is shown.....	34
8. The NMR Spectrum Comparing the Acidities of Germane and Phenyl Germane.....	35
9. The NMR Spectrum of Phenyl Silyl Anion Contaminated with Phenyl Silane and Benzene.....	47
10. The Experimental and Calculated 100 M Hz NMR Spectrum of Phenyl Germane.....	50
11. The Correlation of Ring Coupling Constants of Mono-substituted Benzenes with Electronegativity of Substituent.....	56
12. The Experimental and Calculated 100 M Hz NMR Spectrum of Sodium Phenyl Germyl in Liquid Ammonia.....	58
13. The Experimental and Calculated 100 M Hz NMR Spectrum of Sodium Fluorenyl in Liquid Ammonia.....	64
14. The Correlation of J(P-H) in Phosphine with the Fraction of Vibrationally Excited Molecules.....	69
15. The Symmetry Coordinates of a Pyramidal $MH_3$ Molecule.....	71
16. The Infrared Spectrum of Liquid Ammonia.....	72
17. The Raman Spectrum of Potassium Germyl in Liquid Ammonia.....	75

List of Figures (cont'd.)

	Page
18. The Infrared Spectrum of Sodium Germyl in Liquid Ammonia.....	77
19. The Infrared Spectrum of Potassium Germyl-D <sub>3</sub> in Dimethoxyethane.....	79
20. The Infrared Spectrum of SiH <sub>2</sub> Polymer in Dimethoxyethane.....	84
21. The Infrared Spectrum of SiH <sub>2</sub> Polymer and SiH <sub>3</sub> <sup>-</sup> in HMPA.....	85
22. The Raman Spectrum of Liquid Ammonia: Temperature Dependence.....	89
23. The Raman Spectrum of Liquid Ammonia-D <sub>3</sub> Temperature Dependence.....	90

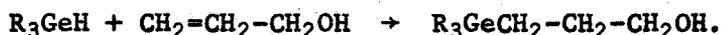
## LIST OF SYMBOLS

- $\text{\AA}$  = angstrom =  $10^{-10}$  cm.  
D = Debye =  $10^{-18}$  esu.cm.  
e = electronic charge =  $4.8 \times 10^{-10}$  esu.  
 $\epsilon$  = dielectric constant.  
G = Gibb's free energy  
HMPA = Hexamethylphosphoramide.  
Hz = Hertz = 1 cycle/sec.  
k = Boltzmann's constant =  $1.3805 \times 10^{-16}$  ergs/ $^{\circ}$ K.  
 $\ln$  =  $\log_e$ .  
 $N_0$  = Avogadro's number =  $6.02 \times 10^{23}$ /mole.  
n = refractive index.  
ppm = parts per million.  
R = Gas constant = 8.3 joules/ $^{\circ}$ K.  
 $\rho$  = density.  
T = absolute temperature.  
 $\chi$  = magnetic susceptibility.  
[x] = concentration in moles/litre.

## CHAPTER 1

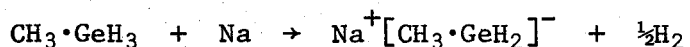
### Introduction

Germanium is element number 32 and the third member of the fourth main group (C, Si, Ge, Sn and Pb). It was discovered in 1887 by C. Winkler and has been comparatively rare and costly until recently when supplies have been developed for the transistor industry. Early research indicated that its properties were intermediate between silicon and tin. It generally forms four tetrahedral covalent bonds, but when bonded to electronegative elements can increase its coordination number to six, e.g.,  $\text{GeCl}_6^{2-}$ . A few divalent compounds are known, e.g.,  $\text{GeF}_2$ , but these are bridged polymers. The most extensive area of study has been organo-germanium compounds and this subject has been reviewed several times (1, 2, 3). The main characteristics of organo-germanium compounds, besides the tetra-valency mentioned above, are the stability of the Ge-C bond, the reactivity of the Ge-Ge and Ge-H bonds and the inability of Ge to form unsaturated compounds analogous to ethylene or acetylene. The most common organo-germanium compounds are of the type  $\text{R}_n\text{GeX}_{4-n}$ , where R is alkyl or aryl, and their reactions are determined principally by the Ge-X function. This thesis is concerned with the hydrides. The Ge-H bond (4, 5) has considerable thermal stability, the bond energy is -70 kcal/mole, but is attacked easily by oxidising agents such as the halogens and less easily by oxygen. The sensitivity to oxidation decreases in the order  $\text{GeH}_4 > \text{RGeH}_3 > \text{R}_2\text{GeH}_2 > \text{R}_3\text{GeH}$  and they are fairly stable to both acid and base. All types of hydride add to carbon-carbon multiple bonds, and such reactions are useful synthetically, e.g.,



The hydrides also exhibit acidic behaviour, i.e., it is possible to abstract

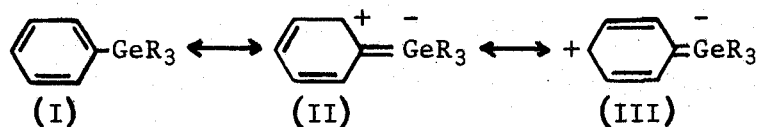
a proton from them to give an organo germanium anion, analogous to a carbanion.



The anions can also be made by cleavage of Ge-Ge bonds using solutions of alkali metals in ammonia (1). Regeneration of the hydride occurs on hydrolysis and this was for a long time the only preparative method for hydrides. Alkyl germanes are obtained on treatment of the anion with an alkyl halide. Other synthetic uses have been production of  $\alpha$ -Ge carboxylic acids (6) and  $\beta$ -Ge ethers (7). There have been suggestions that the dianions,  $\text{R}_2\text{Ge}^{2-}$  where R = H, or phenyl, can be made (1, 8) but this has been disproved for the hydride (9). The solid salts  $\text{NaGeH}_3 \cdot 6\text{NH}_3$  (4) and  $\text{LiGeH}_3 \cdot 2\text{NH}_3$  (10) have been isolated from ammonia solutions but both are unstable at room temperature and no studies have been made on them. Although the germyl ion is well characterized by its reactions in solution, the only physical measurement which has been performed on it is the observation of its proton NMR signal in liquid ammonia solution (11).

There has been considerable activity in the organo-germanium (and organo-silicon) field investigating the interaction of the heteroatom and the organic functional group. In 1954 Chatt and Williams (12) measured the ionization constant for a series of substituted benzoic acids  $\text{R}_3\text{M}-\text{C}_6\text{H}_4-\text{CO}_2\text{H}$  where M = C, Si, Ge and Sn and R =  $\text{CH}_3$  and  $\text{C}_2\text{H}_5$ . The order of acid strength was found to be p-trimethyl silyl > benzoic > p-t-butyl. Silicon and germanium are more electropositive than carbon and are expected to be electron-donating species, which would make the substituted acid weaker than the unsubstituted acid. However, the acidity measurements (12) imply that silyl and germyl groups are electron-withdrawing. The synthesis of  $\alpha$ -silyl and germyl ketones and  $\alpha$ ,

$\alpha'$ -disilyl and digermyl ketones (13, 14) which range in colour from yellow to red violet was of considerable interest, since all analogous carbon compounds are colourless. The shift of the absorption bands to lower frequency and their enhanced intensity implies extension of the chromophore. Both acidity and spectrophotometric results were explained by invoking multiple bonding between the carbon  $\pi$ -electron systems and the empty metalloid d orbitals, i.e., Si and Ge atoms were postulated to form conjugated  $\pi$ -type systems even though they have already formed  $4\sigma$  bonds, by use of low energy vacant orbitals which are not available to carbon (12). In valence bond notation, the following structures were considered to contribute significantly to the ground state:



The acidity measurements (12) of the substituted benzoic acids imply that the resonance structures (II) and (III) outweigh the inductive electron release of the metalloid atoms.

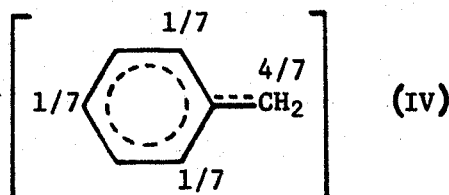
Following these early experiments there have been many attempts to provide additional evidence both for and against such interaction. Structural information such as bond lengths and bond angles (5, 15), dipole moment measurements (16, 17), U.V.-visible spectroscopy using both energy level calculations (18) and transition moments (19), electron spin resonance (20, 21), reaction kinetics (3) and nuclear magnetic resonance (22, 39) have all been used to obtain evidence for or against the participation of d orbitals in the bonding scheme. The position is still not clear; for example some of the most recent evidence (23) shows the original Chatt-Williams acidity

measurements to be incorrectly interpreted. This will be further discussed in the chapter on acidity measurements.

A very interesting observation made by Birchall and Jolly (11) was that triphenyl germane ( $\phi_3\text{GeH}$ ) was much less acidic than germane ( $\text{GeH}_4$ ) in liquid ammonia because the equilibrium of the reaction

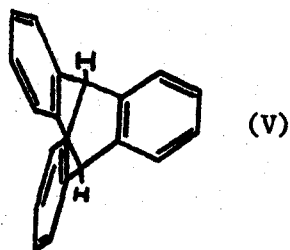


lay to the left. This was considered very surprising because for the analogous carbon compounds the reaction is essentially completely to the right. Indirect measurement on this system (24) indicate that the equilibrium constant is approximately  $10^{20}$ . Phenyl substitution greatly increases the acidity of carbon compounds by two effects (24). The anions formed by the carbon acids can delocalize the negative charge over the  $\pi$ -system of the molecule thus greatly stabilizing the species (40). Evidence for this includes the intense red, orange and purple colours of various conjugated carbanions, equivalence in the NMR spectrum of the protons of species such as the cyclopentadienyl anion (41), and ESR spectra of radical anions (25). Hückel calculations for the benzyl (phenyl methyl) anion (40) indicate the following distribution of the negative charge:

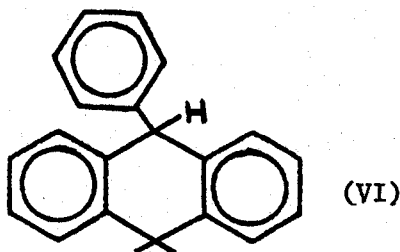


Also important in stabilizing the aryl carbanions is the inductive effect of the phenyl group. This is illustrated well by comparison of the acidities

of triphenyl methane and triptycene (V).



Triptycene is similar to triphenyl methane except that the aromatic rings are constrained to lie orthogonally to the lone pair of the triptyceny anion and so no delocalization is possible. The difference in acidity between cyclohexane and triptycene ( $2 \times 10^7$ ) is greater than the difference between triptycene and triphenyl methane ( $5 \times 10^5$ ) showing both inductive and mesomeric effects to be important in determining the acidity. It is worth noting the effect of steric crowding on the mesomeric effect. While diphenyl methane is approximately  $10^{10}$  more acidic than toluene, triphenyl methane is only 40 times more acidic than diphenyl methane. This is assumed to be because the phenyl groups in the triphenyl methyl anion are too crowded to all lie in one plane and hence cannot obtain maximum  $\pi$ -overlap. Certainly 9,9-dimethyl-10-phenyldihydroanthracene (VI) is  $3 \times 10^3$



times more acidic than the related triphenyl methane and this is ascribed to the increased coplanarity of the phenyl ring.

Thus it can be seen that the germanium hydrides are exhibiting very

markedly different acid behaviour from the corresponding carbon compounds. Birchall and Jolly (11) assumed that Ge in the anionic species could form strong multiple bonds to carbon and cited as evidence the NMR spectrum of the triphenyl germyl anion which showed the aromatic proton resonances split into two groups of relative areas 2:3. These were assigned to the meta and ortho + para protons due to delocalization of charge as shown for the benzyl anion (IV). In order to explain the acidities they (11) suggested that there was extensive multiple bonding in the acid using the Ge 4d orbitals. As shown above in structures (II) and (III) this results in an increase in electron density on the Ge atom and hence makes it harder to remove a positively-charged proton. If correct, this would certainly be one of the most dramatic manifestations of d orbital participation known. However such an explanation is dubious for the following reason. The difference in acidity between triphenyl germane and germane was estimated by Birchall and Jolly to be about 100, i.e., the equilibrium constant for reaction [1] was approximately 1/100. For any equilibrium

$$\Delta G^\circ = -RT \ln K.$$

For reaction [1]  $\Delta G^\circ = 3$  kcal/mole, i.e., it needs 3 kcal/mole more energy to convert triphenyl germane to its anion than it does to convert germane to germyl ion. If this is due entirely to increased electron density on the Ge atom then the size of this charge increase can be calculated using a simple electrostatic model (26). Consider the work done in removing a proton to infinity starting 1.53 Å (GeH bond length (5)) from unit negative charge.

$$\text{Work done} = \int_{1.53 \times 10^{-8}}^{\infty} (e^2 / \epsilon r^2) dr \text{ ergs/mole} \quad (\text{See page viii for symbols.})$$

if the negative charge increases by  $\delta e$

$$\text{Work done} = \int_{1.53 \times 10^{-8}}^{\infty} [e(e + \delta e)/\epsilon r^2] dr \quad \text{ergs/molecule}$$

therefore difference in energy =  $2.65 \times 10^{13} \times \delta e$  cal/mole for  $\text{NH}_3$  solution

$$\text{where } \epsilon = 16.9 \text{ at } 25^\circ\text{C} \quad (36)$$

but this equals  $3 \times 10^3$  cal/mole (from above), so

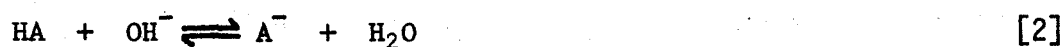
$$\delta e = 1.13 \times 10^{-10} \text{ e.s.u.} = \underline{0.24 \text{ electrons.}}$$

This is a sizable shift of electron density within the neutral molecule and would have large effects upon the aromatic system which is providing these electrons. It therefore seems unlikely that d orbital participation can be the explanation for the acidities since such perturbations would surely have been detected by the physical methods mentioned above and already employed for detection of d-orbital participation. However it did seem worth attempting to estimate the electron densities at the aromatic carbon atoms in both the Ge acid and Ge anion in order to determine the extent to which mesomeric interactions explain the relative acidity measurements. One of the few methods for estimating the electron density of the ground state molecule is by NMR. The technique (as applied here) and its drawbacks are discussed on page 48. There was a further reason for obtaining the NMR parameters of a phenyl group attached to germanium (or silicon). Recently there has been considerable interest in the theoretical calculation of coupling constants (27, 28) and the effect of substituents on the coupling constants of the rest of the molecule; an empirical relationship between electronegativity of the substituent and the proton-proton coupling constants in the attached phenyl group has been proposed (29). Since Si

and Ge are considerably more electropositive than the other substituents considered, it was felt that the results would be of interest by extending the range of such correlations.

Another reason for the study of the germanium hydrides and anions was to obtain some reasonably accurate acidity measurements. Birchall and Jolly's measurements (11) were very approximate and gave no idea of the absolute magnitude of the acidity of these compounds. Very recently the acidity of triphenyl germane was measured in DMSO solution and found to have a  $pK_a$  of 23.1 (30). It was also desirable to extend the measurements to include monophenyl ( $\phi\text{GeH}_3$ ) and diphenyl germane ( $\phi_2\text{GeH}_2$ ). This, however, is not a trivial task. When the acids are very weak it is necessary to use acidity function techniques, the ideas of which are explained below.

In dilute aqueous solutions the concentration of hydroxide ion is a good measure of the basicity of the solution but as the concentration increases it is necessary to use another measure of basicity, commonly the Hammett  $H_-$  value (31) defined from equation [2]



as

$$H_- = pK_{\text{HA}} + \log_{10}([\text{A}^-]/[\text{HA}]) = -\log_{10}(a_{\text{H}^+} f_{\text{A}^-} / f_{\text{HA}}) \quad [3]$$

where  $pK_{\text{HA}} = -\log_{10}(a_{\text{H}^+} \cdot a_{\text{A}^-} / a_{\text{HA}})$ , hence  $K_{\text{HA}}$  = ionization constant of HA,

$a_X$  = activity of species X,

$f_X$  = activity coefficient of X.

The  $pK$  values for some more acidic indicators may be found using the following substitution in equation [3],

$$pK_{\text{W}} - pK_{\text{HA}} = \log_{10}([\text{A}^-]/[\text{HA}]) - \log_{10}[\text{OH}^-] + \log_{10}(a_{\text{W}} f_{\text{A}^-} / f_{\text{HA}} f_{\text{OH}^-})$$

where  $K_W$  = ionic product of water and  $a_W$  = activity of water. At infinite dilution by definition  $a_W$  and all activity coefficients are unity and therefore an extrapolation of a graph of  $\log([A^-]/[HA]) - \log[OH^-]$  against  $[OH^-]$  to  $[OH^-] = 0$  gives a value for  $(pK_W - pK_{HA})$  and hence for  $pK_{HA}$ . If the indicators are very weakly acidic the above method is no longer reliable as the degree of ionization becomes small. In this case a stepwise procedure is used. If two indicators are dissolved in the same solution of given  $H_+$  value then from equation [3] it follows

$$pK_{HA} + \log_{10}([A^-]/[HA]) = pK_{HB} + \log_{10}([B^-]/[HB]). \quad [4]$$

If the  $pK$  of the stronger acid is known, either from the above extrapolation or from a previous stepwise comparison then  $pK_{HB}$  can be found if  $[A^-]/[HA]$  and  $[B^-]/[HB]$  can be measured.

Although the above argument was developed for aqueous solutions it is easily extended to mixed solvents and non-aqueous solvent systems. This has indeed been done for the pyridene-water and DMSO-water (32), pure DMSO (33), cyclohexylamine (24) and ammonia (34) solvent systems. The limitations of the method are discussed in the chapter on the acidity measurements.

It was necessary to choose a suitable solvent for the acidity measurements. Three solvents have been frequently used for preparation of germyl salts: liquid ammonia (1, 11), hexamethylphosphoramide (HMPA) (7) and the chelating ether dimethoxyethane (DME) (6) although other ethers have been used. All these solvents have various advantages and disadvantages and since all three were used in this investigation their relevant properties are listed in Table 1.

It can be seen that none is ideal either for acidity measurements or

TABLE 1

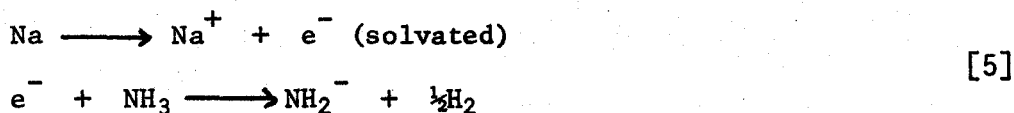
	Ammonia <sup>a</sup>	Dimethoxyethane <sup>b</sup>	HMPA <sup>c</sup>
Boiling point at 76 cm	-33.4°C	+85°C	232°C
Vapour pressure	10 atmospheres at 25°C		0.6 cm at 77 °C
Freezing point	-77.7°C	-58°C	+4°C
Dielectric constant	16.9 at 25°C	approx. 5	30 at 25°C
NMR spectrum		See page 21	
Infrared spectrum	VERY INTENSE and broad fundamentals 1700 - 800 cm <sup>-1</sup> See Fig. 16	COMPLEX See Fig. 20	COMPLEX See Fig. 21
Raman spectrum	Low intensity, effectively no background	Less intense than IR but still complex	

<sup>a</sup>Reference (35); <sup>b</sup>Reference (36); <sup>c</sup>Reference (37).

preparations. Dimethoxyethane has the most convenient liquid range, is easily purified and handled on a vacuum line, but it is the poorest solvent, and has interfering bands in the NMR and vibrational spectra. Alkali metals are very sparingly soluble and reaction times for the less acidic compounds are usually long. HMPA is an excellent solvent but it is difficult to purify, effectively involatile and strongly interferes in both NMR and vibrational spectroscopy. Alkali metals dissolve to give solvated electrons so reactions are rapid.

Ammonia has been previously used for acidity measurements (11) although side reactions do occur (8, 9). It is an excellent solvent and easily purified. The NMR resonances are away from the usual area of interest. The infrared absorptions are very intense, between 1700 and 800 cm<sup>-1</sup>, but the

the Raman scattering is weak. Another considerable advantage of ammonia is the easy, in situ, production of the characteristic base, amide ion ( $\text{NH}_2^-$ ), by the reactions



The quantity of hydrogen evolved can be measured by means of a Toepler pump and thus stoichiometric reactions are feasible without the necessity of accurately weighing small quantities of alkali metal. The major disadvantage of ammonia is its high volatility, necessitating working at low temperatures or high pressures. NMR experiments can conveniently be carried out at high pressures since sealed NMR tubes will withstand 20 atmospheres, however, high pressure infrared work presents some problems. A special cell is necessary and since liquid ammonia dissolves common infrared materials, the windows must be made of  $\text{BaF}_2$  (42) or  $\text{KCl}$  (43). It was decided to carry out the acidity measurements in liquid ammonia at room temperature using the NMR technique. Some measurements were also made in the other solvents using this method.

Extensive use has also been made of vibrational spectroscopy. Early in this study it was considered that solvation of the germyl anions might be responsible for the difference in the acidity of the germanes, rather than d-orbital participation as suggested in (11). In an attempt to gain direct evidence on this subject the vibrational spectra of the germyl anion was measured when dissolved in two dissimilar solvents, ammonia and dimethoxyethane. In conjunction it was planned to measure the relative acidities of some of the germanes in both solvents. Unfortunately the acidity measurements in dimethoxyethane were unsuccessful (see page 45) and the vibrational spectra

in the two solvents are not very different (see page 80 ). However, since the germyl ion was not well characterized by physical measurements it was considered worthwhile to attempt to obtain force constants and bond angles from a normal coordinate analysis of the spectroscopic bands. The Raman spectroscopy was performed using a laser source. The advantages of the laser over conventional excitation are well documented (38). Raman spectroscopy is particularly convenient for use with ammonia solutions; glass sample tubes can be used which withstand the high pressure and the temperature can be easily varied. The Raman spectrum of ammonia is simple (page 89) and two of the bands are of very low intensity.

To summarize, the object of this investigation was further characterization, by physical methods, of some organo-germanium hydrides and anions and comparison of their properties with the corresponding compounds of other group IV elements or the isoelectronic group V compounds. Specific areas to be investigated were the unusual acidities of these compounds in liquid ammonia, estimation of electron densities in the acidic and anionic forms of phenyl germane and estimation of the structure and force constants of the germyl ion by normal coordinate analysis of the vibrational spectra.

## CHAPTER 2

### Experimental

All reactive intermediates and specially dried or purified compounds were handled either in vacuo or under a dry nitrogen atmosphere. Melting points are uncorrected. NMR spectra were recorded on a Varian T60 spectrometer unless otherwise indicated. Mass spectra were recorded on a Hitachi-Perkin-Elmer RMU6A. Infrared spectra were recorded on a Perkin-Elmer model 337 unless otherwise noted.

Solvents: Diethyl ether (Mallinckrodt) and toluene (Shawinigan) were dried over sodium wire. Carbon tetrachloride (Mallinckrodt) was dried over freshly regenerated molecular sieves. Tetrahydrofuran (Allied) was distilled from lithium aluminum hydride. Methanol (Mallinckrodt) and 1,2 dibromoethane (Baker) were used as received. Hexamethylphosphoramide (HMPA) (Aldrich) was vacuum distilled (75-77°C at 0.6 cm) from potassium metal and stored over freshly regenerated molecular sieves. Dimethoxyethane (Eastman) was dried initially over sodium wire, then over lithium aluminum hydride. Ammonia (Matheson) was dried and stored over sodium metal at -78°C.

Reagents: Magnesium turnings (Shawinigan) were treated with a small crystal of iodine before use in Grignard reactions. Aluminium trichloride (Fisher) was sublimed in vacuo before use. Bromine (Shawinigan) was used as received. Sodium borohydride and 4A molecular sieves were obtained from BDH. The molecular sieves were regenerated by heating to 300°C under vacuum before use. Butyl lithium (Alpha) as a solution in hexane was transferred using syringes and septum caps. The concentration was determined by the double titration method (44). Lithium aluminium hydride (Alpha) solutions were

filtered through glass-wool before addition to reaction mixtures. Lithium aluminium deuteride was also obtained from Alpha. Potassium hydride and sodium deuteride (Alpha) obtained as dispersions in oil, were washed and the solvent decanted before use.

#### Preparation of Materials

Germanium Compounds: Germanium tetrachloride and germanium dioxide were donated by the Germanium Research Committee and used without further purification. Tetraphenyl germane ( $\phi_4\text{Ge}$ ) was prepared as has been described (45) by reaction of phenyl magnesium bromide (made from bromobenzene BDH) with  $\text{GeCl}_4$  in toluene and was purified by recrystallization from toluene; M.P.  $232^\circ\text{C}$ , lit.  $233.4^\circ\text{C}$  (44).

Tetra p-tolyl germane ( $\text{pCH}_3\text{-C}_6\text{H}_4$ ) $_4\text{Ge}$  was prepared from p-bromotoluene (Eastman) and purified as for tetraphenyl germane; M.P.  $225^\circ\text{C}$ , lit.  $224$ ,  $227^\circ\text{C}$  (1).

Triphenyl germanium bromide ( $\phi_3\text{GeBr}$ ) was prepared by reaction of  $\phi_4\text{Ge}$  and the stoichiometric quantity of bromine in 1,2-dibromoethane solution (45).

Triphenyl germane ( $\phi_3\text{GeH}$ ) was prepared by the lithium aluminium hydride reduction (45) of  $\phi_3\text{GeBr}$  and purified by recrystallization from methanol; M.P.  $40^\circ\text{C}$ , lit.  $\alpha$  phase  $41^\circ\text{C}$  (1).

Tris p-tolyl germane ( $\text{pCH}_3\text{-C}_6\text{H}_4$ ) $_3\text{GeH}$  was prepared by reactions analogous to those for the triphenyl compound; M.P.  $81^\circ\text{C}$ , lit.  $81^\circ\text{C}$  (46).

Diphenyl germanium dibromide ( $\phi_2\text{GeBr}_2$ ) was prepared by the reaction of  $\phi_4\text{Ge}$  and the stoichiometric quantity of bromine in 1,2-dibromoethane solution (45).

Diphenyl germane ( $\phi_2\text{GeH}_2$ ) was prepared by the lithium aluminium hydride reduction of  $\phi_2\text{GeBr}_2$  and purified by vacuum distillation,  $100^\circ\text{C}$  at approximately 0.1 cm, lit.  $95^\circ\text{C}$  at 0.1 cm (45). It was stored in a stoppered

flask in a refrigerator.

Phenyl germanium trichloride ( $\phi\text{GeCl}_3$ ) was prepared by the  $\text{AlCl}_3$  catalysed exchange reaction between  $\phi_4\text{Ge}$  and  $\text{GeCl}_4$  (3) and purified by vacuum distillation,  $60^\circ\text{C}$  at approximately 1 cm. It was important to recrystallize the  $\phi_4\text{Ge}$  carefully to remove all  $\phi_6\text{Ge}_2$  for the reaction to proceed in good yield.

Phenyl germane ( $\phi\text{GeH}_3$ ) was prepared by the  $\text{LiAlH}_4$  reduction of  $\phi\text{GeCl}_3$  and purified by trap-to-trap distillation in vacuo, collecting the fraction at  $-22^\circ\text{C}$ ; lit. vapour pressure 0.12 cm at  $42^\circ\text{C}$  (47). It was stored under vacuum at  $-78^\circ\text{C}$ . The mass spectrum of this compound had not been previously reported, Figure 1. Peaks from  $m/e$  156-147 were observed, corresponding to all ions from  $\phi^{76}\text{GeH}_3^+$  to  $\phi^{70}\text{Ge}^+$  as well as peaks to lower mass number corresponding to break-up of the aromatic ring. After correction for up to one  $^{13}\text{C}$  atom per molecule the intensities were shown to agree with the following ion ratios:  $\phi\text{GeH}_3^+$  0.99;  $\phi\text{GeH}_2^+$  0.90;  $\phi\text{GeH}^+$  1.00;  $\phi\text{Ge}^+$  0.52.

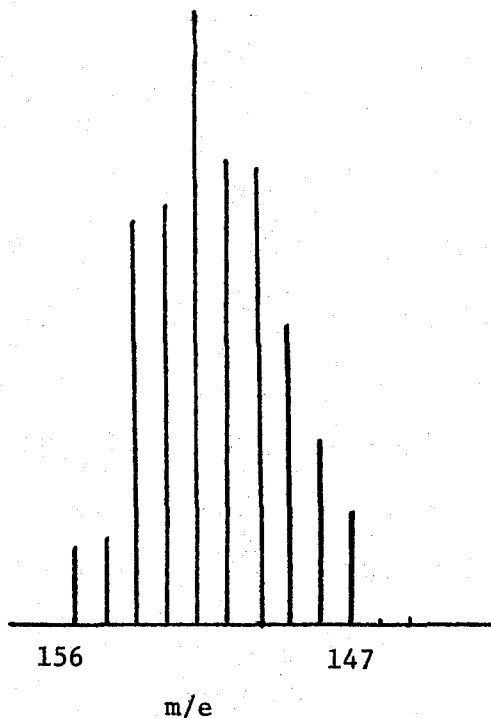
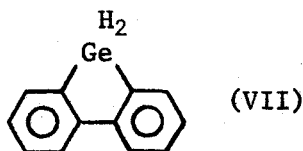


Figure 1. The Mass Spectrum of  $\phi\text{GeH}_3$  in the Molecular Ion Region.

Germane ( $\text{GeH}_4$ ) was prepared by the sodium borohydride reduction of  $\text{GeO}_2$  (48) and purified by distillation through a trap containing ascarite and a  $-126^\circ\text{C}$  trap (methyl cyclohexane slush). It was stored in a glass bulb at room temperature.

Germane- $\text{D}_4$  ( $\text{GeD}_4$ ) was prepared by lithium aluminium deuteride reduction of  $\text{GeCl}_4$  (49) and purified as for germane. It was stored in a glass bulb at room temperature.

2,2' diphenylene germane (VII)



2,2' dibromo-biphenyl was first synthesized by adding 23.4 mls of a 2.34 M solution of butyl-lithium in hexane to 25.9 grams of  $\sigma$ -dibromo benzene in 250 mls of anhydrous THF; the temperature was not allowed to rise above  $-65^\circ\text{C}$ . After one hour the solution was warmed to room temperature and hydrolysed with 100 mls of 10% HCl. The organic layer was separated, dried and distilled until the temperature reached  $85^\circ\text{C}$ . The residue was recrystallized from 25 mls of absolute ethanol to yield 10.8 g of 2,2' dibromo-biphenyl, M.P.  $79^\circ\text{C}$ . Fifteen mls of a 2.34 M solution of butyl-lithium in hexane plus 30 mls of ether were added slowly to 5.46 gms of 2,2' dibromo-biphenyl in 80 mls of ether at  $0^\circ\text{C}$ . The mixture was warmed to room temperature and added slowly to excess (10 gms) of  $\text{GeCl}_4$  in 250 mls of toluene at  $80^\circ\text{C}$ . The mixture was then refluxed for 2 hours, filtered to remove the  $\text{LiCl}$  and the solvent evaporated to leave an oil. This was then reduced with  $\text{LiAlH}_4$  as described above. The oil then obtained by evaporation of the petroleum ether solution was distilled in vacuo,  $100^\circ\text{C}$  at approximately

0.01 cm. The oil obtained fumed on contact with air and the NMR spectrum showed that it still contained ether. The ether was still present after a second vacuum distillation and it was assumed to be due to an aluminium hydride/ether complex which had distilled with the product. Only two drops of product were obtained; the infrared spectrum showed a strong absorption at  $3050\text{ cm}^{-1}$  characteristic of aromatic protons and a strong band at  $2060\text{ cm}^{-1}$  characteristic of Ge-H bonds. The NMR spectrum showed besides ether absorptions, peaks in the aromatic region which strongly resembled those of the hydrocarbon fluorene and a  $\text{GeH}_2$  resonance at 5.07 ppm relative to internal TMS. This spectral evidence strongly suggested that the desired product, although impure, had been synthesized. The above procedure was repeated using 10 gms of methyl germanium trichloride  $\text{CH}_3\cdot\text{GeCl}_3$  (Alpha) instead of  $\text{GeCl}_4$ . The petroleum ether solution from the  $\text{LiAlH}_4$  reduction was treated with 0.2 mls of ethanol to destroy any remaining  $\text{LiAlH}_4$  before vacuum distillation,  $120^\circ\text{C}$  at 0.01 cm. The resulting clear liquid had an infrared spectrum similar to that of the previous product and the NMR spectrum, Figure 2, showed the following peaks, chemical shifts measured relative to internal TMS:  $\text{GeH}$  -5.16 ppm (q);  $\text{GeCH}_3$  -0.65 ppm (d);  $J(\text{H-Ge-C-H})$  3.25 Hz, and a complex multiplet in the aromatic region which closely resembled the spectrum of fluorene. This spectrum is good evidence that the methyl derivative of (VII) had been made. In addition the compound ionized upon dissolution in liquid ammonia containing amide ion, as shown by the following changes which occurred in the NMR spectrum. A  $\text{GeH}$  resonance could not be observed and the  $\text{GeCH}_3$  resonance was observed as a singlet at +0.15 ppm relative to external TMS. The aromatic protons were split into two multiplets of area 3:1, the larger

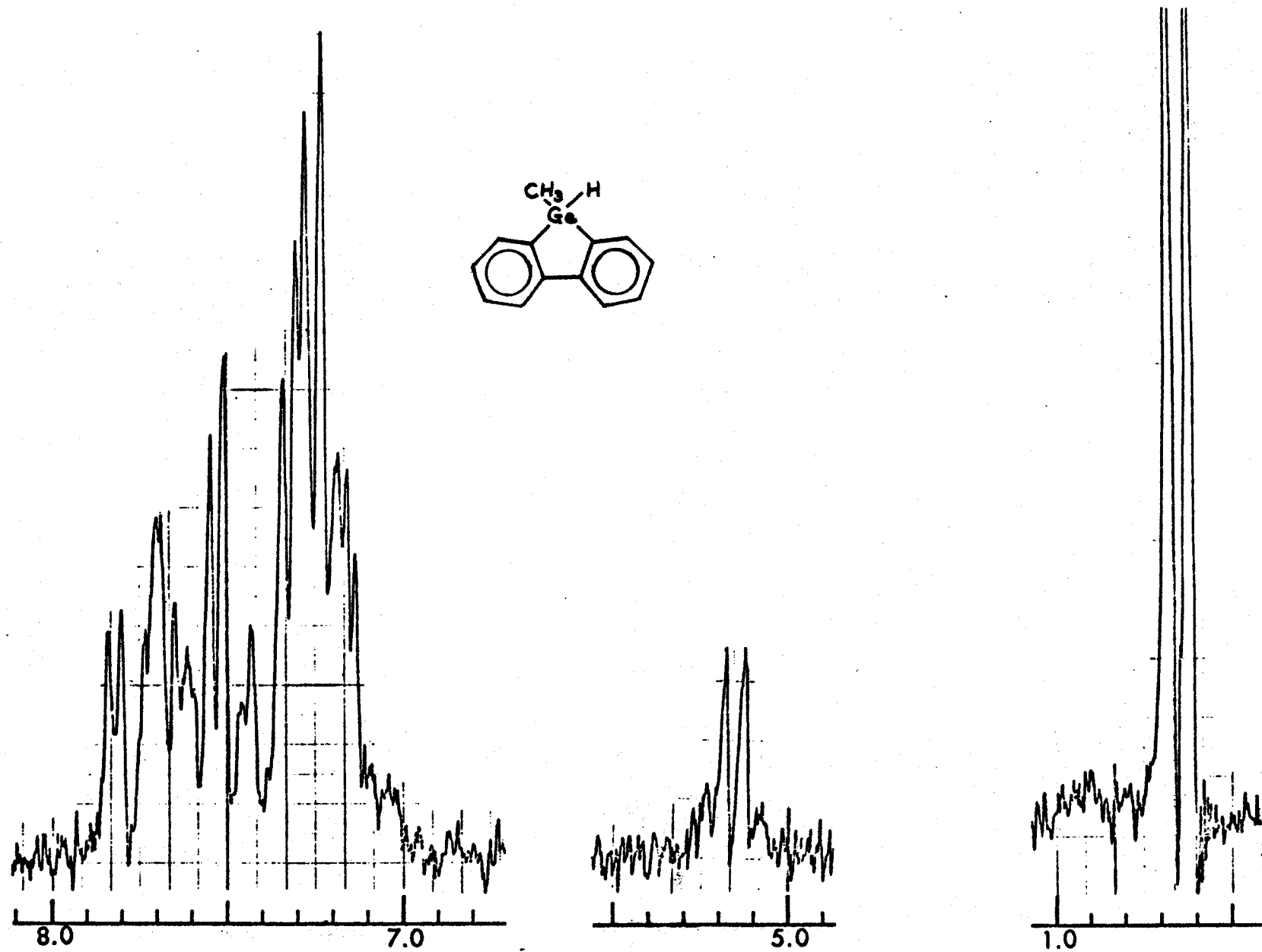


Figure 2. The NMR Spectrum of Bis Diphenylene Methyl Germanium Hydride.

resonance being centred at  $-7.4$  ppm, the smaller at  $-6.8$  ppm. A mass spectrum of the hydride showed peaks at  $m/e$  244 - 237 of the correct relative intensities corresponding to the diphenylene methyl hydride molecular ion and peaks to lower  $m/e$  corresponding to loss of methyl and hydrogen. In addition there were other groups of peaks up to  $m/e$ : 325. The intensity patterns of these groups were very complex and were thought to correspond to derivatives of digermane formed by coupling reactions of the lithium compounds (44). These reactions have been repeated several times but in no case was a pure product isolated. The hydride reacted with alumina or silica gel preventing chromatographic separation.

Silicon Compounds: Triphenyl silane ( $\phi_3\text{SiH}$ ) (Alpha) was used as purchased. Phenyl silane ( $\phi\text{SiH}_3$ ) was prepared by reduction of phenyl trichlorosilane ( $\phi\text{SiCl}_3$ , Alpha) with lithium aluminium hydride (50) and purified by trap-to-trap distillation in vacuo, the fraction from the  $-22^\circ\text{C}$  trap was collected. It was stored in vacuo at  $-78^\circ\text{C}$ .

Silane ( $\text{SiH}_4$ ) was prepared by the lithium aluminium hydride reduction of silicon tetrachloride ( $\text{SiCl}_4$ , Fisher) as described (49) and purified by distillation through a  $-126^\circ\text{C}$  trap.

Silane-D<sub>4</sub> ( $\text{SiD}_4$ ) was prepared by  $\text{LiAlD}_4$  reduction of  $\text{SiCl}_4$  (49), purified by distillation through a  $-126^\circ\text{C}$  trap and stored in a glass bulb at room temperature.

Disilane ( $\text{Si}_2\text{H}_6$ ) and disilane-D<sub>6</sub> ( $\text{Si}_2\text{D}_6$ ) were prepared by reduction of hexachlorodisilane ( $\text{Si}_2\text{Cl}_6$ , Alpha) with lithium aluminium hydride and deuteride respectively (51). Both compounds were purified by vacuum distillation through a  $-95^\circ\text{C}$  (toluene slush) trap and collection in a  $-126^\circ\text{C}$  trap. They were stored at room temperature in glass bulbs.

Phosphine ( $\text{PH}_3$ ) was prepared by heating phosphorous acid ( $\text{H}_3\text{PO}_3$ , Allied) in vacuo, purified by distillation through a  $-126^\circ\text{C}$  trap (52), and stored in a glass bulb at room temperature.

Ammonia- $\text{D}_3$  (Merck) was dried over sodium metal before use.

Ammonia- $^{15}\text{N}$  (Mallinckrodt-Nuclear) was dried over sodium before use.

1,1,3-triphenyl propene ( $\phi_2\text{C}=\text{CH}-\text{CH}_2\phi$ ) was prepared by the reaction of 2-phenylethyl magnesium bromide ( $\phi\cdot\text{CH}_2\cdot\text{CH}_2\text{Br}$ , Aldrich) with benzophenone (Fisher) in ether. The resulting solution was hydrolysed with saturated  $\text{NH}_4\text{Cl}$  solution, the organic layer separated and evaporated to an oil. The crude alcohol was then dehydrated using 20%  $\text{H}_2\text{SO}_4/\text{CH}_3\cdot\text{CO}_2\text{H}$  by heating on a steam bath for 5 minutes. The resulting mixture of isomers was purified by vacuum distillation,  $210^\circ\text{C}$  at 0.8 cm, lit.  $225^\circ\text{C}$  at 1.2 cm (53). The pasty white solid isolated was shown by NMR to be mainly the 1,1,3-triphenyl prop-1-ene isomer (54) and it was used directly in the acidity measurements. Both isomers yield the same anion and it was therefore unnecessary to separate them.

Fluorene was recrystallized from methanol before use, M.P.  $114^\circ\text{C}$ , lit.  $115^\circ\text{C}$  (36).

2-Methyl fluorene (Koch-Light) was used as purchased.

Indene was distilled before use, B.P.  $180^\circ\text{C}$ , lit.  $180^\circ\text{C}$  (36).

#### NMR Measurements

Bulk susceptibilities of solvents. Several different solvents have been used for recording NMR spectra; since these solvents have different diamagnetic susceptibilities it is necessary to use an internal reference in order to compare the chemical shifts of various species in these solvents (55). Unfortunately the usual material, tetramethylsilane (TMS) reacts with

many of the species studied here. Thus the chemical shifts were measured with respect to the solvent absorptions or with respect to an external standard of 12% tetramethylsilane (TMS) in chloroform and corrected for differences in susceptibility of the solution and reference. The first method is more accurate provided the solvent protons are not involved in chemical exchange, e.g., ammonia solutions in the presence of excess amide ion. Table 2 provides the information necessary to compare the chemical shifts of compounds measured in the three basic solvents used here.

TABLE 2

## NMR Parameters of Basic Solvents Used in this Work

Solvent	Chemical Shifts	
	ppm relative to INTERNAL TMS	ppm relative to EXTERNAL TMS
AMMONIA (Liquid at +30°C)	-0.61; $J(^{14}\text{N-H}) = 43 \text{ Hz}$	-0.27
Dimethoxyethane	CH <sub>3</sub> -3.11	CH <sub>3</sub> -2.76
	CH <sub>2</sub> -3.25	CH <sub>2</sub> -2.90
Hexamethyl- phosphoramide (HMPA)	-2.46; $J(\text{H-C-N-P}) = 9.0 \text{ Hz}$	-2.30

Comparative acidity spectra in liquid ammonia solution. The apparatus shown in Figure 3 was washed with a  $10^{-4}$  M solution of chloroplatinic acid, dried and heated under vacuum to decompose the acid to platinum metal which acts as a catalyst for the reaction between the electron and ammonia. The vessel was transferred to a dry box and approximately  $2 \times 10^{-4}$  moles of sodium metal introduced. The vessel was returned to the vacuum line, re-evacuated and approximately 0.4 mls of liquid ammonia distilled into it. It was then sealed at A and warmed to room temperature when reaction [5] occurred. The reaction was complete when the blue colour of

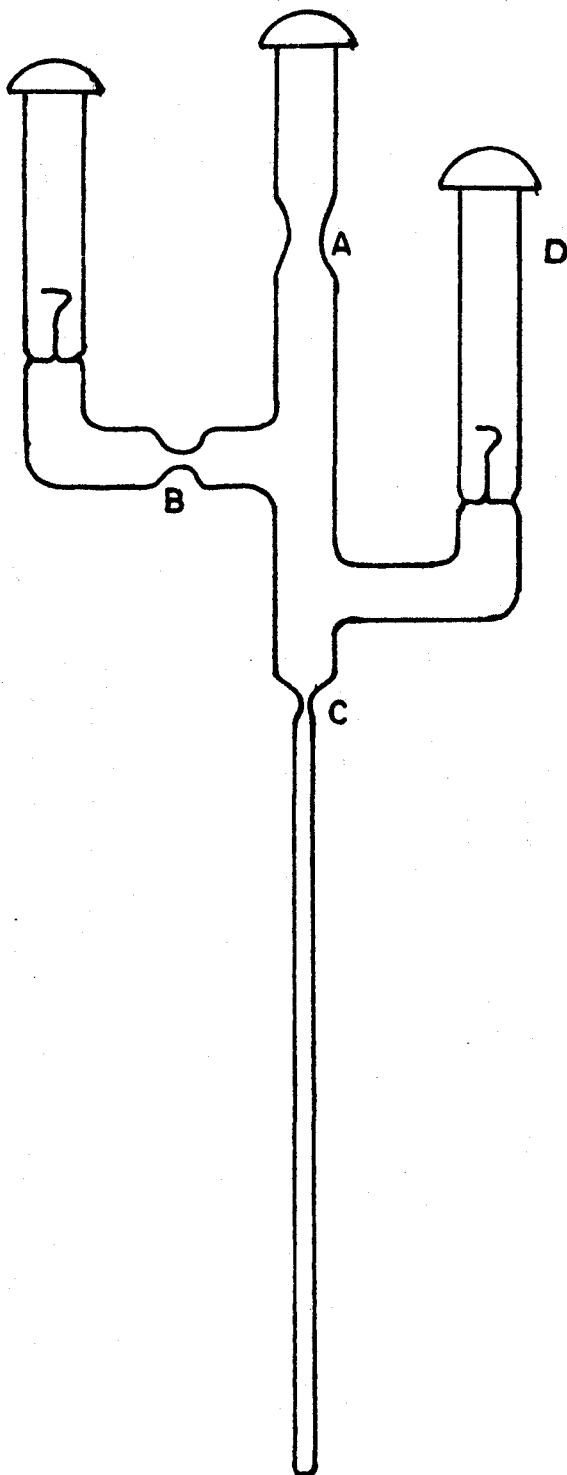


Figure 3. The Apparatus for Preparation of Solutions of Anions in Liquid Ammonia for NMR Spectroscopy.

the solvated electron had been discharged. This could take from several hours to several days. Clear cubic crystals of sodium amide were formed on the side of the tube. If potassium amide was prepared, no crystals precipitated as it is more soluble than the sodium salt and the solutions were often slightly yellow. The vessel was then attached to the vacuum line via side-arm B and after freezing the ammonia with liquid nitrogen, the break-seal was broken and the hydrogen pumped into a calibrated volume through two liquid nitrogen traps to remove any ammonia still present. The vessel was then sealed at B. The quantity of amide ion produced was calculated from the quantity of  $H_2$  evolved and equimolar quantities of the two acids to be compared weighed into the other side-arm. Volatile liquids such as indene and phenyl germane were sealed under vacuum in small glass break-seals. These substances were easily distilled into the NMR tube after evacuating the side-arm and breaking the break-seals. For compounds with low vapour pressures at room temperature, the side-arm was evacuated, sealed at D and the compounds driven into the NMR tube using a Bunsen burner. It was necessary to avoid having any sodium amide near the top of the NMR tube as the molten acids reacted vigorously with the solid and charring occurred. After sealing at C the NMR tube was warmed to room temperature while shaking vigorously to prevent local excesses of amide ion from causing side reactions. All NMR samples with liquid ammonia as solvent were placed in a water-bath at  $40^\circ C$  for  $\frac{1}{2}$  hour prior to recording the spectrum to ensure they did not explode in the spectrometer.

$^{15}NH_3/PH_3$  coupling constant measurements. The  $^{15}NH_3$  was dried over sodium and a sufficient quantity condensed into an NMR tube to give 5 atmospheres pressure at room temperature. The  $PH_3$  sample was made by degassing 0.5 mls

of tetradecane ( $C_{14}H_{30}$ ) in an NMR tube and condensing in enough  $PH_3$  to give 5 atmospheres pressure at room temperature. Both samples were pressure tested by heating to  $190^\circ C$ . The spectra were recorded on a Varian A60 spectrometer, the temperature of the probe being measured by the chemical shift difference of the absorptions of an ethylene glycol sample. Fifteen minutes was allowed for equilibration of the samples each time the temperature or sample was changed. The coupling constant was measured by generating 190 Hz sidebands using a Muirhead-Wigan D-890-A decade oscillator. Six sweeps giving 12 measurements were made at each temperature.

Analysis of the spectra of monosubstituted benzenes. The spectra were analysed using LAOCN3 (56), a computer program which can calculate the spectrum expected from a given set of parameters. If the spectrum so calculated resembles the experimental spectrum the program can then obtain the best set of parameters to match the two spectra. The procedure for monosubstituted benzenes is well-established (29, 57). As soon as the pattern of the calculated spectrum became similar to that of the experimental spectrum, the transitions were assigned and the chemical shifts and coupling constants 2,3 and 5,6; 2,4 and 4,6; 3,4 and 4,5 were iterated to provide a better fit while the other coupling constants were held constant at the previously estimated values. Then one-by-one the remaining sets of parameters were brought into the iterative process until all parameters were varied synchronously in a final iteration. After each step it was often necessary to reassign two or three lines; in these cases the iteration was repeated before bringing the next set of parameters into the calculation. Unless this procedure was used the iterations would not converge properly as

the assignment of the lines would change.

#### Preparation of solutions of the germyl ion for laser Raman spectroscopy.

The apparatus used is shown in Figure 4 . To prepare the solutions in liquid ammonia, potassium amide was prepared in situ and the exact quantity measured as described above for the NMR samples. An equimolar quantity of germane was then condensed into the apparatus which was sealed at B and warmed to  $-45^{\circ}\text{C}$  (chlorobenzene slush). The solution was then filtered into the sample tube, frozen with liquid nitrogen and sealed at C.

To prepare the dimethoxyethane solutions, excess potassium metal was distilled in vacuo to form a mirror inside the apparatus. The dimethoxyethane and germane were then condensed into the vessel which was sealed at A. After warming to room temperature and allowing the reaction to proceed to completion as shown by cessation of gas evolution at the surface of the potassium, the hydrogen was pumped away via the break-seal and the solution filtered into the sample tube and sealed.

The Raman spectra were recorded using the transverse excitation, transverse viewing method with either a Spectro Physics He/Ne laser ( $6328 \text{ \AA}$ ) or an Argon ion laser ( $5145 \text{ \AA}$ ) with a Spex 1400 spectrophotometer system. Samples were cooled by passing cold nitrogen gas, boiled from a Dewar of liquid nitrogen, over the sample which was contained in a clear-walled Dewar. Temperatures were measured using a thermocouple. The spectrometer was calibrated using indene by Mrs. B. Spiers.

#### High pressure infrared cell.

A full-scale diagram of the cell used to obtain spectrum of liquid ammonia solutions at room temperature is shown in Figure 5 . It was

SAMPLE TUBE  
5 m.m. O.D. pyrex

10 m.m. fine frit

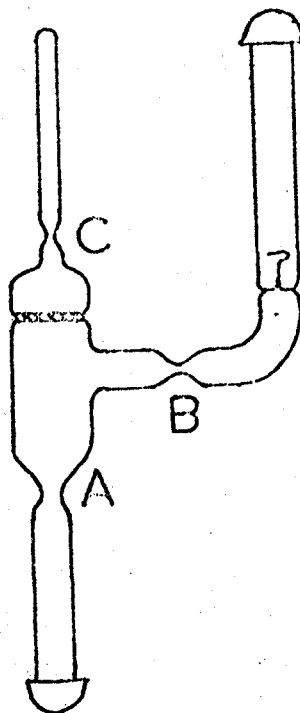
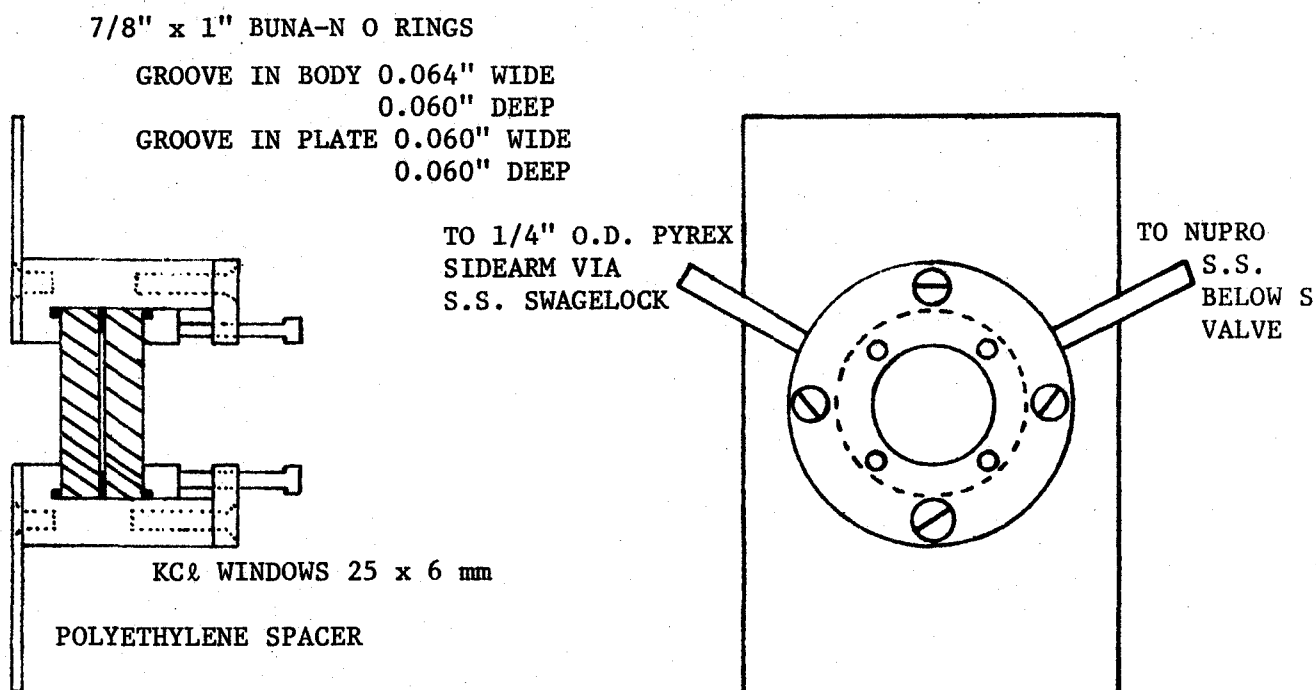


Figure 4. The Apparatus for Preparation of Laser Raman Samples.



NOTE: All material is stainless steel unless noted otherwise. For pressures above 10 atmospheres, 25 x 12 mm windows are necessary.

Figure 5. A Full-scale Diagram of the High Pressure Infrared Cell.

adapted from a design by K. Noack (58). The windows used with the liquid ammonia solution were KCl disks 6 mm thick. The strength of the windows was marginal and several sets of windows were broken because of the high pressure in the cell. It was necessary to assemble the cell very carefully making sure there was no dirt on the window-seats and to avoid sudden pressure changes within the cell. On no account were the screws compressing the windows and o-rings done up more than finger tight. This was quite sufficient for a good vacuum seal if the o-rings were in good condition. Some of the problems could have been avoided by use of windows 12 mm thick but this would have involved construction of a new cell body. These thicker windows are available from Harshaw Chemical Co.

The samples were prepared as described above for the NMR or Raman samples. Sodium or potassium amide was prepared in the side-arm of the cell and the quantity of hydrogen produced measured by Toepler pump. An equimolar quantity of germane was condensed into the side-arm with liquid nitrogen and it was then allowed to warm to room temperature. The solution was then filtered into the cell through a glass-wool plug. The spectra were recorded using a Perkin-Elmer 521 or 337.

#### Dipole moments of phenyl silane and phenyl germane.

A series of solutions of accurately known concentration by weight were prepared in Na dried spectrophotometric grade cyclohexane (Baker). The refractive indices of these solutions were measured with an Abbé refractometer which was calibrated using pure cyclohexane and carbon tetrachloride. The dielectric constants of the solutions were measured using a WTW dipolemeter DM01 at a measuring frequency of 2MHz and which was calibrated with

air and cyclohexane.

The magnitude of the dipole moment was calculated by the method of Smith (59) using the following expression:

$$\mu_X^2 = \frac{27 kT}{4\pi N_o} \cdot \frac{\text{Mol. Wt. (X)}}{\rho_o (\epsilon_o + 2)^2} \cdot \left( \frac{\partial(\epsilon - \epsilon_o)}{\partial c} - \frac{\partial(n^2 - n_o^2)}{\partial c} \right) \text{ cm.esu.}$$

where  $\partial/\partial c$  is the differential with respect to concentration (in weight fraction of compound X), subscript o refers to the pure solvent and the other symbols have their usual meaning (see page viii). Using cyclohexane as a solvent where  $\rho_o = 0.7791$  gms/ml and  $\epsilon_o = 2.0228$  at  $20^\circ\text{C}$  (36) this simplifies to

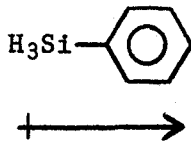
$$\mu_X^2 = 0.01145 \times \text{Mol. Wt. (X)} \times \left( \frac{\partial(\epsilon - \epsilon_o)}{\partial c} - \frac{\partial(n^2 - n_o^2)}{\partial c} \right) \text{ Debye.}$$

The derivatives were evaluated graphically, Figure 6, using the experimental data in Table 3. The dipole moments were found to be

phenyl silane ( $\phi\text{SiH}_3$ )       $0.88 \pm 0.03$  D.

phenyl germane ( $\phi\text{GeH}_3$ )       $0.68 \pm 0.03$  D.

The direction of the dipole moment in phenylsilane can be found from a comparison of the dipole moments of p-chlorophenylsilane and chlorobenzene. The dipole moment of (p chlorophenyl)silane is 0.99 D (16) and since the dipole moment of chlorobenzene is 1.59 D (60) the direction of the phenylsilane dipole moment must be the same as chlorobenzene. By analogy the



dipole moment of phenylgermane acts in the same direction.

TABLE 3

## Data for Calculation of Dipole Moments

Wt. fraction of compound in solution	Phenyl silane in cyclohexane at 20°C	
	Refractive index	Dielectric Constant
0.09938	1.4346	2.1057
0.06098	1.4320	2.0775
0.03285	1.4290	2.0509
0 (a)	1.4266	2.0228
	Phenyl germane in cyclohexane at 20°C	
0.16139	1.4388	2.0985
0.10326	1.4341	2.0701
0.08615	1.4327	2.0624
0.04479	1.4293	2.0438
0 (a)	1.4266	2.0228

(a) reference (36).

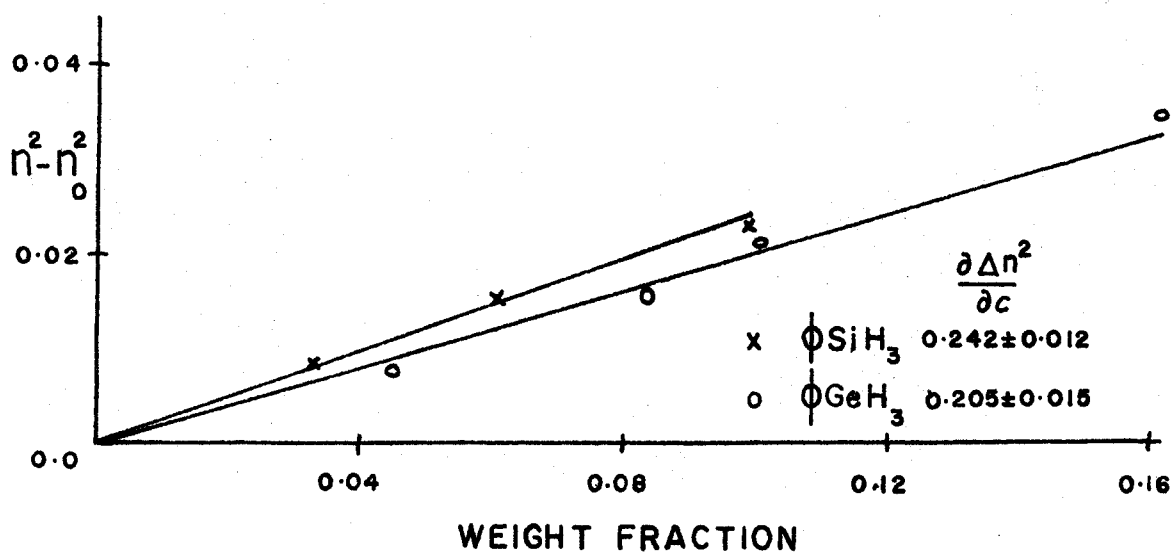
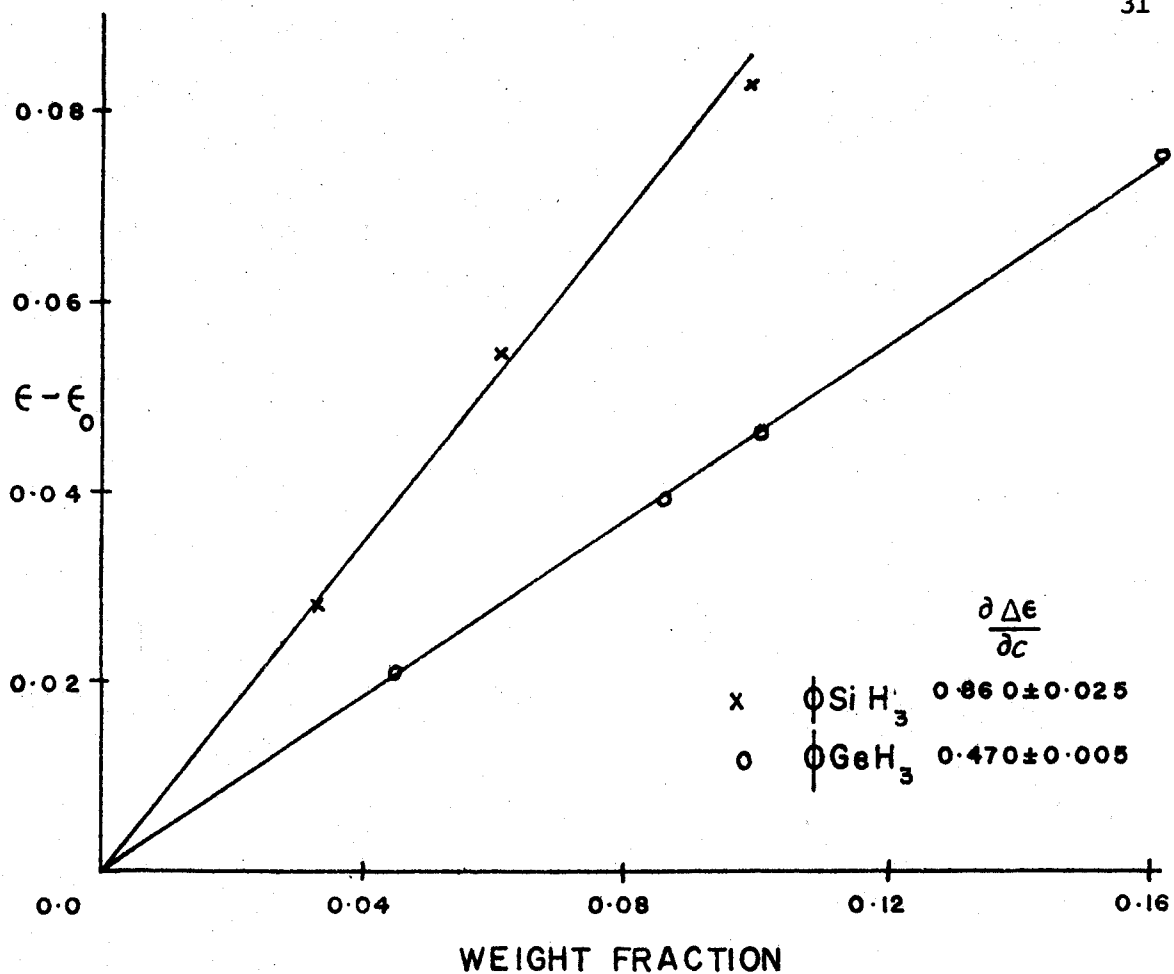


Figure 6. The Evaluation of the Differentials for Calculation of the Dipole Moments of Phenyl Silane and Phenyl Germane.

## CHAPTER 3

### The Acidity of Aryl Germanes

As described in the Introduction the acidity of two acids HA and HB dissolved in the same medium are related by equation [4], page 9, derived from the Hammett  $H_{\text{}}$  equation. This can be rearranged to give

$$pK_A - pK_B = -\log_{10} \frac{[A^-][HB]}{[B^-][HA]} \quad [6]$$

Following the preliminary work of Birchall and Jolly (11,34) an NMR technique has been used to evaluate the concentration ratios for the aryl germanes and some hydrocarbon indicators in liquid ammonia solution.

The type of NMR spectrum observed for a mixture of an acid and its anion depends upon the rate of proton exchange between the two species. There are three situations which may occur (61). If two proton species of resonant frequencies  $V_A$  and  $V_B$  Hz and concentrations  $[A]$  and  $[B]$  are interchanging sites with a frequency of  $1/t$ , then if  $t < 1/\pi(V_A - V_B)$  proton exchange is said to be fast on the NMR time scale and a single peak at the weighted average frequency  $([A]V_A + [B]V_B)/([A] + [B])$  is observed. When  $t \approx 1/\pi(V_A - V_B)$  the rate of exchange is intermediate and two broad lines of intermediate separation are observed, but when  $t > 1/\pi(V_A - V_B)$  the exchange is slow and two peaks at  $V_A$  and  $V_B$  are observed. The areas under the peaks are proportional to the concentration of the species present in solution. Acidity measurements have been made using spectra showing fast proton exchange for a series of substituted anilines in liquid ammonia (34). In these spectra the solvent ammonia was always observed to be a broad triplet resonance due to coupling of

the protons with the  $^{14}\text{N}$  nucleus ( $I = 1$ ), with sharp satellites due to coupling to the 0.4% abundant  $^{15}\text{N}$  nucleus ( $I = \frac{1}{2}$ ) as illustrated in Figure 7 . This showed that the solvent ammonia was not involved in the mechanism by which rapid proton exchange occurs between the acid and its anion. Such spectra have been previously observed in liquid ammonia where the ammonium ion concentration has been reduced by buffering the solution with a weak acid and its salt (62). In this work all of the spectra obtained of solutions containing acid/anion mixtures were of the slow proton exchange type and thus consisted of the superimposed spectra of the acid, its anion and the solvent, Figures 7 and 8. This agrees with previous observations (11) which suggested that for acid/anion mixtures the rates of proton exchange of group IV, V and VI hydrides were slow, intermediate to fast, and fast respectively on an NMR time scale. All of the species studied here had at least one clearly resolvable absorption so that the relative concentrations of the acid and anion could easily be measured from the spectra, generally by electronic integration. In some cases the characteristic absorption occurred close to the solvent absorptions making electronic integration impossible, as for the germyl ion, Figure 8 . In these cases the area of the peak was obtained by cutting out the peak and weighing the paper. It was assumed that the paper was of uniform density and thickness. The details of the actual resonances used for the measurements are shown in Table 4 . The chemical shifts were measured relative to the centre peak of the ammonia triplet and varied with concentration and constitution of the solutions but always occurred within 0.1 ppm of the value given in the table.

A complete analysis of the NMR spectra was not attempted in all

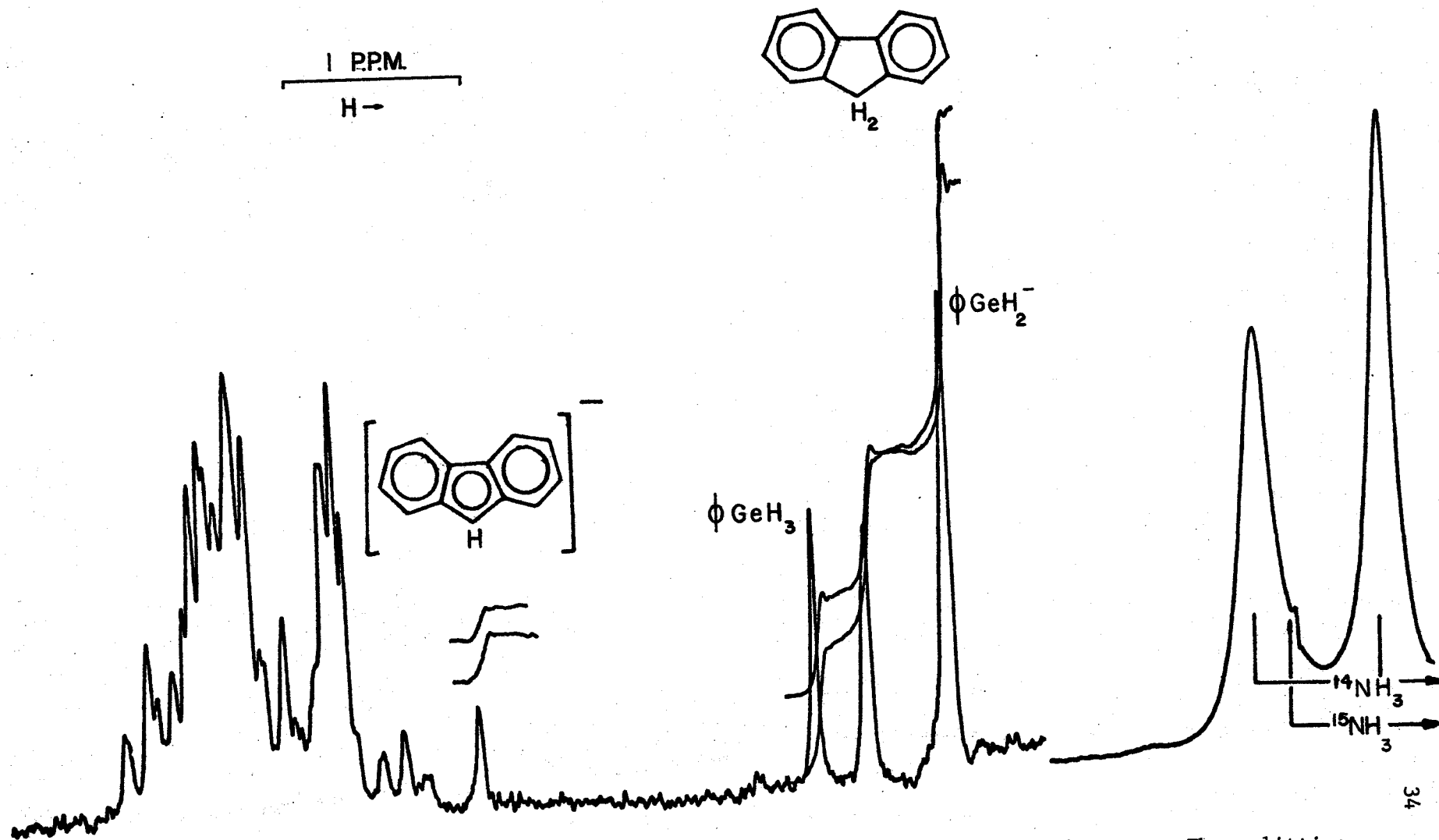


Figure 7. The NMR Spectrum Comparing the Acidities of Phenyl Germane and Fluorene. The splitting of the solvent protons by the nitrogen nuclei is shown.

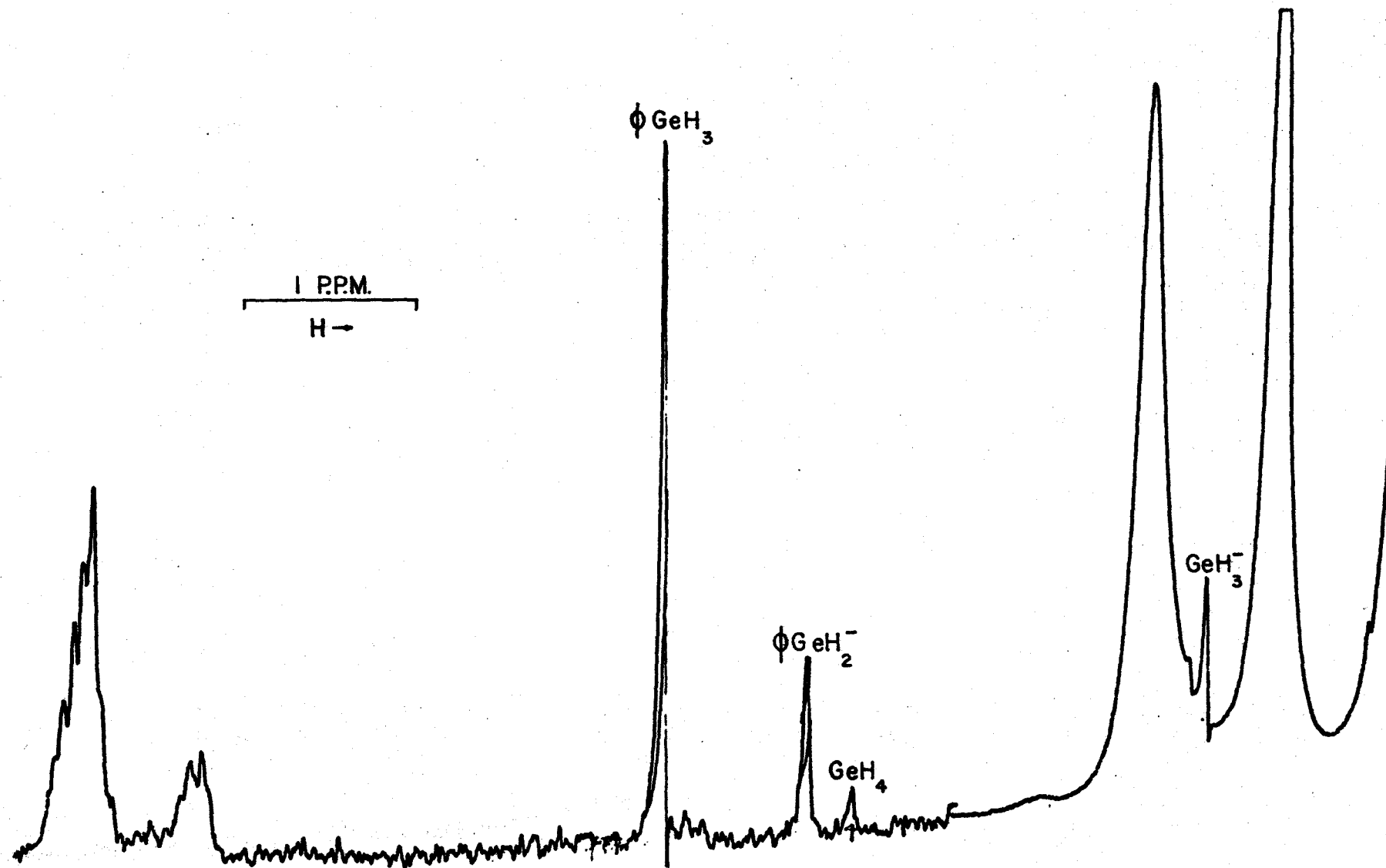


Figure 8. The NMR Spectrum Comparing the Acidities of Germane and Phenyl Germane.

TABLE 4

## NMR Parameters of the Acids and Anions Used in Acidity Measurements

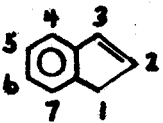
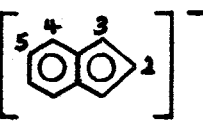
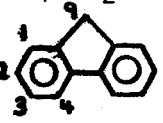
Compound	Chemical Shift* of resonance used for acidity measurement (ppm downfield from NH <sub>3</sub> )	Further details of spectrum	
		Chemical Shifts (ppm downfield)	Coupling Constants (Hz)
 <p>Indene</p>	(1) 2.68 broad singlet	Ref. (89). Pure indene; TMS ref. (1) 2.96; (2) 6.14; (3) 6.66; (4,5,6,7) broad multiplet ~6.9.	(1,2) +2.02; (1,3) -1.98; (2,3) +5.58.
 <p>Indenyl anion</p>	(3) 5.18 (d) J = 5 Hz	Ref. (73). THF solution. C <sub>6</sub> H <sub>12</sub> ref. (2) 5.1 (t); (3) 4.4 (d); (4) 5.8 (q); (5) 4.9 (q).	
Germane	2.41		
Germyl ion	0.43		
φGeH <sub>3</sub>	(GeH <sub>3</sub> ) 3.47	multiplet at ~6.7	
φGeH <sub>2</sub> <sup>-</sup>	(GeH <sub>2</sub> ) 2.66	2 multiplets area 2:3 at ~6.8 and ~6.1	
 <p>Fluorene</p>	(9) 3.21 broad singlet	Ref. (88). CCl <sub>4</sub> solution. TMS ref. (1) 7.41; (2) 7.16; (3) 7.25; (4) 7.66; (9) 3.82.	(1,2) 7.65; (1,3) 0.85; (1,4) 0.7; (2,3) 7.4; (2,4) 1.25; (3,4) 7.25.

TABLE 4 (cont'd.)

Compound	Chemical shift* of resonance used for acidity measurement (ppm downfield from NH <sub>3</sub> )	Chemical Shifts (ppm downfield)	Coupling Constants (Hz)
	(9) 5.40 broad singlet	(1) 6.71; (2) 6.19; (3) 5.80; (4) 7.30.	(1,2) 8.06; (1,3) 0.99; (1,4) 0.83; (2,3) 6.63; (2,4) 1.28; (3,4) 7.82; (4,9) 0.70.
Fluorenyl anion			
$\phi_2\text{GeH}_2$	(GeH <sub>2</sub> ) 4.36	broad multiplet at ~6.5	
$\phi_2\text{GeH}^-$	(GeH) 4.23	2 broad multiplets, area 4:6, at ~6.7 and ~6.1.	
tol <sub>3</sub> GeH (a)	(CH <sub>3</sub> ) 1.70	CCl <sub>4</sub> solution. TMS ref. (CH <sub>3</sub> ) 2.27; (GeH) 5.39; (ortho) 7.08; (meta) 6.88.	(ortho, meta) 7.4
tol <sub>3</sub> Ge <sup>-</sup>	(CH <sub>3</sub> ) 1.60	(ortho) 6.71; (meta) 6.23.	(ortho, meta) 7.5
113 triphenyl propene	(CH <sub>2</sub> ) 2.75 (d) J = 8 Hz	Ref. (54). CCl <sub>4</sub> solution. TMS ref. (CH <sub>2</sub> ) 3.42 (d); (CH) 6.22 (t); broad multiplet at ~7.3.	
113 triphenyl propenyl ion	(CH $\phi$ ) 4.66 (d) J = 14 Hz	2 broad multiplets at ~6.7 and ~6.2.	

\* (d) indicates a doublet resonance; (t) a triplet; and (q) a quadruplet.

(a) tol represents p-CH<sub>3</sub>-C<sub>6</sub>H<sub>4</sub>-

cases since it was only necessary to know one characteristic absorption for each species in order to estimate its relative concentration. However, the parameters are summarised in Table 4 if they are known. The spectra of some of the species are discussed in more detail later in this thesis.

The results of the relative acidity measurements are shown in Table 5, the errors quoted were estimated from the accuracy with which the NMR spectra could be integrated. In view of the difficulty of sample preparation (page 21) and the inherent limitations of the method, which are discussed below, it was considered unnecessary to repeat the measurements more than twice. The difference in acidity observed between any pair of acids is clearly outside the errors of measurement. Table 5 shows the compounds retabulated in order of acidity. Also included in this table are the results of a spectrophotometric determination of the relative acidities of the relevant hydrocarbons in cyclohexylamine (63) and a potentiometric determination of these hydrocarbon acidities in DMSO (64). In order to facilitate comparison the  $pK_a$  of fluorene has been taken as 20.6 in liquid ammonia. It can be seen that the agreement between the results obtained in the different solvents is quite good. This is a further check on the reliability of the NMR measurements. The results confirm Birchall and Jolly's observation (11) that germane is more acidic than triphenyl germane; each successive aryl substitution reduces the acidity of the germane by approximately 2 orders of magnitude. This is an extremely surprising result by comparison with the analogous carbon compounds where each aryl substitution causes a large increase in acidity [ $pK \text{ CH}_4 \sim 50$ ,  $\phi \text{CH}_3 \sim 40$ ,  $\phi_2 \text{CH}_2 = 33.1$  and  $\phi_3 \text{CH} = 31.5$  (24)]. The

TABLE 5

Comparative Acidity Measurements of the Aryl Germanes  
in Liquid Ammonia using Na Salts (+30°C)

HA	HB	$+\log_{10} \frac{[A^-][HB]}{[B^-][HA]}$	probable error
Indene	GeH <sub>4</sub>	0.3, 0.3	±0.1
GeH <sub>4</sub>	φGeH <sub>3</sub>	~ 2.3, 2.1, 2.1	±0.2
φGeH <sub>3</sub>	Fluorene	0.8, 0.8	±0.1
Fluorene	φ <sub>2</sub> GeH <sub>2</sub>	0.75, 0.8	±0.1
φ <sub>2</sub> GeH <sub>2</sub>	tol <sub>3</sub> GeH (a)	2.2	±0.2
φ <sub>3</sub> GeH	tol <sub>3</sub> GeH (a)	0.5, 0.4	±0.1
113 triphenyl propene	tol <sub>3</sub> GeH (a)	0.4, 0.5	±0.1

Acids in Order of Strength referred to Fluorene (pK<sub>a</sub> = 20.6)

Acid	pK <sub>a</sub> in liquid ammonia	pK <sub>a</sub> in C <sub>6</sub> H <sub>11</sub> ·NH <sub>2</sub> (63) (pK <sub>a</sub> 9φFluorene = 16.4) (65, 33)	pK <sub>a</sub> in DMSO (33, 65)
Indene	17.4	18.1	18.5
GeH <sub>4</sub>	17.7		
φGeH <sub>3</sub>	19.8		
Fluorene	(20.6)	20.7	20.5
φ <sub>2</sub> GeH <sub>2</sub>	21.4		
113 triphenyl propene	23.1	24.3	23.1
φ <sub>3</sub> GeH	23.2		23.0 (b)
tol <sub>3</sub> GeH (a)	23.6		
C <sub>2</sub> H <sub>5</sub> GeH <sub>3</sub>	23.9 (c)		

(a) tol represents (p-CH<sub>3</sub>-C<sub>6</sub>H<sub>4</sub>).

(b) Ref. (30).

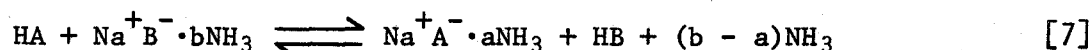
(c) Ref. (11).

NMR parameters of phenyl germane (page 48) show that there is almost no perturbation of the aromatic system in this acid and hence (p-d) $\pi$  bonding probably has little effect in deciding the acidity of the phenyl germanes. Much more important, the NMR parameters of the phenyl germyl anion (page 57) show that there is little or no delocalization of the negative charge on to the aromatic ring. Thus aryl substitution would not be expected to increase the acidity of the germanes as greatly as with the carbon acids because the corresponding anions are not resonance stabilized. Table 5 also shows that ethyl germane is a weaker acid by a factor of  $\sim 10^6$  than germane, a result inexplicable by simple inductive electronic effects as was shown by the simple electrostatic argument in the Introduction. However the substitution of a large uncharged group (phenyl or ethyl) for a hydrogen will greatly change the extent of solvation of the localized charge of the germyl anions.

At this point it is appropriate to discuss the assumptions and the standard states of the species involved in the calculations of the acidity differences. The standard state of a compound is the state where, by definition, the activity is equal to unity. As shown in the Introduction, the  $pK_a$  of the reference acid is estimated by extrapolation of the measurements to infinite dilution when the activity coefficients  $\rightarrow 1$ , thus the standard state is the hypothetical unit concentration with each molecule behaving as if it were surrounded only by pure solvent. The standard state of the solvent is pure solvent. Thus it is indeed surprising that the values in Table 5 agree so well. The dissociation constants were calculated using activities based on very different states, namely dilute solution in the various solvents. However, the values estimated in cyclo-

hexylamine were based on a determination of the  $pK_a$  of 9 phenyl fluorene in DMSO solution (65). The cyclohexylamine and DMSO scales show a large discrepancy if the  $pK_a$  value for 9 phenyl fluorene measured in an aqueous solution is used as the reference value for the cyclohexylamine scale (33).

Equation [6] above can also be derived by considering the equilibrium constant of the reaction between the acids and anions, [7], studied here



where the anionic species are shown as strongly solvated ion pairs. Thus the equilibrium constant for this reaction is

$$K = K_A/K_B = \frac{f_A^- f_{HB} [A^-][HB]}{f_B^- f_{HA} [B^-][HA]} \times a_{NH_3}^{(b-a)} \quad [8]$$

where  $f_X$  = activity coefficient of species X

and  $a_{NH_3}$  = activity of ammonia.

This reduces to equation [6] if the assumptions are made that the ratio of the activity coefficients is unity and the solution is sufficiently dilute so that the activity of the solvent in solution is equal to that of the pure solvent, i.e., unity. As stated above, the experimental errors quoted in Table 5 are estimated from the accuracy with which the NMR spectra could be integrated. From the agreement with the other acidity scales (Table 5) these would seem to be realistic overall errors. Since the solutions used here were 0.2 - 0.5 M in each acid, the assumptions noted above are certainly not true and one might have expected a poorer correlation between the different scales.

Another uncertainty in the interpretation of results arises because of the possibility of ion-pairing in solution. Lagowski has shown that

salts in liquid ammonia solution exist mainly as ion aggregates (66) and Streitweiser has shown that in cyclohexylamine the acidity of certain compounds depends on the counter ion (67). By using lithium or cesium as the counter ion he observed changes in acidity for a series of hydrocarbons of generally 0 - 0.3 pK units but occasionally as high as 0.5 pK units. These differences were attributed to the different types of ion-pair formed. Li was thought to form a solvent separated ion-pair while cesium formed contact ion-pairs. The contact ion-pair favours the formation of the anion in cases where the charge is relatively localized, thus increasing the acidity of that species. Since the chemical shift of a proton in a molecule is sensitive to electric fields arising from dipoles (68), the NMR spectra of the Li, Na, K and Cs salts of the germyl ion were measured. It was expected that the results would give a qualitative idea of the nature of the ion-pairing in ammonia solutions (69). The results presented in Table 6 are considered to be more accurate than the previous measurement of the chemical shift of the germyl ion (11) as the measurements reported here were made relative to an internal reference rather than to an external reference of unknown susceptibility. The spectra of the Li, Na and K salts were the same within experimental error, but different from that of the

TABLE 6

Chemical Shift of the Germyl Ion in Ammonia Solution at +30°C

Alkali metal cation	$\delta(\text{GeH}_3^-)$	$\delta(\text{GeH}_4)$
Li <sup>+</sup>	-0.38 ppm	-2.40 ppm
Na <sup>+</sup>	-0.42 ppm	-2.43 ppm
K <sup>+</sup>	-0.42 ppm	-2.43 ppm
Cs <sup>+</sup>	-0.50 ppm	-2.40 ppm

Chemical shifts to  $\pm 0.01$  ppm relative to the centre peak of  $\text{NH}_3$  triplet solutions  $\sim 0.4$  M in both germane and salt.

cesium salt. This data suggests that the Li, Na and K salts all form solvent-separated ion-pairs in ammonia, while the cesium salt probably forms contact ion-pairs. If this is so and Streitweiser's arguments to explain the effect of the counterion are correct, then it can be anticipated that the germanes, whose anions have their charges localised on the germanium atom, would be more acidic compared to the hydrocarbons if cesium were used as counterion for the measurements.

From the above discussion it is apparent that the acidities presented in Table 5 are calculated from a standard state in ammonia solution but based on a reference compound, fluorene, whose  $pK_a$  is derived from measurements in DMSO solution. Thus the relative acidities ( $\Delta(\Delta G^\circ)$  for the ionization of the two acids) are a measure of the difference in both the gas phase ionization and the solvation energies of the various acids and anions. Any arguments concerning changes in acidity as a result of electronic effects in the acid or anion refer only to the gas phase ionization. Thus it is not possible to make deductions concerning the electronic effects within these molecules from the acidity measurements unless solvation effects are constant. This statement may appear to be obvious but it has often been ignored. Chatt and Williams (12) measured the ionization constant of trimethyl silyl and trimethyl germyl substituted benzoic acids and claimed that since these compounds are more acidic than benzoic acid the silyl and germyl groups must be electron-withdrawing. Recently the temperature dependence of these acidities was measured (23) and the  $\Delta H^\circ$  and  $\Delta S^\circ$  of ionization obtained; the  $\Delta S^\circ$  term arising mainly from the effects of solvation. Some of the results are shown in Table 7

TABLE 7

Thermodynamic Data for Ionization of Substituted Benzoic Acids  
at 25°C (23) in Aqueous Solution

Acid	$\Delta G^\circ$ (cals/mole)	$\Delta H^\circ$ (cals/mole degree)	$\Delta S^\circ$ (cals/mole degree)
p-nitro benzoic acid	+4696	+ 122	-15.3
p-trimethylsilyl benzoic acid	+5719	+3060	- 8.9
benzoic acid	+5735	+ 150	-18.7

One can see from this table that the enhanced acidity of the silyl substituted acid over benzoic acid is due entirely to the small  $\Delta S^\circ$  term compared to the other acids. The  $\Delta H^\circ$  value suggests strongly that silicon is an electron-donating species as predicted by electronegativity arguments. Therefore it is felt that the solvation energies of the germyl anions are responsible for the apparently anomalous acidities of the aryl germanes. The germyl ion will be strongly solvated in solution as it is small in size (compared to organic anions). The covalent radii of Si and Ge differ by approximately 0.05 Å and the ionic radius of the silyl ion in crystals of  $\text{KSiH}_3$  is 2.24 Å (70), much the same size as the iodide ion. The large increase in effective radius of the ion on alkyl or aryl substitution would be expected to greatly change the solvation parameters, that is both  $\Delta H^\circ$  and  $\Delta S^\circ$ . Several attempts were made to confirm this hypothesis. The temperature dependence of the relative acidity of fluorene and diphenyl germane was investigated but no change could be detected within the estimated experimental error over a temperature range of 25°C. The upper temperature (45°C) was determined by the vapour pressure of the ammonia and the lower temperature (20°C) by the solubility of the acids. Another

approach was to measure the relative acidities in a different solvent. Dimethoxyethane was chosen since it was anticipated that the solvation energies of the germyl ions would be smaller in this solvent than in ammonia and hence the difference in acidities between the germanes would be smaller. Unfortunately the NMR absorptions of the solvent were so intense that the characteristic absorptions of many of the acids and their anions were obscured. An attempt was made to compare the acidities of germane and phenyl germane by adding phenyl germane to a solution of  $\text{KGeH}_3$  in dimethoxyethane but decomposition occurred rapidly to give a dark red-brown gelatinous precipitate and a non-condensable gas, presumably hydrogen. By shaking the precipitate to the top of the tube an NMR spectrum was obtained which showed no peak due to the germyl ion but in the aromatic region the characteristic spectrum of the phenyl germyl ion (page 57) was observed. It was presumed that a reaction of the following type had occurred.



One further reason for the reduced acidity of the triphenyl germane compared to the other aryl germanes may be steric crowding of the anion. There is no structural information on the triphenyl germyl anion but it may be reasonably inferred that the C-Ge-C bond angle is less than tetrahedral. The bond angle of the germyl ion is approximately  $95^\circ$  (Table 14) and C-P-C angle of the structurally-related molecule triphenyl phosphine is  $103^\circ$  (71). Certainly the triphenyl germyl anion would not be expected to be planar about the central atom as is the triphenyl methyl anion, since it has been shown that there is negligible delocalization of the charge from the Ge atom to the aromatic ring (page 57). Given the

assumption that the bond angles at Ge decrease on ionization this would be most unfavourable for formation of the triphenyl germyl anion and thus partially account for the reduced acidity of triphenyl germane.

#### The Acidity of Silanes

An attempt was made to measure the relative acidity of silane and phenyl silane in dimethoxyethane by adding phenyl silane to a solution of potassium silyl and allowing the mixture to react in a sealed NMR tube. Initially the NMR spectrum showed peaks due to silyl ion and phenyl silane but bubbles formed in the solution and the spectrum slowly changed over a period of time. After one week the silyl ion resonance was much smaller and a new multiplet had appeared upfield of the existing aromatic resonances. In addition a small peak due to benzene had also appeared. After several weeks crystals grew from the yellow solution and no further changes occurred in the NMR spectrum, Figure 9. By analogy with the spectrum of  $\phi\text{GeH}_2^-$  this spectrum is assigned to  $\phi\text{SiH}_2^-$  but contaminated with  $\phi\text{SiH}_3$ . It is not known if the crystals which precipitated were  $\text{K}\phi\text{SiH}_2$  or some other compound resulting from attack of an anionic species on dimethoxyethane. The results of this experiment suggest that silane and phenyl silane are of comparable acidity in dimethoxyethane. The phenyl silyl ion has not been reported previously. The triphenyl silyl and diphenyl methyl silyl anions have been synthesized previously but an attempt to make phenyl dimethyl silyl anion failed (72).

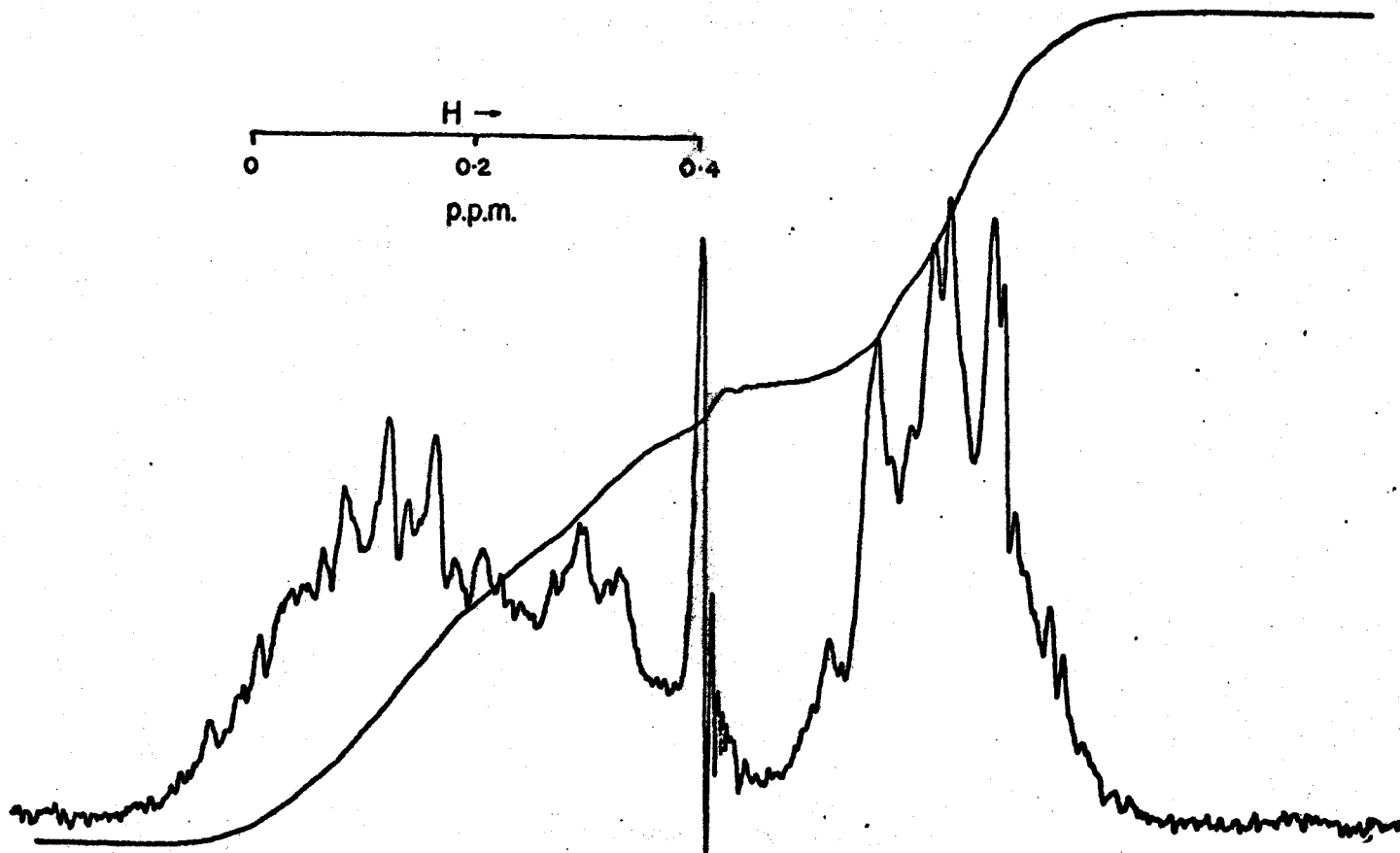


Figure 9. The NMR Spectrum of  $\phi\text{SiH}_2$  contaminated with  $\phi\text{SiH}_3$  and benzene.

## CHAPTER 4

### NMR Spectra

#### The NMR Spectra of Phenyl Silane and Phenyl Germane

As discussed in the Introduction (page 6 ) it had been suggested that multiple bonding was responsible for the reduced acidity of triphenyl germane compared to germane in liquid ammonia solution. Doubt has already been cast upon the validity of this explanation due to the magnitude of the electron shift required (see Introduction). To test this hypothesis further, the  $^1\text{H}$  NMR parameters of the above molecules were obtained.

The chemical shift of a proton is a measure of the magnetic screening provided by the surrounding electrons and thus depends on the electron density around that point in the molecule (68). Since other factors also affect the chemical shift such as magnetic anisotropy of adjacent bonds in the molecule and interaction with neighbouring molecules in the solution it is usual to compare chemical shifts with that of an internal reference which must be closely related structurally and of known electron density distribution. Benzene was chosen as the standard in this work. The best procedure to minimize solvent effects is to use a non-polar solvent and to extrapolate the measurements to zero concentration, but it is common procedure to compare spectra recorded at a constant low concentration. For benzenoid systems the chemical shift of a proton has been shown to increase by  $10.7 \pm 1.0$  ppm per electron on the neighbouring carbon atom (73). Thus fairly small changes of electron density in an aromatic system would give easily detectable changes in the chemical shifts of the protons. The method has been used to explain the NMR spectra of the non-alternant hydro-

carbons, azulene and acepleiadylene and to make experimental determinations of electron density which agree well with M.O. calculations for hydroxy-benzenes (74) and various anionic species (73,75). Careful analysis of the NMR parameters of phenyl silane and phenyl germane was therefore expected to give a measure of the extent of perturbation of the electrons of the aromatic ring by the metalloid atom.

Phenyl silane has been shown by NMR methods to form complexes by association with donor solvents and to self-associate in non-polar solvents (76). The study was based on the observations that the phenyl and silyl proton chemical shifts were solvent and concentration dependent. Phenyl germane exhibits similar behaviour, the phenyl resonances moving to lower field and the germyl resonances to higher field on dilution of the solutions. To eliminate the effect of these intermolecular interactions the spectra were recorded and analysed at several different concentrations and the parameters at infinite dilution obtained by extrapolation. The spectra observed in this work were of considerably higher resolution than the previously reported spectrum of phenyl silane (76) and consisted of a very complex resonance in the aromatic region (Figure 10) and a very sharp singlet resonance from the  $MH_3$  protons approximately 3 ppm upfield of the aromatic protons. Double irradiation of the  $MH_3$  resonance did not detectably change the aromatic region for either the silicon or germanium compound indicating that there is no spin-spin coupling of the  $MH_3$  protons with the ring protons, unlike toluene where such coupling does exist (57). Because of this lack of coupling it was only necessary to analyse a five-spin  $AA'BB'C$  spectrum to obtain the NMR parameters. This analysis was performed using a computer program LAOCN3 (56) as described in the experimental section. Criteria

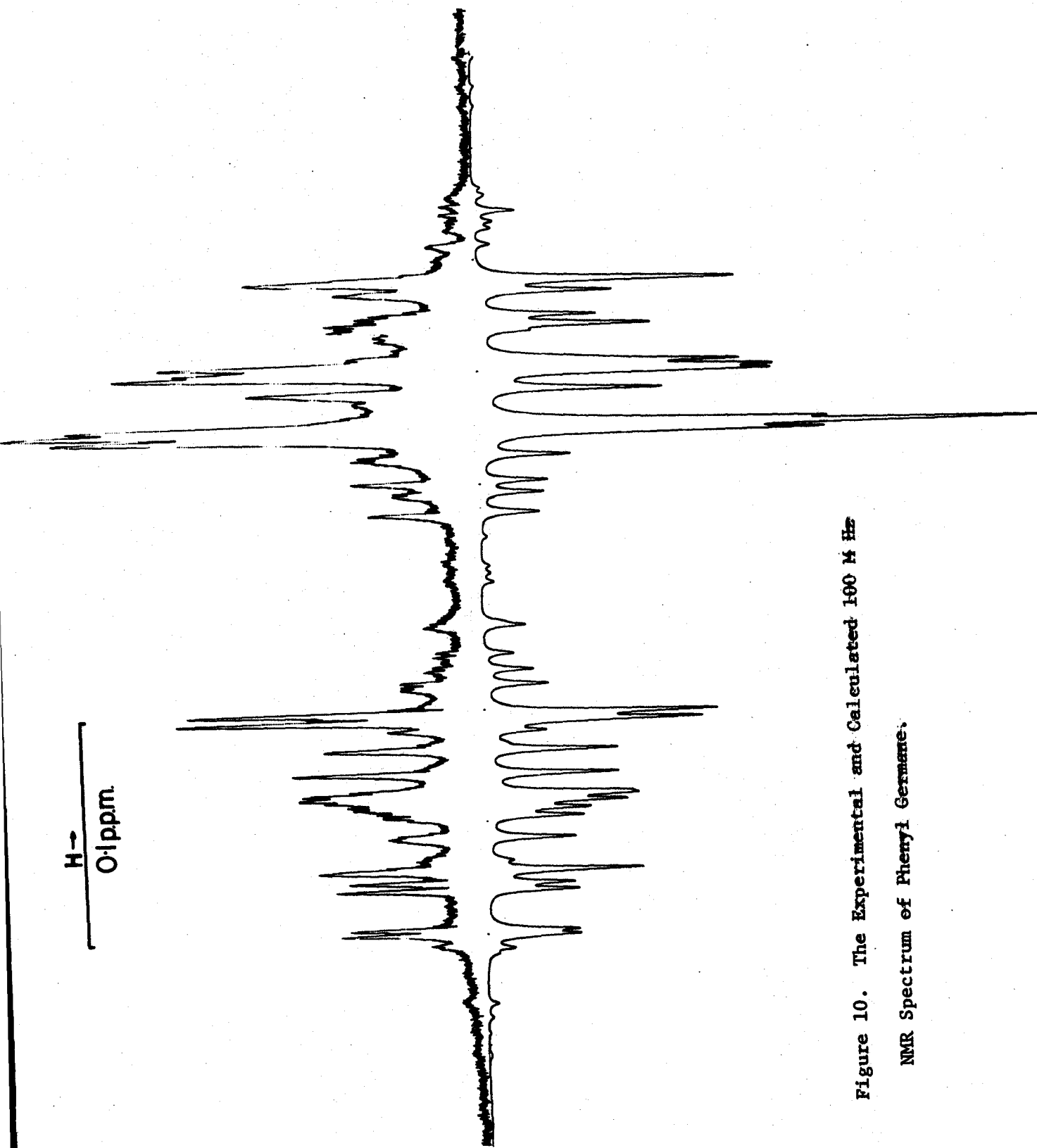


Figure 10. The Experimental and Calculated 100 Mc Hz

NMR Spectrum of Phenyl Germane.

for accuracy of analysis were visual agreement of calculated and experimental spectra (see Figure 10) which is a good check on the calculated intensities of the transitions and the value of the root mean square error calculated by LAOCN3. This latter value is a check on the accuracy of the calculated positions of the transitions and should be around 0.1 Hz since this is the error of measuring the position of a single peak. It is of interest to note that a phenyl group has 110 symmetry-allowed transitions (Appendix I). LAOCN3 calculates 76 transitions of reasonable intensity and approximately 50 transitions were assigned for each analysis performed. The results of the analyses are shown in Table 8. The chemical shifts relative to benzene for phenyl silane at infinite dilution were found to be -0.263, -0.012 and -0.061 ppm for ortho, meta and para protons respectively. The corresponding values for phenyl germane are -0.185, +0.020 and -0.020 ppm. Clearly, there is no drastic perturbation of the aromatic ring by substitution of a silyl or germlyl group for hydrogen. As explained above, interaction of the system with the empty d orbitals of the metalloid would result in an electron deficiency at the ortho- and para-positions and a consequent downfield shift. However, the magnitude of the observed shift is so small that other factors become important.

The presence of a dipole moment in a molecule causes an electric field which tumbling does not average to zero. The magnitude and sign of the shift caused by this electric field can be estimated from knowledge of the molecular dipole moment and dimensions. Buckingham has worked out a general formula (68):

$$\sigma = -2 \times 10^{-12} E_z - 10^{-18} E^2$$

where  $\sigma$  = the screening constant of the proton

TABLE 8

<sup>1</sup>H NMR data for phenylsilane and phenylgermane in carbon tetrachloride solution

	Phenylsilane				Phenylgermane			
	Concentration of CCl <sub>4</sub> solution (moles/l.)							
	0	0.55	2.1	3.0	0	0.65	2.5	
	Chemical shift (p.p.m.) relative to C <sub>6</sub> H <sub>6</sub>							
2,6	-0.263 ±0.001	-0.2619 ±0.0001	-0.2571 ±0.0002	-0.2469 ±0.0001	-0.185 ±0.002	-0.1780 ±0.0004	-0.1723 ±0.0001	
3,5	-0.012 ±0.001	-0.0110 ±0.0002	-0.0018 ±0.0002	+0.0164 ±0.0002	+0.020 ±0.002	+0.0215 ±0.0005	+0.0302 ±0.0001	
4	-0.061 ±0.001	-0.0591 ±0.0003	-0.0477 ±0.0003	-0.0307 ±0.0003	-0.020 ±0.003	-0.0149 ±0.0007	+0.0105 ±0.0002	
MH <sub>3</sub>	+3.07 ±0.05	+3.06	+3.02	+2.93	+3.045 ±0.003	+3.030 ±0.001	+2.991 ±0.001	
	J (Hz)							
2,6	1.32 ±0.05	1.28 ±0.03	1.29 ±0.03	1.37 ±0.02	1.33 ±0.09	1.24 ±0.07	1.35 ±0.02	
3,5	1.35 ±0.04	1.33 ±0.03	1.39 ±0.02	1.32 ±0.02	1.36 ±0.07	1.41 ±0.07	1.36 ±0.01	
2,3;5,6	7.28 ±0.06	7.23 ±0.03	7.34 ±0.03	7.27 ±0.02	7.41 ±0.09	7.32 ±0.08	7.45 ±0.02	
2,4;4,6	1.43 ±0.04	1.47 ±0.03	1.39 ±0.03	1.44 ±0.02	1.41 ±0.09	1.50 ±0.08	1.38 ±0.02	
3,4;4,5	7.62 ±0.04	7.58 ±0.04	7.63 ±0.02	7.66 ±0.02	7.66 ±0.08	7.72 ±0.10	7.66 ±0.02	
2,5;3,6	0.64 ±0.02	0.64 ±0.02	0.64 ±0.02	0.64 ±0.02	0.64 ±0.07	0.64 ±0.07	0.64 ±0.02	
R.m.s. error	-	0.088	0.086	0.081	-	0.157	0.052	

$E$  = the electric field at H

$E_z$  = the component of the electric field along the X - H bond

for a monosubstituted benzene with dipole moment  $\mu$  cm.esu.

$$\text{ortho } E_z = 8.74 \times 10^{22} \mu \quad E^2 = 82.8 \times 10^{44} \mu^2$$

$$\text{meta } E_z = 2.32 \times 10^{22} \mu \quad E^2 = 5.88 \times 10^{44} \mu^2$$

$$\text{para } E_z = 1.75 \times 10^{22} \mu \quad E^2 = 3.07 \times 10^{44} \mu^2$$

The dipole moments of phenyl silane and phenyl germane are  $0.88 \times 10^{-18}$  cm.esu. and  $0.68 \times 10^{-18}$  cm.esu. and are positive as defined by Buckingham for the above formula (see page 29). The chemical shifts caused by these dipoles were calculated to be:

phenyl silane	ortho	-0.16 ppm	meta	-0.04 ppm	para	-0.03 ppm
phenyl germane	ortho	-0.12 ppm	meta	-0.03 ppm	para	-0.02 ppm

The presence of a dipole moment also causes a shift due to the electric field induced in the solvent. Buckingham developed the theory which has been experimentally verified (55). The magnitude of the induced field was estimated using Onsager's model of a point dipole at the centre of a sphere:

$$E = \frac{\epsilon - 1}{2\epsilon + 2.5} \cdot \frac{\mu}{\alpha}$$

where  $\alpha$  = polarizability of a sphere of molecular diameter.

Then  $E_z = E \cos \theta$  where  $\theta$  = angle of X - H bond to the dipole. Using a value of  $\mu/\alpha = 0.9 \times 10^5$  the chemical shifts due to the reaction field were estimated to be:

ortho	+0.01(5) ppm	meta	-0.01(5) ppm	para	-0.03 ppm
-------	--------------	------	--------------	------	-----------

The remaining effect to be considered is the magnetic anisotropy of the  $\text{MH}_3$  substituent. The magnitude of this effect is given by (77)

$$\sigma = \frac{(\chi_{\parallel} - \chi_{\perp})}{3R^3} \cdot (1 - 3\cos^2\theta)$$

where R = distance of resonant nucleus from anisotropic bond;

$\theta$  = angle between the bond axis and the nucleus.

The effect varies as the inverse cube of the distance, thus contributions at the meta and para positions will be very small. The contribution at the ortho position is also expected to be small since  $\chi_{\parallel} - \chi_{\perp}$  will be small and will be negative by analogy with the  $\beta$  protons of ethyl iodide (77).

The above discussion indicates that the effect of the permanent dipole moment on the chemical shifts is the same order of magnitude as the observed shifts. Thus we can conclude that perturbations of the aromatic  $\pi$  system by multiple bonding are very small in phenyl silane and phenyl germane. Certainly the most generous estimation of the electron shift is an order of magnitude less than that required to cause the observed change in acidity of the aryl germanes (page 7). Recently the spectral parameters of some  $\text{RMX}_3$  compounds (where R = phenyl 2,5 D<sub>2</sub>; M = C, Si, Ge, Sn and Pb and X = Cl or C<sub>2</sub>H<sub>5</sub>) were reported (78). Table 9 summarizes some of the relevant data.

TABLE 9

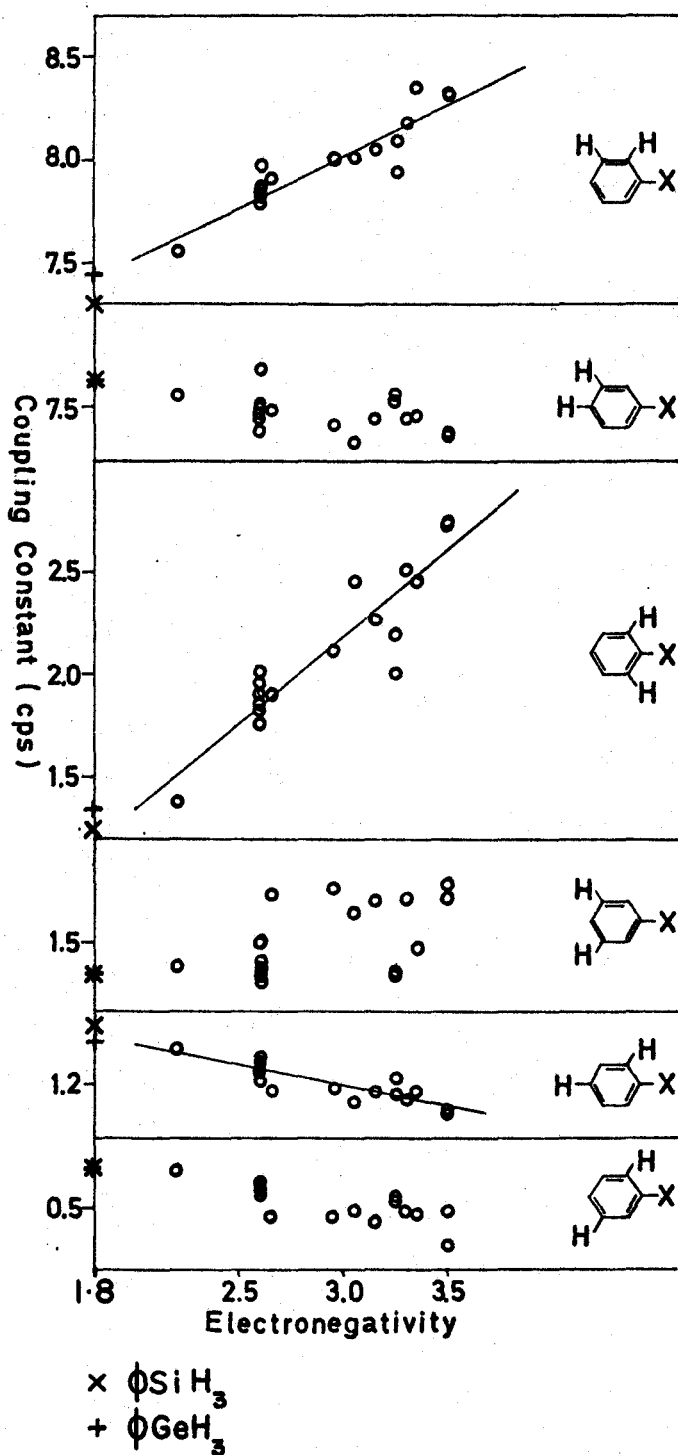
Compound	Chemical shifts (ppm downfield from TMS)		
	ortho	meta	para
C <sub>6</sub> H <sub>6</sub> (a)		7.26	
C <sub>6</sub> H <sub>5</sub> ·CH <sub>3</sub> (a)	7.10	7.14	7.09
C <sub>6</sub> H <sub>5</sub> ·C(CH <sub>3</sub> ) <sub>3</sub> (a)	7.27	7.17	7.03
C <sub>6</sub> H <sub>5</sub> ·Si(C <sub>2</sub> H <sub>5</sub> ) <sub>3</sub> (b)	7.48	7.31	7.22
C <sub>6</sub> H <sub>5</sub> ·Ge(C <sub>2</sub> H <sub>5</sub> ) <sub>3</sub> (b)	7.34	7.20	7.20
C <sub>6</sub> H <sub>5</sub> ·CCl <sub>3</sub> (b)	7.87	7.30	7.31
C <sub>6</sub> H <sub>5</sub> ·SiCl <sub>3</sub> (b)	7.73	7.44	7.37
C <sub>6</sub> H <sub>5</sub> ·GeCl <sub>3</sub> (b)	7.67	7.56	7.46

Spectra recorded in 25% w/w solution in CCl<sub>4</sub>. (a) Ref. (79). (b) Ref. (78).

The presence of the alkyl groups as opposed to hydrogens upon the M atom causes significant changes in the chemical shifts of the ring protons. This shift is explained in part by the difference in dipole moment of the compounds. Trimethylsilyl benzene has a dipole moment of 0.42 D but in the opposite direction to that of phenyl silane (87). Whitesides et al. chose to compare the chemical shifts of the silicon and germanium compounds with the analogous carbon compound and made no attempt to correct for dipole moment, anisotropy or solvent effects. On these grounds the alkyl derivatives of Si, Ge, Sn and Pb were considered to exhibit weak (p-d) $\pi$  bonding, Si > Ge  $\approx$  Sn > Pb. The pit-falls of this approach are shown when considering the chloro compounds. Here the dipole moments are nearly an order of magnitude greater, and the magnetic anisotropy of the substituent is greater, than for the corresponding alkyl compounds. It was concluded that the order of  $\pi$  bonding effectiveness was C < Si < Ge < Sn, a result contrary to previous conclusions (17 and references therein). Although the theory for changes in chemical shift due to dipole moments is admitted to be approximate (68) it has been applied to  $\phi\text{CCl}_3$ ,  $\mu = 2.14$  D (60) and  $\phi\text{GeCl}_3$ ,  $\mu = 3.15$  D (17) and the corrected chemical shifts are:

	ortho	meta	para
$\phi\text{CCl}_3$	7.54 ppm	7.20 ppm	7.15 ppm
$\phi\text{GeCl}_3$	7.12 ppm	7.20 ppm	7.06 ppm

The corrections to the chemical shifts are slightly greater than the observed shifts of the compounds relative to benzene for the meta and para protons. Thus the results in reference (78) do, in fact, support the conclusion that the chemical shifts of phenyl silane and phenyl germane arise mainly from the dipole moment of the molecule rather than



All other points from reference (29).

Figure 11. The Correlation of Ring Coupling Constants of Monosubstituted Benzenes with Electronegativity of Substituent.

from perturbations of the  $\pi$  system by (p-d) $\pi$  bonding. The discussion above clearly underlines the need for extreme care when interpreting small changes in chemical shift.

#### Coupling constants of phenyl silane and phenyl germane

The coupling constants of many monosubstituted benzenes have now been accurately measured (29,80) and a strong correlation between the magnitude of the coupling constants and the electronegativity of the substituent has been established, Figure 11. The coupling constants within the phenyl groups of phenyl silane and phenyl germane obtained in this work are constant, within experimental error, over the concentration range studied and thus can be compared with the values in Figure 11 which were obtained from neat liquid spectra. As can be seen, phenyl silane and phenyl germane agree well with the previous results if an electronegativity of 1.8 is assumed for both substituents (26). As the electronegativity of the substituent decreases, the values of the coupling constants tend to the values of pyridene (80). This is reasonable as pyridene is isoelectronic with the phenyl anion. The coupling constants of the phenyl germyl anion could not be measured with sufficient accuracy to predict an effective electronegativity for the  $\text{GeH}_2^-$  group.

#### The NMR Spectrum of the Phenyl germyl anion

The spectrum of a solution of the sodium salt of phenyl germane in liquid ammonia is shown in Figure 12 together with the computed spectrum. The spectrum of the triphenyl germyl anion has been observed previously (11) and is very similar. The two multiplets of relative areas 2:3 of the triphenyl anion had been assigned to the meta and (ortho + para) protons respectively. Attempts to analyse the sodium phenyl germyl

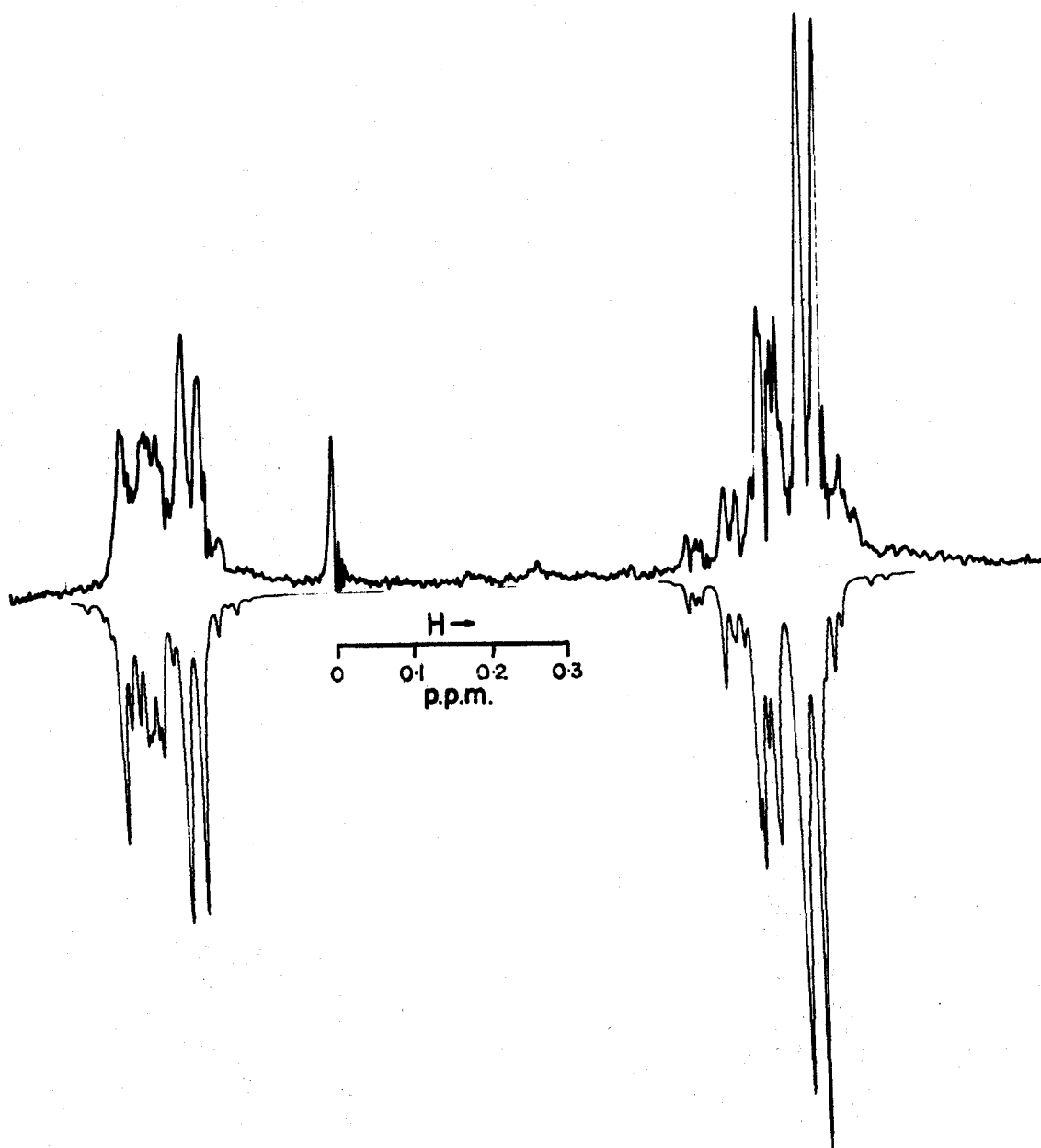


Figure 12. The Experimental and Calculated 100 M Hz NMR Spectrum of Sodium Phenyl Germyl in Liquid Ammonia. Peak at 0 ppm is Benzene.

spectrum using this assignment failed, and only when the low field multiplet was assigned to the ortho protons and the high field multiplet to the (meta + para) protons could the analysis be completed. Spectra were recorded for solutions in the concentration range 0.1 - 1.0 M and while the more dilute spectra could not be analysed due to the low signal-to-noise ratio, direct superposition of the spectra indicated that the positions of the resonances changed by less than 1 Hz relative to an internal benzene reference. This was taken as evidence that the sodium phenyl germyl was fully ionized in the solutions examined. The spectral lines were somewhat broader (ca. 0.5 Hz) than the lines observed for phenyl silane and phenyl germane which may have been due to the presence of a small quantity of white solid in the samples. Since germanium imide is produced during the reaction of potassium amide with germane in liquid ammonia (9), the white material observed here is presumably similar. The quantity of this white material could be greatly reduced by vigorous shaking of the NMR tube as it warmed up thus preventing any local excess of one reactant over the other. In spite of the broader lines an unambiguous assignment and an almost complete analysis of the spectrum was possible. The parameters obtained are listed in Table 10.

The negative charge was expected to be delocalized into the aromatic ring and to reside largely at the ortho and para positions. This would shift these resonances to higher field as was found for benzyl lithium in tetrahydrofuran solution (Table 10) (75). Large shifts to higher field have been noted in other anionic systems where the possibility of conjugation of the aromatic system with the negative charge exists (34,73,75). The chemical shifts of the aromatic protons of phenyl germyl anion are

TABLE 10

<sup>1</sup>H NMR data for sodium phenylgermyl and benzyl-  
lithium solutions

	$\phi$ GeH <sub>2</sub> Na Liquid NH <sub>3</sub> solution	$\phi$ CH <sub>2</sub> Li <sup>†</sup> THF solution
	$\delta$ (p.p.m.) relative to C <sub>6</sub> H <sub>6</sub>	
2,6	-0.203 ±0.005	+1.19
3,5	+0.528 ±0.005	+0.98
4	+0.576 ±0.005	+1.78
MH	4.010 ±0.005	-
	J (Hz)	
2,6	1.20*	
3,5	1.20*	
2,3;5,6	7.40 ±0.10	8.0
2,4;4,6	1.42 ±0.10	
3,4;4,5	6.89 ±0.09	6.2
2,5;3,6	0.60*	
R.m.s. error	0.369	

\*Assigned not calculated values.    †Data from reference (75).

ortho  $-0.203$  ppm; meta  $+0.528$  ppm and para  $+0.576$  ppm relative to benzene. Clearly there is little delocalization of the negative charge into the ring. If it were assumed that the negative charge was entirely resident upon the germanium atom, this would strongly polarize the electrons of the aromatic ring, producing the upfield shift of the meta and para protons by increasing the electron density at these sites and deshielding the ortho protons by reducing the electron density. In addition the considerable electric field around the negative charge would help deshield the ortho protons. That the germanium atom does carry a large negative charge is confirmed by the upfield shift of the Ge-H resonance by  $0.8$  ppm, Table 4, compared to the unionized compound. The change in chemical shift on ionization of  $\text{CH}_3\cdot\text{GeH}_3$  to  $\text{CH}_3\cdot\text{GeH}_2^-$  is  $1.03$  ppm (11) where there is no possibility of charge delocalization and here the charge must reside entirely on the Ge atom.

Additional evidence for the lack of charge delocalization in aryl germane anions is given by the anion of bis diphenylene germane. The spectrum of this compound shows only two multiplets in the aromatic region separated by  $\sim 0.6$  ppm, page 17, a completely different spectrum to the formally analogous fluorenyl anion (page 62) which is known to be highly delocalized (40,73).

#### The proton NMR spectrum of the silyl ion ( $\text{SiH}_3^-$ )

The NMR spectrum of an approximately  $1$  M solution of potassium silyl shows, in addition to the intense absorptions of the solvent, the associated spinning sidebands and  $^{13}\text{C}$  satellites, a single sharp peak with two satellite peaks. These resonances are assigned to the silyl ion, the satellites arising from coupling to the  $4.7\%$  abundant  $^{29}\text{Si}$  isotope which

has  $I = \frac{1}{2}$ . Observation of these singlet satellite resonances confirms that the central resonance is due to protons bonded to silicon. The values of the chemical shift reported in Table 11 are close to that measured for the germyl ion (Table 6) after correction for bulk susceptibility of the solvents.

TABLE 11

## NMR Parameters of Potassium Silyl (1 Molar Solutions)

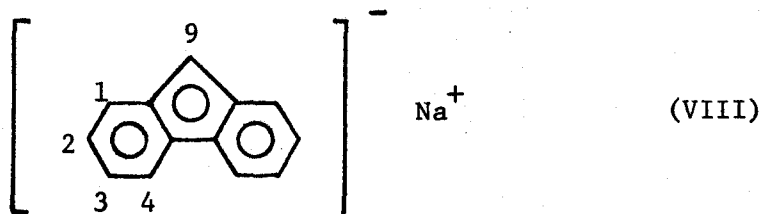
Solvent	$\delta$ relative to solvent	$\delta$ relative to 'internal' TMS	$J(^{29}\text{Si-H})$
Dimethoxyethane	+2.02 ppm from $\text{CH}_3$	-1.09 ppm	77 Hz
HMPA	+1.26 ppm	-1.19 ppm	73 Hz

The value of the coupling constant is considerably smaller than previously measured coupling constants between directly bonded silicon and hydrogen nuclei; the smallest previous measurement being 183 Hz for the compound  $\text{C}_6\text{H}_5\text{Si}(\text{H})(\text{CH}_3)_2$  (81). The approximate bond angle of the silyl ion can be calculated from the coupling constant as shown in Appendix 2. The value calculated for the H-Si-H bond angle is  $96^\circ$ . The accuracy of this figure may be judged by considering the value calculated for the isoelectronic molecule phosphine ( $\text{PH}_3$ ). The  $^{31}\text{P-H}$  coupling constants of  $\text{PH}_4^+$  and  $\text{PH}_3$  are 547 and 184 respectively (82,83) which predicts a bond angle of  $95^\circ$  for phosphine, compared to  $93^\circ$  measured by spectroscopic methods.

The NMR Spectrum of the Fluorenyl Anion (VIII)

The spectrum of the sodium salt of fluorene (VIII) in dilute solution in THF has been previously observed (73) but only chemical shifts from a first order treatment were reported and there was ambiguity in assignment

of the resonances. Detailed knowledge of the parameters of this system was of interest as the analogous compound, bis diphenylene germane (VII), was being prepared. Good spectra of the fluorenyl anion were obtained while using the hydrocarbon for acidity measurements. A more complete analysis of the NMR spectrum was therefore carried out and the data presented below.



The spectrum of an approximately 0.5 M solution of sodium fluorenyl in liquid ammonia, recorded at 100 MHz, is shown in Figure 13. The relative areas of the multiplets at 7.3, 6.7, 6.2, 5.8 and 5.4 ppm downfield from ammonia are 2:2:2:2:1 with the high field peak obviously assigned to the 9 proton. The spectrum is approximately first order, thus the doublet structures are due to protons 1 and 4 split by protons 2 and 3 respectively and the triplet-type peaks are due to protons 2 and 3 split by 1+3 and 2+4 respectively. To aid the assignment spin-tickling experiments were performed. Double irradiation of the multiplet at -7.3 ppm caused collapse of the structure at -5.8 ppm. Double irradiation of the resonance at -6.7 ppm caused collapse of the structure at -6.2 ppm. Two assignments are consistent with the above observations, namely H(1), H(4), H(3), H(2), H(9) or H(4), H(1), H(2), H(3), H(9) on going from low to high field. The usual procedure to distinguish between such assignments is to consider the magnitudes of the coupling constants and the intensities of

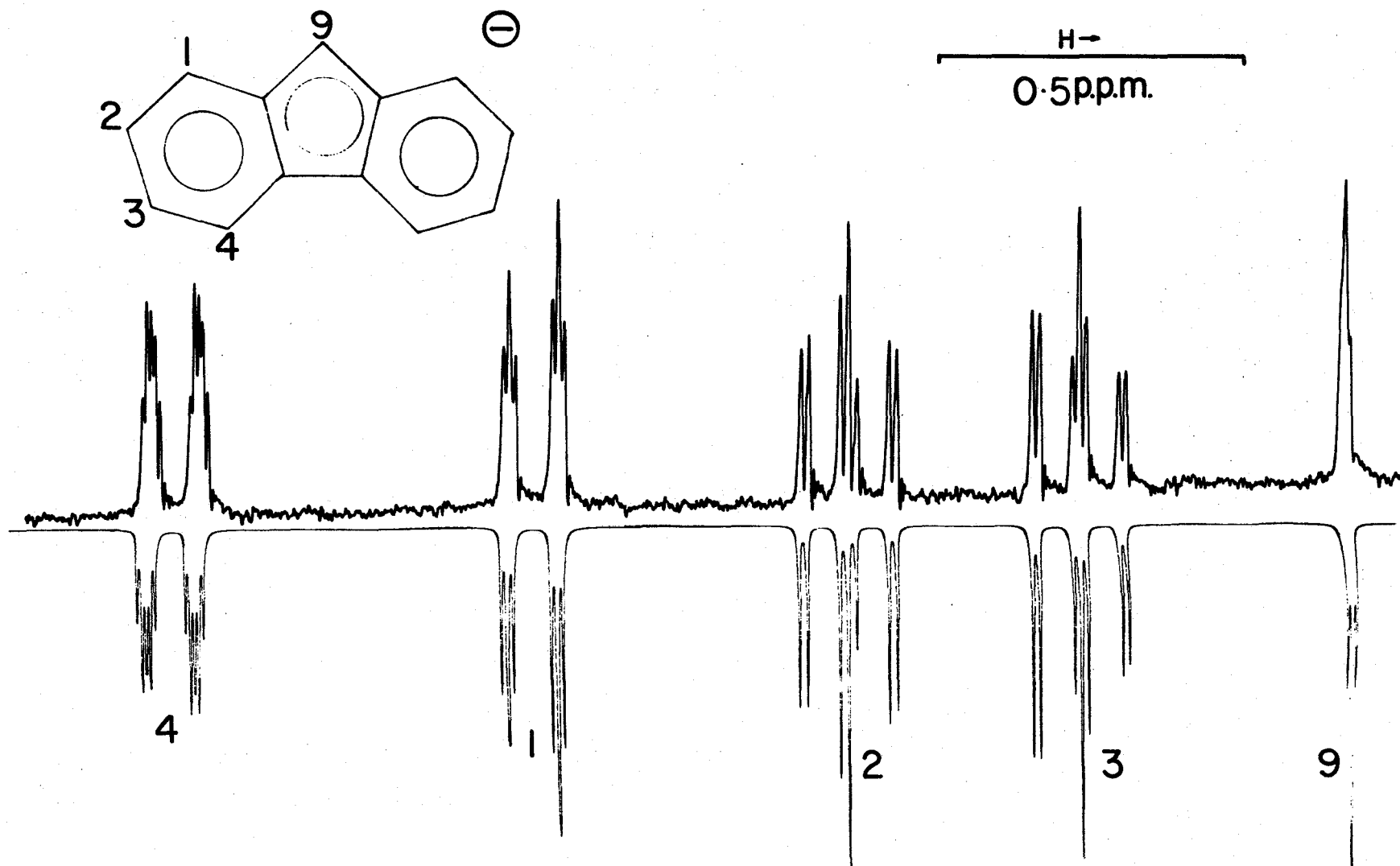


Figure 13. The Experimental and Calculated 100 M Hz NMR Spectrum of Sodium Fluorenyl in Ammonia.

the transitions of the second-order spectrum. Unfortunately the aromatic protons in this molecule are nearly symmetric in arrangement and it is not possible to distinguish the assignments by this technique. Therefore the spectrum of the 2-methyl fluorenyl anion was examined. This spectrum was very similar to the fluorenyl anion spectrum except for the presence of the 2-methyl resonance at -1.77 ppm from ammonia and the areas of the aromatic proton multiplets were now in the ratio 2:2:1:2:1. Thus the correct assignment is as shown in Figure 13 and in Table 12, confirming the original assignment which had been suggested on the basis of electron density calculations.

TABLE 12

Nucleus	Chemical Shift (ppm) (a)	Coupling Constants (Hz) (b)			
		2	3	4	9
1	-6.707	8.06	0.99	0.83	0
2	-6.185		6.63	1.28	0
3	-5.803			7.82	0
4	-7.301				0.7
9	-5.360				

(a) Relative to  $\text{NH}_3$ , accurate to  $\pm 0.005$  ppm. Benzene = -6.99 ppm relative to  $\text{NH}_3$ .

(b) Probable errors are  $\pm 0.03$  Hz.

R.M.S. of fit = 0.107; 64 lines assigned.

#### Variation of Coupling Constants with Temperature

##### Ammonia and phosphine

The variation of coupling constant with temperature has already been noted for  $\text{BF}_3$  (84) and two possible explanations were suggested for this

unusual observation. Intermolecular association must be important in neat liquid  $\text{BF}_3$  and the observed variation may be due to changes in the state of aggregation in the liquid. However a more interesting possibility is that thermal excitation of the molecule to a vibrationally excited state may change the coupling constant by vibronic interaction. Dr. J. Bacon of this department is currently conducting a theoretical investigation of this problem by calculation of coupling constants as averaged over molecular vibrations. Since both the NMR and vibrational spectra of ammonia and phosphine have been studied here, the temperature dependence of the spin-spin coupling in these molecules was investigated. Both nitrogen and phosphorous have a spin  $I = \frac{1}{2}$  nucleus so that problems associated with quadrupole relaxation phenomena do not arise. The major difficulty associated with these molecules is the relatively high energy of the lowest vibrationally excited state, namely  $950 \text{ cm}^{-1}$  for  $\text{NH}_3$  and  $991 \text{ cm}^{-1}$  for  $\text{PH}_3$  (85), making measurements at high temperatures necessary. The initial measurements were made on gas-phase samples in order to eliminate intermolecular effects and to allow fullest use of the range of temperatures available in the NMR spectrometer, i.e., up to  $160^\circ\text{C}$ .

$^{15}\text{N}$  ammonia gave a reasonably sharp doublet signal from the gaseous sample and at  $35^\circ\text{C}$  the coupling constant was found to be 61.0 Hz with  $\sigma = 0.25$  Hz. This value did not change significantly on heating to  $143^\circ\text{C}$ . The value reported for liquid ammonia is 61 Hz (62) so that it would appear that the coupling constant of ammonia does not change either with temperature or intermolecular association.

A gaseous sample of phosphine gave a very broad doublet signal with  $J(\text{P-H}) \approx 160$  Hz. The broadness of the peaks and the small value of  $J(\text{P-H})$

suggest that the proton and phosphorous nuclei respectively are relaxing at an intermediate rate on the NMR time scale. It was therefore necessary to use a solution of phosphine to overcome this problem by slowing the rate of nuclear relaxation. Tetradecane ( $C_{14}H_{30}$ ) was chosen because of its high-boiling point and because it was likely to behave as a non-interacting solvent. The results are presented in Table 13 along with some previously reported measurements at low temperature in cyclopentane solution (83).

TABLE 13

	J(P-H) Hz	$\sigma$ Hz	Temperature °K	$\chi_1$
(a)	183.4	0.2	251.2	0.0035
(a)	183.3	0.4	273.2	0.0055
(a)	183.0	0.3	294.2	0.0078
	182.94	0.05	308.2	0.0098
	182.54	0.05	353.2	0.0177
	182.11	0.36	385.7	0.0248
	181.86	0.24	419.2	0.0333
	181.38	0.37	437.2	0.0383

(a) Taken from reference (83).

As can be seen there is a significant variation of the coupling constant with temperature and as with  $BF_3$  the value becomes numerically smaller as the temperature increases. If this variation is caused by the thermal excitation of molecules to a state where the coupling constant is different from the ground state, the magnitude of the excited state coupling constant can be calculated from the data in Table 13. Of the

four fundamental vibrations of phosphine, Figure 15, only  $\nu_2$  and  $\nu_4$  are of sufficiently low energy to be thermally excited at the temperatures used here. Preliminary calculations using the Pople and Santry theory (86) showed that distortions of a phosphine molecule by the  $\nu_4$  vibration did not change the coupling constant significantly but the  $\nu_2$  vibrational distortions caused a considerable variation. Accordingly it was assumed that

$$\begin{aligned} J(\text{P-H})_{\text{observed}} &= (1 - \chi_1)J_0 + \chi_1J_1 \\ &= J_0 + \chi_1(J_1 - J_0) \end{aligned}$$

where  $\chi_1$  = fraction of molecules with  $\nu_2$  in first excited state;

$J_0$  = ground state coupling constant;

$J_1$  = coupling constant with  $\nu_2$  in first excited state.

Using the Boltzmann equation,

$$\chi_1 = \exp\left(-\frac{\Delta E}{kT}\right) \quad \text{where } \Delta E = 991 \text{ cm}^{-1}.$$

Thus a plot of  $J(\text{P-H})$  observed against  $\chi_1$  should give a straight line of gradient  $(J_1 - J_0)$  and intercept  $J_0$ . Such a straight line was fitted by a weighted least sum of squares method and is shown in Figure 14 .

The values of  $J_0$  and  $J_1$  were estimated to be

$$J_0 = 183.43 \text{ Hz} \quad J_1 = 133 \text{ Hz}.$$

Although ammonia unlike phosphine does not apparently show a variation of coupling constant with temperature it should be noted that the magnetogyric ratio ( $\gamma$ ) of  $^{31}\text{P}$  is four times greater than  $^{15}\text{N}$ . Thus similar electronic perturbations on each molecule, giving similar changes in the reduced coupling constant  $K(\text{AB})$  (86) will show four times the effect for the phosphorous compound since:

$$J(\text{AB}) = \gamma_A \gamma_B \cdot \frac{h}{4\pi^2} \cdot K(\text{AB}) \text{ Hz}.$$

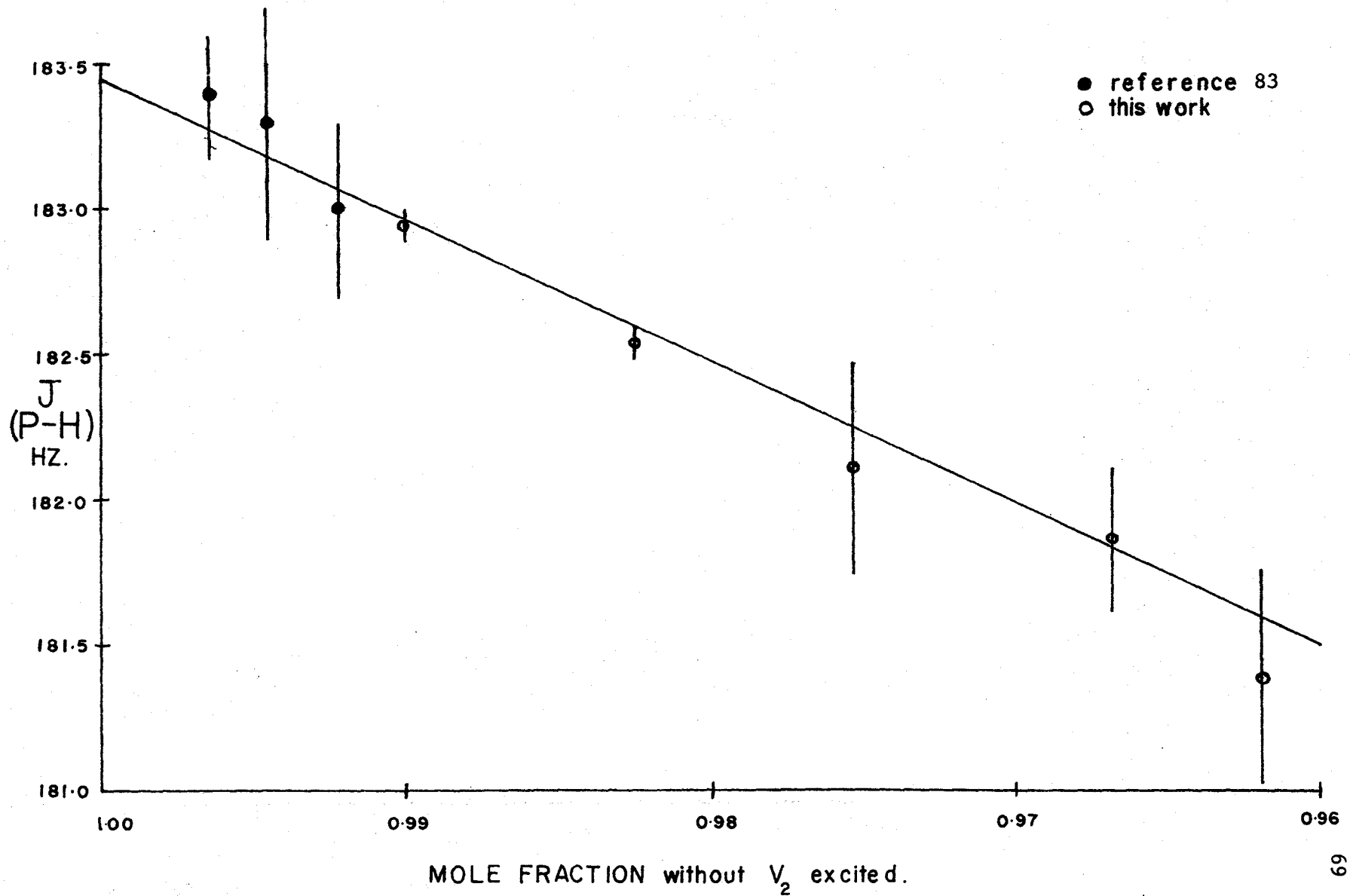


Figure 14. The Correlation of  $J(P-H)$  in Phosphine with the Fraction of Vibrationally Excited Molecules.

## CHAPTER 5

### Vibrational Spectra

#### Vibrational Spectra of Pyramidal $MH_3$ Molecules

A non-linear molecule with  $n$  atoms has  $(3n - 6)$  vibrations associated with it and these vibrations must belong to the symmetry types of the point group of the molecule. Pyramidal molecules of formula  $MH_3$  belong to the  $C_{3v}$  point group which has symmetry types  $A_1 + A_2 + E$  (85). The types of the vibrations for the  $C_{3v}$  group are obtained by dividing the atoms of the molecule into groups in the following manner. Let  $m_o$  = the number of atoms on all elements of symmetry;  $m_v$  = the number of sets of atoms on a plane of reflection but not on the principal axis, and  $m$  = the number of atoms on no element of symmetry.

$$\begin{aligned} \text{Then number of atoms in the molecule} &= 6m + 3m_v + m_o \\ \text{number of } A_1 \text{ vibrations} &= 3m + 2m_v + m_o - 1 \\ \text{number of } A_2 \text{ vibrations} &= 3m + m_v - 1 \\ \text{number of } E \text{ vibrations} &= 6m + 3m_v + m_o - 2 \end{aligned}$$

For a pyramidal  $MH_3$  molecule  $m_o = 1$ ,  $m_v = 1$  and  $m = 0$ . Therefore  $MH_3$  has four fundamental vibrations, two fully symmetric  $A_1$  and two doubly degenerate  $E$ , making up the total of  $(3n - 6)$  vibrations for the molecule. The six vibrations described in terms of symmetry coordinates are shown in Figure 15. If a simple valence force field is assumed and the mechanics of the situation are solved as described in detail in reference (85) then the following equations are found for the fundamental frequencies of vibration.

$$4\pi^2(v_1^2 + v_2^2) = \left(1 + \frac{3H}{M} \cos^2\beta\right) \frac{k}{H} + \left(1 + \frac{3H}{M} \sin^2\beta\right) \frac{12 \cos^2\beta}{(1+3 \cos^2\beta)} \frac{k_d}{\ell^2 H}$$

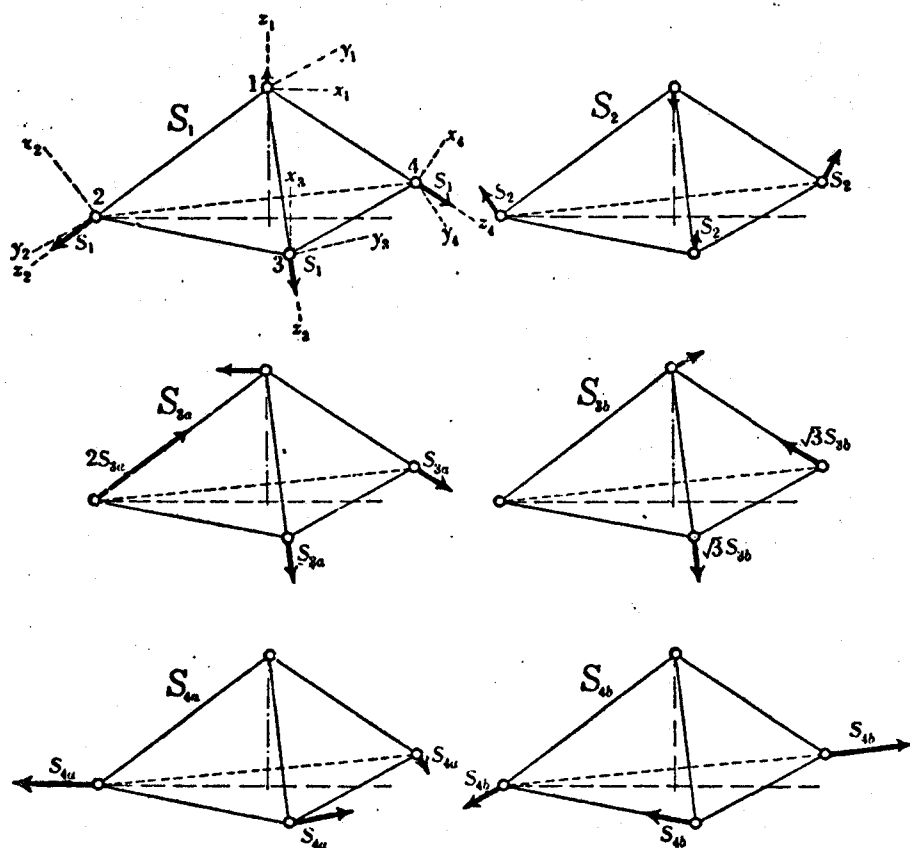


Figure 15. The Symmetry Coordinates of a Pyramidal  $MH_3$  Molecule.

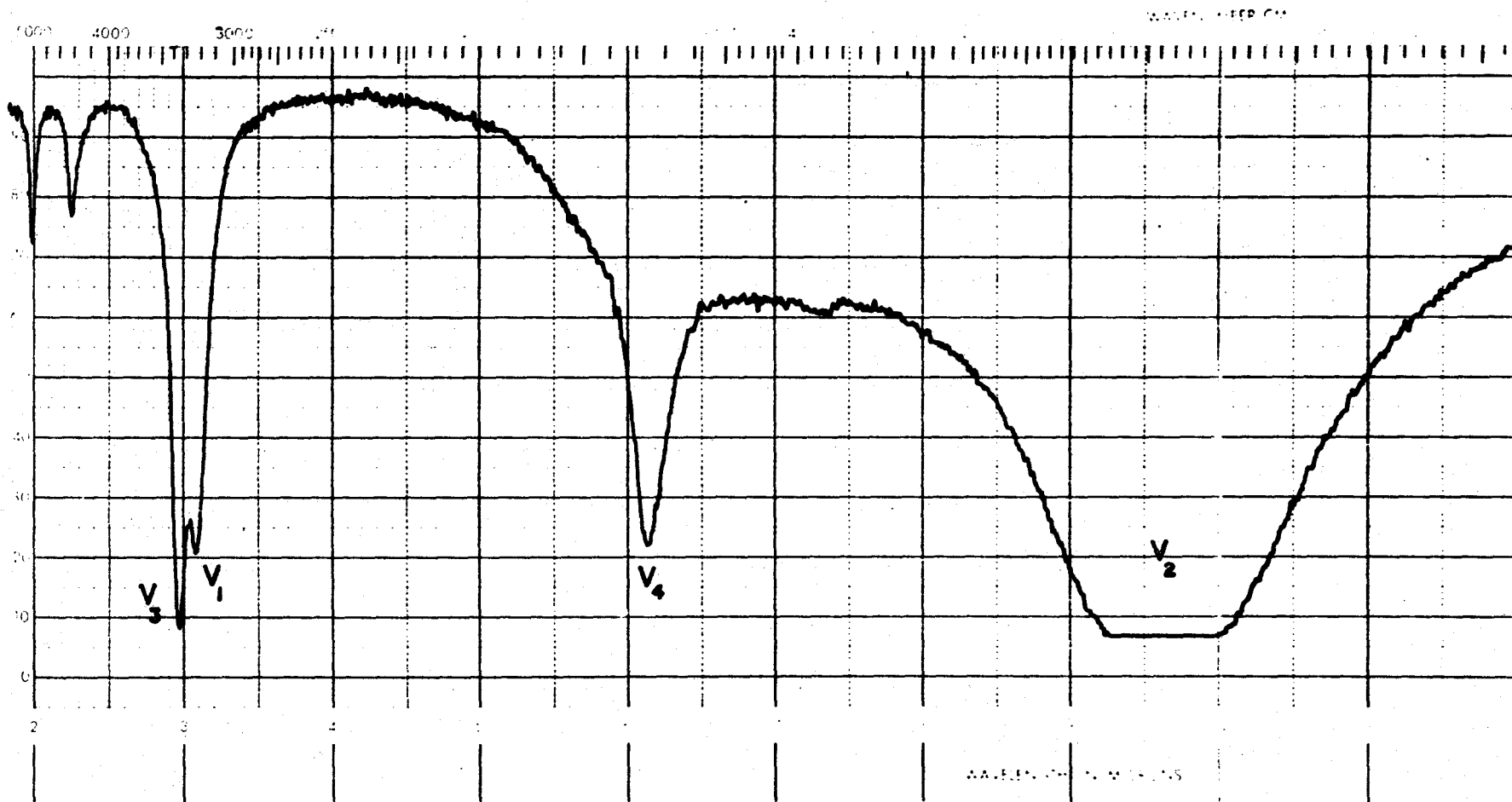


Figure 16. The Infrared Spectrum of Liquid Ammonia Showing the Four Fundamentals and the Two Combination Bands  $\nu_3 + \nu_2$  and  $\nu_3 + \nu_4$ .

$$16\pi^4 v_1^2 v_2^2 = \frac{12 \cos^2 \beta}{(1+3 \cos^2 \beta)} \left(\frac{3H}{M} + 1\right) \frac{k}{H^2} \cdot \frac{k_d}{\ell^2} \quad [9]$$

$$4\pi^2 (v_3^2 + v_4^2) = \left(1 + \frac{3H}{2M} \sin^2 \beta\right) \frac{k}{H} + 3\left(1 + \cos^2 \beta + \frac{3H \sin^4 \beta}{2M}\right) \frac{k_d}{(1+3 \cos^2 \beta) \cdot H \cdot \ell^2}$$

$$16\pi^4 v_3^2 v_4^2 = 3\left(1 + \cos^2 \beta + \frac{3H}{M} \sin^2 \beta\right) \frac{k}{(1+3 \cos^2 \beta) H^2} \frac{k_d}{\ell^2}$$

where  $v_i$  = frequency of  $i$ th vibration;

H = either the mass of a hydrogen or deuterium atom;

M = the mass of the central atom;

$\beta$  = the angle between the principal axis and a bond;

k = the stretching force constant; and

$k_o/\ell^2$  = the bending force constant.

These can be rearranged to give

$$\cos^2 \beta = 1/[4(v_3^2 v_4^2 / v_1^2 v_2^2) - (M-3H/M+3H)] \quad [10]$$

where the bond angle  $\alpha$  is related to  $\beta$  by  $\cos^2(\alpha/2) = \frac{1}{4}(1+3 \cos^2 \beta)$ .

If the fundamental frequencies can be obtained then an estimate of molecular geometry is possible. Unfortunately  $v_3$ , the antisymmetric stretch, is often of low intensity in both Raman and infrared experiments and is therefore difficult or impossible to observe. An estimate of the geometry can however still be obtained by assuming  $v_3/v_1 \approx 1$ . This assumption is not as drastic as it would appear and has been used previously for  $PD_3$  and  $AsD_3$  to give bond angles later found to agree to within  $3^\circ$  (91) and is experimentally verified for the symmetric and antisymmetric stretching vibrations of phenylgermane (92).

All four fundamentals are both infrared and Raman active since components

of the dipole moment vector and polarizability tensor have symmetry species corresponding to both  $A_1$  and E types. Moreover in the Raman spectrum it is expected that the two fully symmetric  $A_1$  vibrations will scatter polarized light, thus aiding assignment of vibrations.

### The Germyl Ion ( $\text{GeH}_3^-$ )

Because hydrides are generally weak Raman scatterers and very thin films were necessary for the IR experiments in order to overcome the very intense ammonia absorptions, it was necessary to use fairly concentrated solutions, i.e., around 1 M. Solutions of both Na and K salts in liquid ammonia were used and there was no change of frequency within experimental error. Only potassium germyl was used in dimethoxyethane since these solutions were easier to prepare with the more reactive potassium metal and are rather more stable than the solutions of the sodium salts, as is outlined in the section on polymeric germanium hydride.

### Raman Spectra

The Raman spectrum of a solution of potassium germyl in liquid ammonia is shown in Figure 17. The starred peak is a plasma line from the exciting laser radiation and the two broad low intensity peaks are due to the solvent ammonia. The two most prominent peaks are assigned to the germyl ion and are >95% polarized, indicating they are due to  $A_1$  type fully symmetric vibrations and accordingly are assigned as  $\nu_1$  and  $\nu_2$ , the symmetric stretching and bending modes. The polarization measurements eliminate the alternative planar  $D_{3h}$  structure for the germyl ion as this would give only one polarized band, having vibrations of types  $A_1' + A_2'' + 2E'$  (85). Despite careful observation it was not possible to detect the two antisymmetric

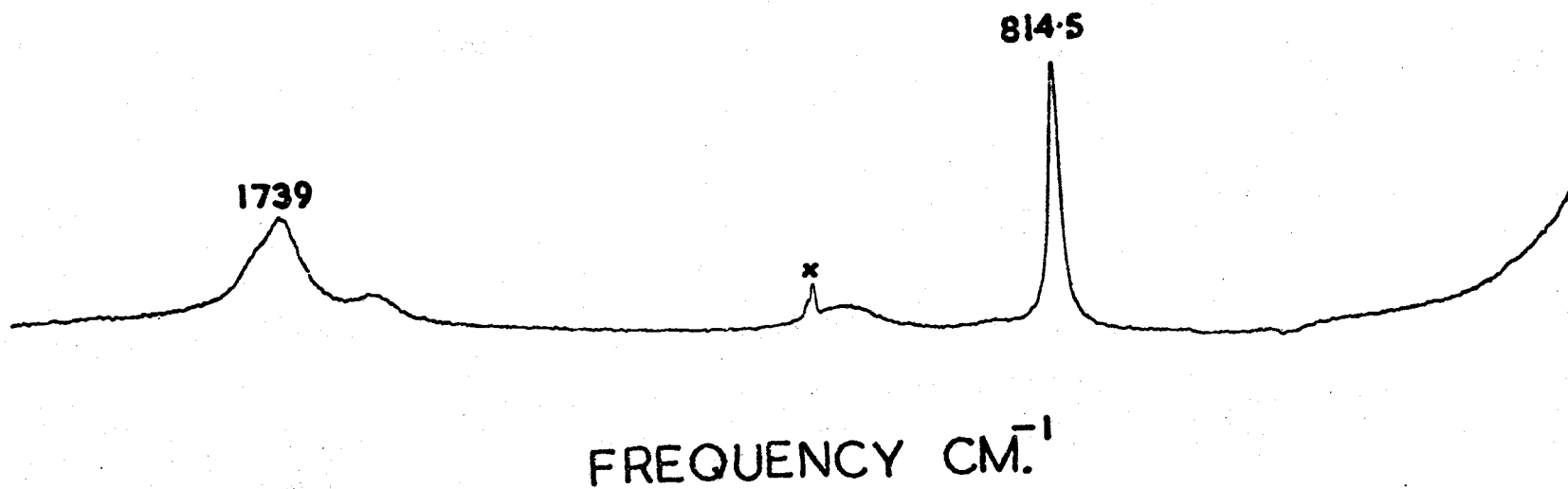


Figure 17. The Raman Spectrum of Potassium Germyl in Liquid Ammonia. The starred peak is a plasma line from the laser radiation. The unmarked peaks are due to the solvent.

vibrations of the germyl ion, but Herzberg (85) notes that antisymmetric vibrations frequently give weak Raman scattering.

To help confirm the assignment, the deuteriated analogue was prepared in liquid  $\text{ND}_3$  solution. Spectra were also recorded of potassium germyl and potassium germyl- $\text{D}_3$  in dimethoxyethane solution. The data are summarized in Table 14.

The simple valence force field, from which the equations at the beginning of the chapter are derived, describes the molecule in terms of three parameters, a stretching force constant, a bending force constant and the angle between the  $\text{C}_3$  axis and the GeH bond. Since by isotopic substitution, four vibrational frequencies are known, the unknown parameters could, in principle, be found from this information. In practice, however, the errors in measurement and the assumptions of the force field are greater than the changes in  $\nu_1$  caused by varying the angle. Thus the geometry cannot be determined from the observed Raman frequencies alone but the assignment can be verified. Equation [9] page 73 can be rearranged to give:

$$\frac{12 \cos^2 \beta}{16\pi^4 (1 + 3 \cos^2 \beta)} \cdot k_1 \cdot \frac{k_d}{l^2} = \frac{\nu_1^2 \nu_2^2 H^2}{(1+3H/M)}$$

If the assignments are correct then the value given by the right-hand side of the above expression should be equal for the two isotopic species. For the ammonia solutions the ratio for hydride/deuteride = 1:0.924; for the dimethoxyethane solutions, 1:0.913. This is as good as the agreement for gaseous  $\text{NH}_3$  and  $\text{ND}_3$  using the same force field.

### Infrared Spectra

The infrared spectrum of sodium germyl in liquid ammonia is shown in

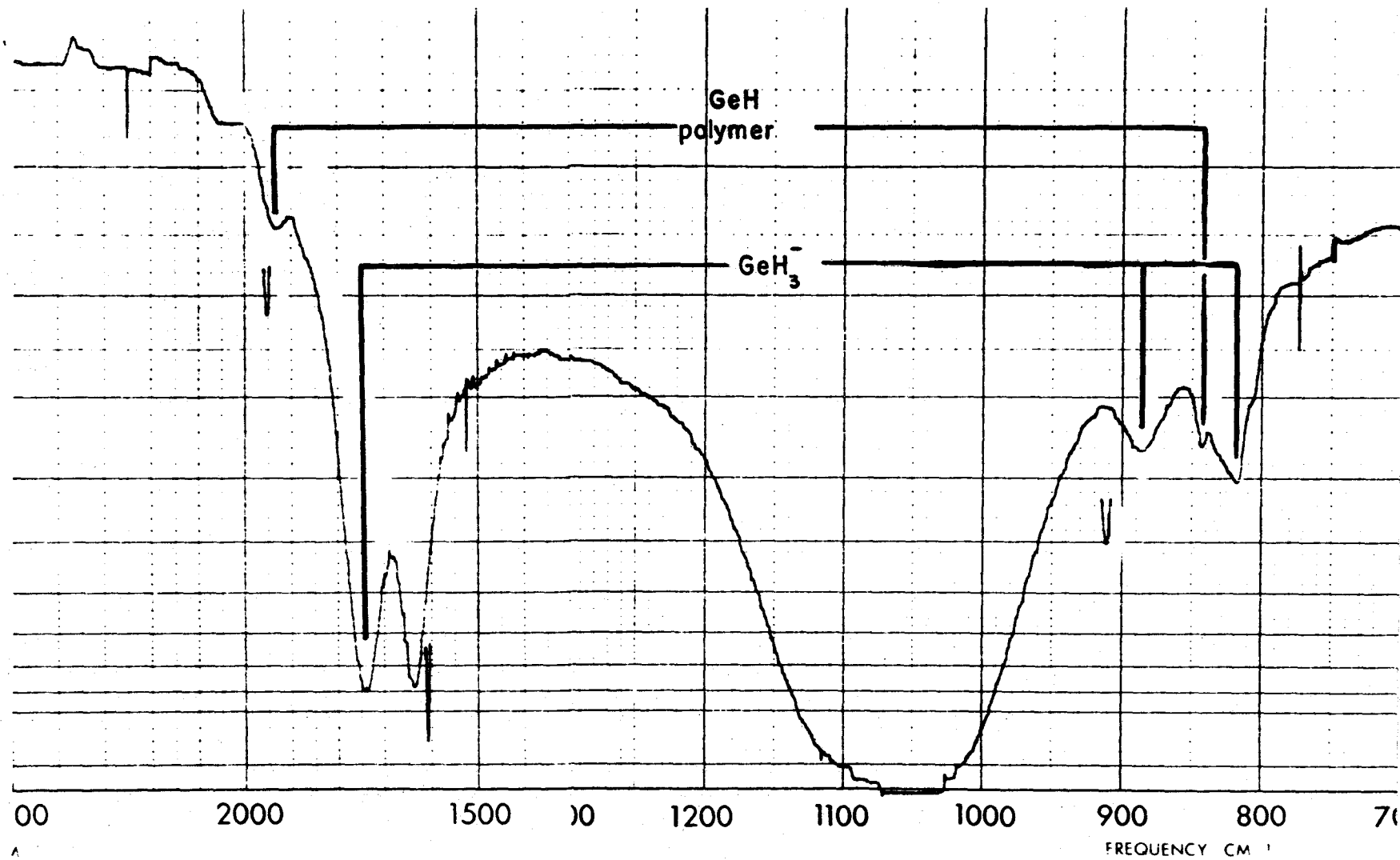


Figure 18. The Infrared Spectrum of Sodium Germyl in Liquid Ammonia Showing Impurity Peaks from Polymeric Hydrides.

Figure 18 . Of the three peaks assignable to the germyl ion, two have the same frequencies as observed in the Raman spectrum. The third peak is in the Ge-H bending region and is assigned to  $\nu_4$  the antisymmetric bend or 'scissors' vibration. The antisymmetric stretch  $\nu_3$  which is not observed is either very weak or just hidden under the very strong  $\nu_1$  band. Unfortunately in dimethoxyethane solution only the symmetric stretch could be observed as the solvent peaks obscured the bending modes; in the Raman experiment the interfering peaks were relatively weak and the position of the germyl resonance could be observed. For the deuterated compound only the bending region can be observed and the stretching region is obscured, Figure 19 . The observed frequencies are tabulated in Table 14 .

The procedure used to solve the equations given on page 70 to obtain the bond angle and force constants was as follows. The angle was estimated from equation [10], by assuming  $\nu_3/\nu_1 = 1$  (91) and then using a computer program (VAO4A (105)) to find the best values of the force constants determined by the least sum of squares method. This calculation was performed on each of the three complete sets of observations and the results are given in Table 14 . It would have been possible to use a more complex force field with extra force constants to give a better description of the vibrations but the simple model used gives quite a good description and the physical meaning of the force constants obtained is more readily appreciated (see page 93 ). The agreement between the sets of parameters obtained is a good check that it is indeed the pyramidal monomeric germyl ion which is being observed.

As indicated in the Introduction, the purpose of obtaining the

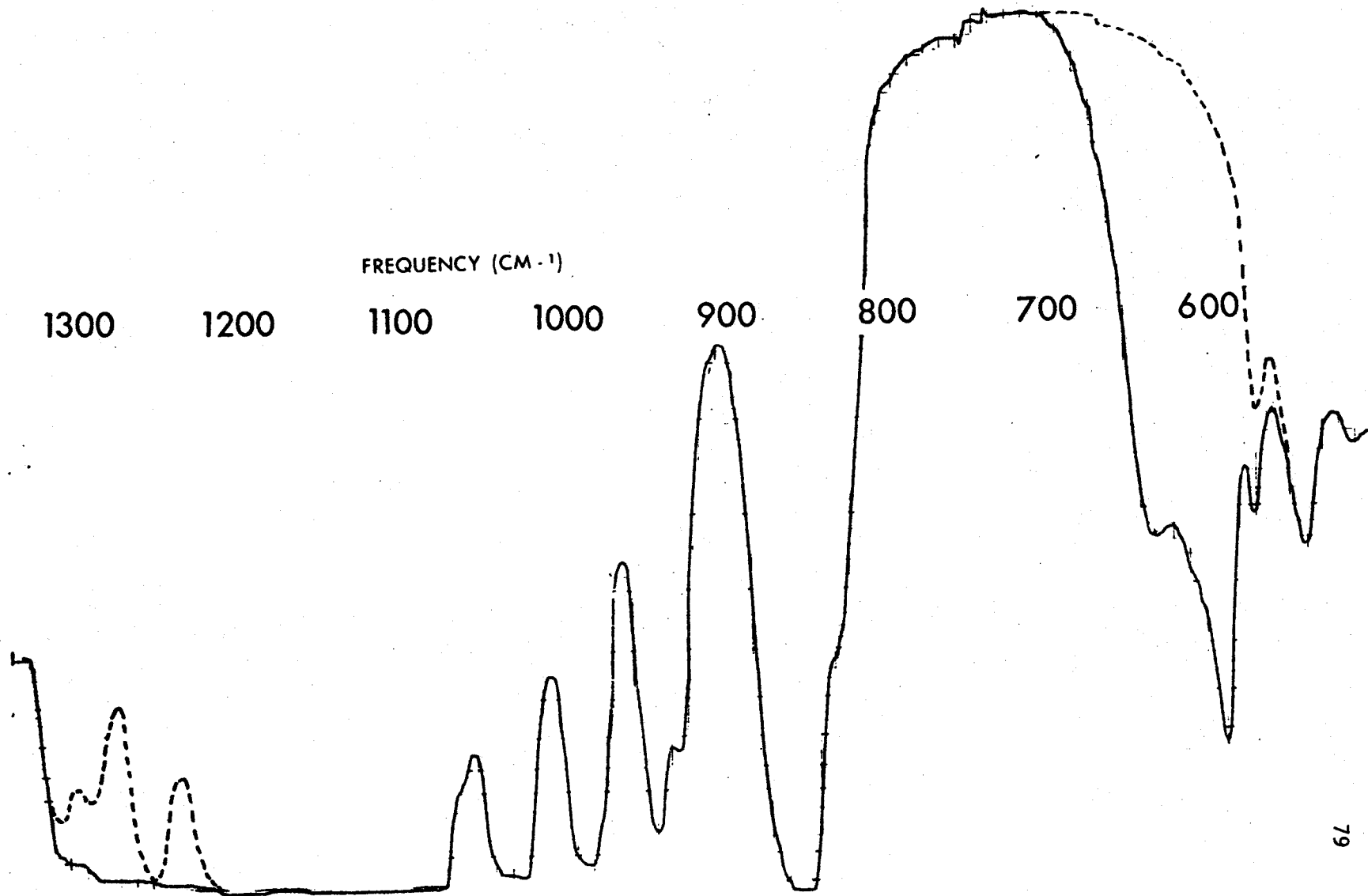


Figure 19. The Infrared Spectrum of Potassium Germyl-D<sub>3</sub> in Dimethoxyethane. The dotted line indicates solvent absorption where different.

TABLE 14

Potassium Germyl in Liquid Ammonia				
	$\text{GeH}_3^-$		$\text{GeD}_3^-$	
$\nu_1$	$1739 \pm 6$	IR + R	$1256 \pm 6$	IR + R
$\nu_2$	$814.5 \pm 1.5$	IR + R	$588 \pm 3$	IR + R
$\nu_3$	-		-	
$\nu_4$	$883 \pm 5$	IR	$625 \pm 5$	IR
Potassium Germyl in Dimethoxyethane				
	$\text{GeH}_3^-$		$\text{GeD}_3^-$	
$\nu_1$	$1744 \pm 8$	IR + R	$1272 \pm 8$	R
$\nu_2$	$839 \pm 9$	R	$596 \pm 4$	IR + R
$\nu_3$	-		-	
$\nu_4$	-		$635 \pm 5$	IR

Frequencies in  $\text{cm}^{-1}$ ; all Raman bands observed were >95% polarized.

#### Calculated Frequencies and Parameters

	$\text{KGeH}_3/\text{NH}_3$		$\text{KGeD}_3/\text{ND}_3$		$\text{KGeD}_3/\text{DME}$	
	Calc.	error	Calc.	error	Calc.	error
$\nu_1$	1739	0	1256	0	1272	0
$\nu_2$	816	+1	589	+1	596	+1
$\nu_3$	1743	-	1260	-	1277	-
$\nu_4$	882	-1	624	-1	634	-1
$k_1$	1.76		1.82		1.86	
$k_d/\ell^2$	0.22		0.22		0.22	
$\beta$	$59.0^\circ$		$58.5^\circ$		$58.7^\circ$	
$\alpha$	$95.8^\circ$		$95.2^\circ$		$95.4^\circ$	

Force constants in millidynes/ $\text{\AA}$ .

vibrational spectra was the investigation of possible strong solvent-solute interactions. It can be seen from Table 14 that the observed frequencies hardly change with solvent, being slightly lower in ammonia solution in each case. Such small shifts are common when changing solvents and it has been suggested that it is due to simple electrostatic interactions of an oscillating dipole with its dielectric surroundings (85). The frequencies are, indeed, lower in the solvent of greater dielectric constant (ammonia  $\sim 16$ , dimethoxyethane  $\sim 5$ ).

#### Polymeric Germanium Hydride

Impurity peaks were sometimes observed in the vibrational spectra of the germyl ion, Figure 18. Usually these peaks were quite weak but their intensity depended upon the exact conditions of the preparation. It was discovered that they were more prominent if the solutions were prepared in dimethoxyethane rather than ammonia, if the counter-ion was sodium rather than potassium, or if the reactions were carried out at room temperature. If the solutions were coloured yellow-brown rather than light yellow or colourless then the amount of impurity was likely to be appreciable. The absorptions were assumed to be due to one of the ill-defined lower polymeric hydrides of germanium (4). A yellow to orange solid formulated as  $\text{GeH}_x$  where  $0.9 < x < 1.2$  was isolated by Drake (93) as a by-product of the borohydride reduction of  $\text{GeO}_2$  and infrared bands were observed at 2060, 832 and  $775 \text{ cm}^{-1}$ , measured as a KBr pellet. Royen and Rocktaeschel (94) isolated a similarly formulated compound from the hydrolysis of  $\text{CaGe}$  and reported infrared bands at 2000, 822, 770 and  $550\text{--}600 \text{ cm}^{-1}$ . These latter workers also claimed there was no evidence for a compound with the formulation  $\text{GeH}_2$ . Kraus and Glarum (4) claimed to have isolated  $\text{GeH}_2$  but it was unstable above  $-33^\circ\text{C}$  when it disproportionated into germane and  $(\text{GeH})$  polymer,

the composition of the polymer being deduced from the stoichiometry of the reaction. Peaks observed in this work at 1945 and 837  $\text{cm}^{-1}$  have been attributed to polymeric germanium hydrides. No further characterization of the material was attempted.

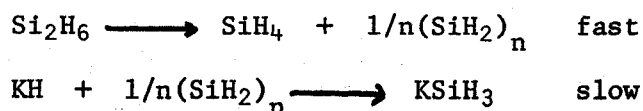
The silyl ion ( $\text{SiH}_3^-$ ) and polymeric silicon hydride ( $\text{SiH}_2$ )<sub>n</sub>

Following the successful analysis of the vibrational spectra of the germyl ion, attempts were made to record the spectra of the silyl ion ( $\text{SiH}_3^-$ ). An NMR signal had already been observed which was attributed to the silyl ion (page 61). These solutions were made by shaking silane, dimethoxyethane and Na/K alloy in a sealed tube for 3 weeks (70, 95). The resulting solutions, after filtering, were green at low temperature, greenish-yellow at room temperature and fluoresced in the laser beam thus preventing the observation of Raman spectra. This behaviour is thought to be due to the presence of a colloidal suspension of elemental silicon; the reaction mixtures, before filtering, were brown-black, indicating that extensive decomposition had occurred. The filtered solutions also decomposed at room temperature in the 5145 Å laser beam to give a white solid, soluble in the solution on shaking. Because of the long reaction times and the unsuitable solutions prepared by the above method, a different method was used to prepare solutions for infrared spectroscopy. Cleavage of disilane ( $\text{Si}_2\text{H}_6$ ) using hydride ion (70) proceeds rapidly and gives light yellow to colourless solutions.

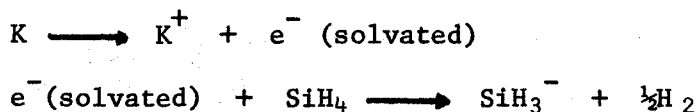


This reaction was used as an in situ preparation of the silyl ion in the side-arm of the high pressure infrared cell, the silane produced being

pumped off while the solution was held at  $-78^{\circ}\text{C}$ . The spectrum obtained is shown in Figure 20 . Traces of silane were still present in this spectrum, being identified by the two weak peaks at  $2190$  and  $900\text{ cm}^{-1}$  (85). There are in addition two prominent peaks at  $2060$  and  $873\text{ cm}^{-1}$ . The deuteride spectrum, which was obtained in a similar manner from  $\text{Si}_2\text{D}_6$  and  $\text{NaD}$ , shows in addition to solvent bands only two strong peaks at  $1495$  and  $648\text{ cm}^{-1}$ . It is known that the reaction of hydride ion with disilane is complex, proceeding in at least two steps (96,97).



Thus it is possible that the observed spectra of solutions prepared by this cleavage reaction are due to the polymeric hydride rather than the silyl ion. To check on this possibility the silyl ion was prepared by a third method, namely the reaction of monosilane with the solvated electron in HMPA solution (7). The silyl ion is produced as a deep yellow solution in approximately 90% yield.



Samples were taken from the preparations and the NMR spectra recorded to confirm the presence of the silyl ion (see page 61). Only three bands could be observed in the infrared spectrum because of the intense HMPA absorptions. These bands occurred at  $2040$  (weak),  $1850$  (strong) and  $894$  (weak)  $\text{cm}^{-1}$ . The observation supports the proposal that the bands observed in the dimethoxyethane solutions prepared by the cleavage of

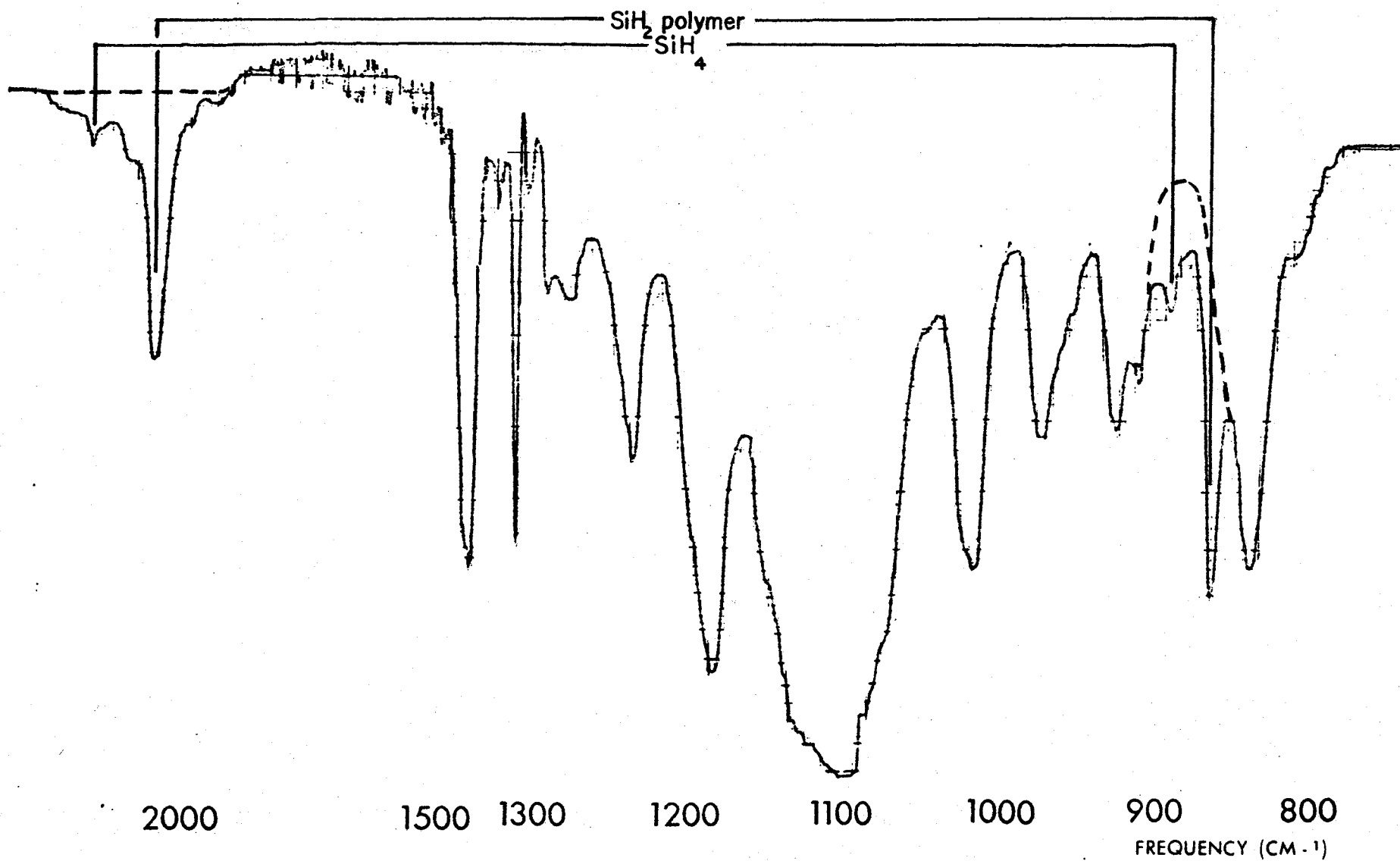


Figure 20. The Infrared Spectrum of SiH<sub>2</sub> Polymer in Dimethoxyethane. The dotted line shows the pure solvent spectrum.

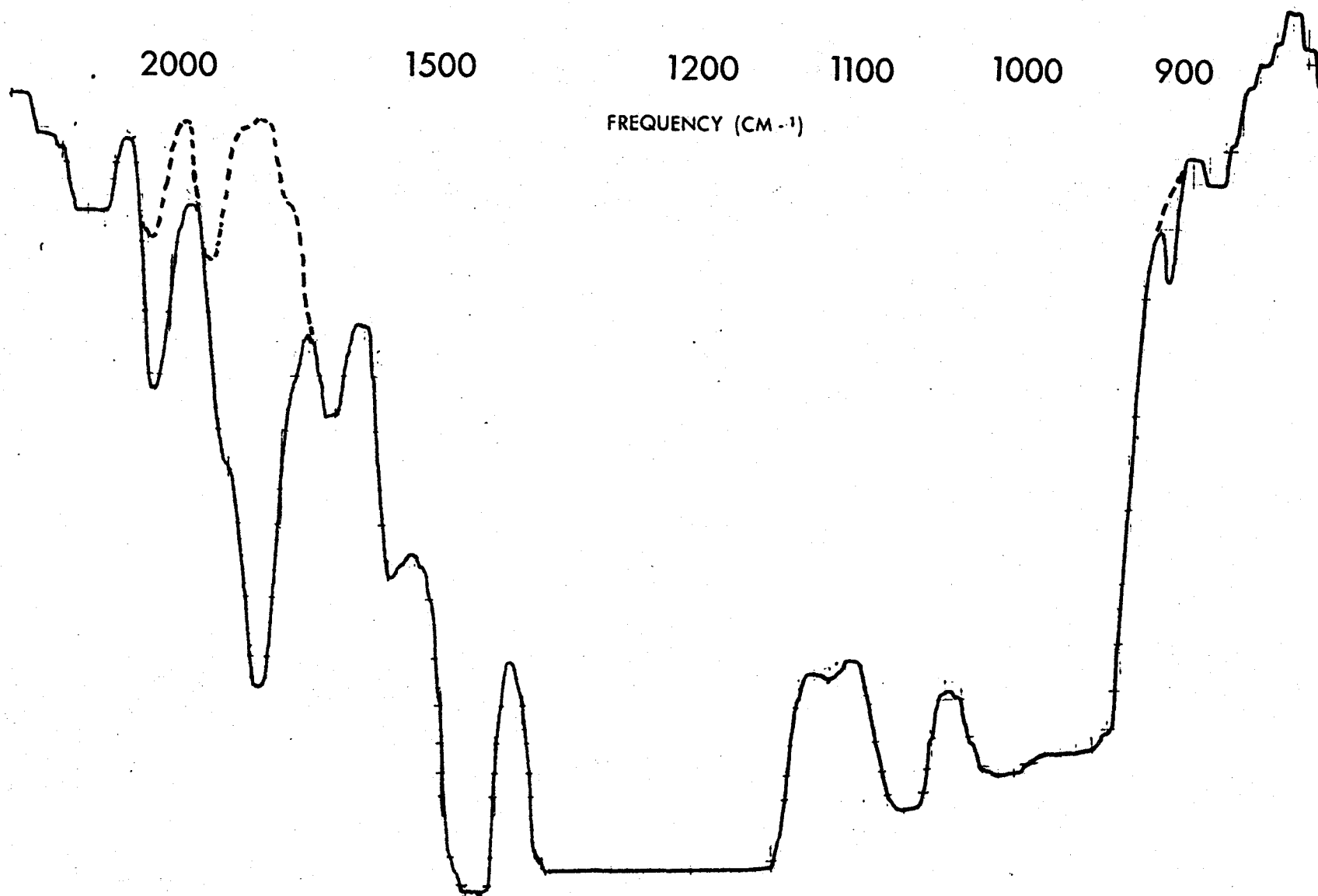


Figure 21. The Infrared Spectrum of  $\text{SiH}_3^-$  and  $\text{SiH}_2$  Polymer in HMPA. The dotted line shows pure solvent spectrum.

disilane were due to the polymeric hydride. The frequencies measured compare with the values 2090, 870 and 635  $\text{cm}^{-1}$  quoted for  $\text{SiH}_x$  where  $0.7 < x < 0.9$  (94).

The strong band at 1850  $\text{cm}^{-1}$  observed in the HMPA solution is tentatively assigned to the silyl ion. Unfortunately no other bands could be observed because of the solvent and it is not possible to isolate the salt from HMPA because the solvent is involatile at room temperature.

#### The vibrational spectra of liquid ammonia

The Raman spectrum of potassium germyl in liquid ammonia (Figure 17) shows two broad peaks of low intensity near 1640 and 1060  $\text{cm}^{-1}$  and no other peaks assignable to the solvent between 2000 and 200  $\text{cm}^{-1}$ . In order to confirm that these were, indeed, the solvent absorptions, the evidence for the vibrational spectrum of liquid ammonia was re-examined and some considerable confusion uncovered. The most careful study of the Raman spectrum of liquid ammonia was performed by Plint and coworkers (98) who observed three bands (Table 15) which varied in intensity with temperature. Only two fundamental vibrations,  $\nu_1$  and  $\nu_3$ , are expected in the NH stretching region at about 3,300  $\text{cm}^{-1}$  and so the band at lowest frequency was assigned to the first overtone of the  $\nu_4$  fundamental. Previous workers had suggested that the  $\nu_1$  fundamental was split as a result of dimerization of the molecules (98). The high intensity of the overtone was assumed to be due to Fermi resonance of the symmetric sublevel of the overtone with the symmetric  $\nu_1$  fundamental; both Raman bands are fully polarized, a result confirmed in this study. Plint and coworkers had not been able to observe either the  $\nu_2$  or the  $\nu_4$  fundamentals when making their assignment which had

TABLE 15

Vibrational Spectra of Ammonia and Ammonia-D<sub>3</sub>

				<u>Ammonia</u>				
Phase	Temperature	Method	Reference	Observed Frequencies (cm <sup>-1</sup> )				
gas	Room temp.	IR	(85)	3444(a)	3336	3219	1628	950(d)
liquid	-34° → -70°C	R	(98)	3373	3330	3218		
liquid	-50°C	IR	(101)	3375	3285	3220	1632	1050(d)
	+25°C	IR		3380	3250		1635	1055
liquid	+25°C	R		3379	3301(p)	3215(p)	1638	1066(p)
	-55°C	R		3363	3296(p)	3206(p)	1641	1070(p)
solid	-190°C	IR	(102)	3378	3297	3223	1646	1060
				<u>Ammonia-D<sub>3</sub></u>				
gas	Room temp.	IR	(85)	2555	2419		1191	749(d)
Liquid	+25°C	IR		2520	2370		1195	815
liquid	+25°C	R		2517	2399(p)	2344(p)	1203	816(p)
	-55°C	R		2514	2396(p)	2338(p)	1200	820(p)
solid	-190°C	IR	(102)	2500	2392	2318	1196	815

(a) Alternative assignment by Hertzberg confirmed in ref. (99).

(d) Average of doublet peak.

(p) Polarized band in Raman spectrum.

Measurements in this work estimated to be  $\pm 3$  cm<sup>-1</sup> except the broad  $\nu_2$  peak which is  $\pm 7$  cm<sup>-1</sup>. In addition the IR spectrum of liquid NH<sub>3</sub> showed peaks at 4400 and 5000 cm<sup>-1</sup> (very approximate) and liquid ND<sub>3</sub> at 3345 and 3710 cm<sup>-1</sup> assignable to  $\nu_3 + \nu_2$  and  $\nu_3 + \nu_4$  respectively.

presumably been based on intensity arguments. At room temperature the central peak was most intense and assigned to the fundamental. This assignment was also made by Kinumaki and Aida (100) and by Demidenkova and Shcherba (101). These latter studies claimed to have observed the  $\nu_2$  and  $\nu_4$  fundamentals in addition to the three peaks discussed above. The alternative assignment whereby the central peak of the three at  $\sim 3300 \text{ cm}^{-1}$  is assigned to the  $2\nu_4$  overtone and the low frequency peak to  $\nu_1$  has been given by Reding and Hornig (102) who examined the infrared spectrum of crystalline ammonia and ammonia- $\text{D}_3$ . If Fermi resonance is causing the intensity of the overtone then this second assignment must be correct for the liquid spectra as well, for the following reason. Fermi resonance causes the two interacting levels to move apart in energy (85), the lower level decreasing in energy by the same amount as the upper level increases in energy. If the frequency of the  $\nu_4$  fundamental is known, then the magnitude of the perturbation of  $2\nu_4$  and hence  $\nu_1$  can easily be calculated. This was done using the value for the  $\nu_4$  fundamental measured by Demidenkova et al. and it showed that the more intense central peak must be the overtone and the lower frequency peak the fundamental since the levels would have to cross for the alternative assignment and this is not possible.

There is also disagreement as to the form of the band due to the  $\nu_2$  vibration (101,103). In the gas phase spectra, both infrared and Raman, the band is split into doublets because of the inversion of the molecule (85). The separation of the infrared bands is  $36.5 \text{ cm}^{-1}$  and corresponds to the sum of the splittings of the upper and lower levels. The separation in the Raman bands is  $30.3 \text{ cm}^{-1}$  and corresponds to the difference in splitting of the upper and lower levels. This is due to the different selection rules,

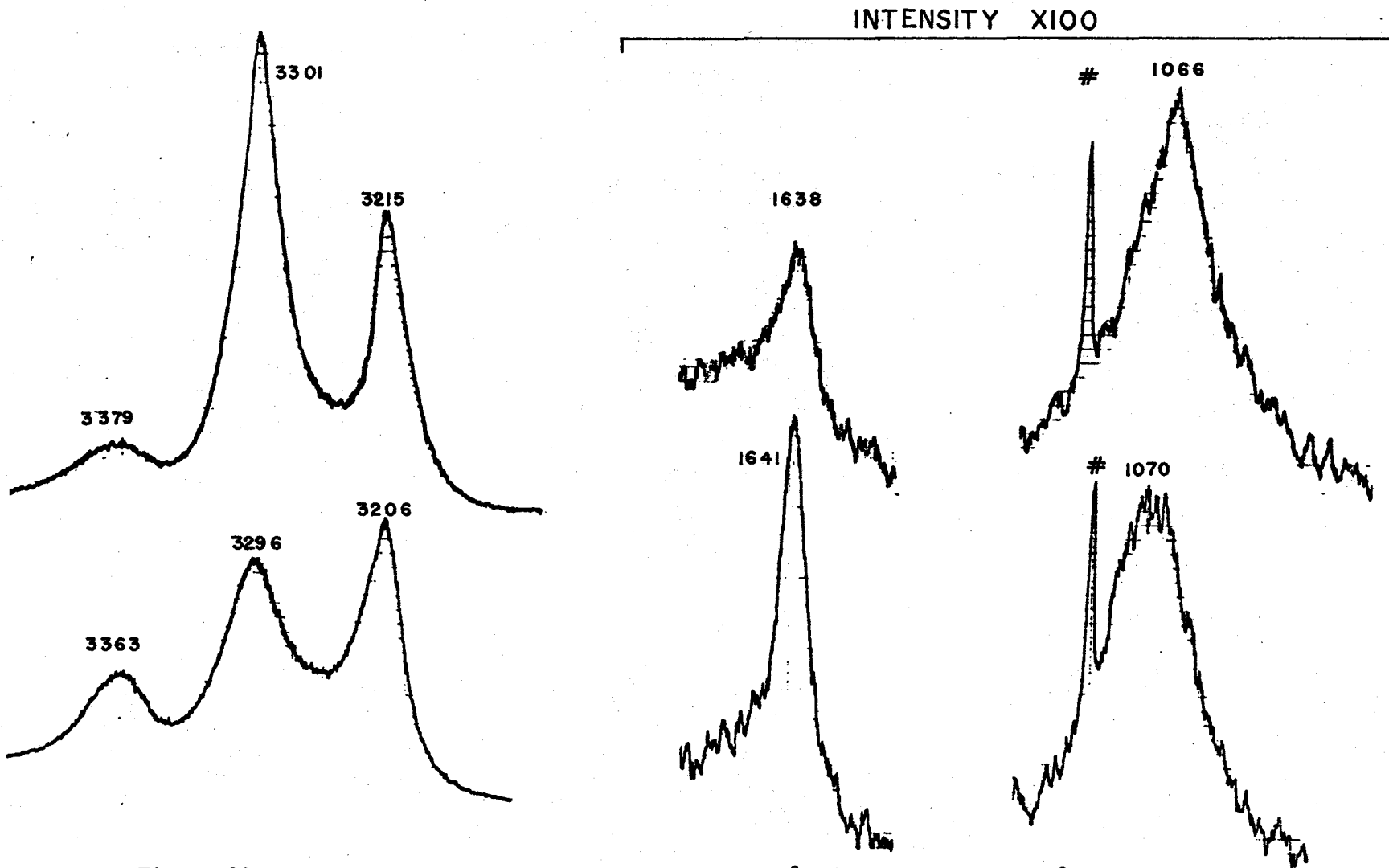


Figure 22. Raman Spectrum of Liquid Ammonia at +25°C (upper trace); -55°C (lower trace).  
The starred peak is a plasma line from the laser radiation.

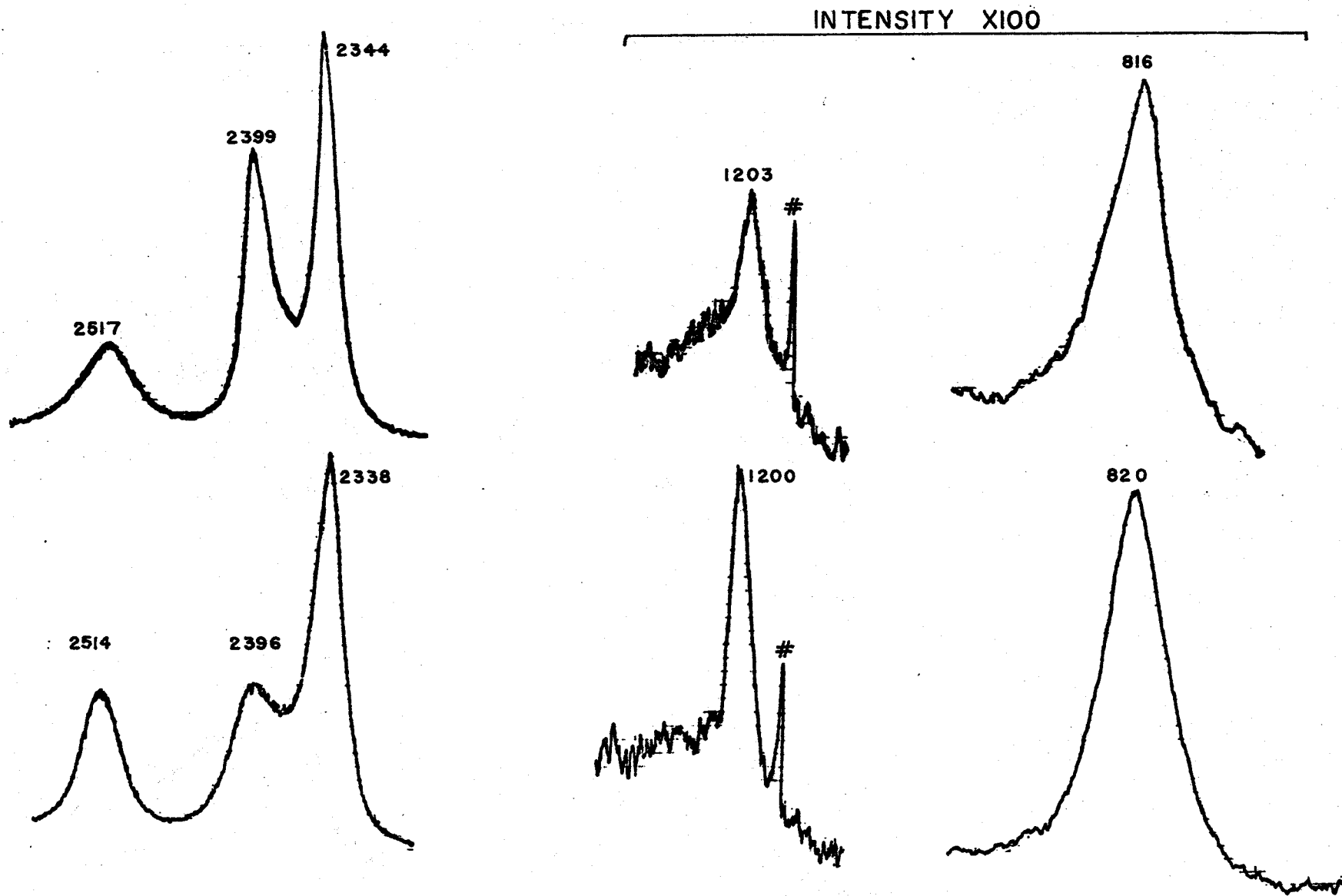


Figure 23. Raman Spectrum of Liquid Ammonia-D<sub>3</sub> at +25°C (upper trace); -55°C (lower trace). The starred peak is a plasma line from the laser radiation.

infrared being  $+\leftrightarrow-$  and Raman being  $+\leftrightarrow+$  or  $-\leftrightarrow-$ . In the liquid phase Kinumaki and Aida (100) claim to observe a doublet for this band although their Raman spectrum is of poor quality. In the infrared spectra Demidenkova et al. (101) observe a double peak but Corset et al. (103) show only a single absorption.

In view of this confusion it was decided to investigate further the Raman spectrum of liquid ammonia and ammonia-D<sub>3</sub>; the latter compound not having been studied in the liquid phase previously. The spectra obtained are shown in Figures 22 and 23 and the frequencies are tabulated in Table 15.

The assignment of the deuteride spectrum would seem to be straightforward, the central band of the high frequency triplet is weaker than in the hydride spectra and occurs at twice the  $\nu_4$  frequency within experimental error and is clearly the  $2\nu_4$  overtone.

The hydride spectral frequencies agree reasonably well with the previous work and confirm that the more intense central peak at room temperature is due to the overtone. The magnitude of the Fermi resonance shift is estimated to be  $25 \text{ cm}^{-1}$  which gives an unperturbed value of  $3240 \text{ cm}^{-1}$  for the  $\nu_1$  vibration. If this value is used together with the other fundamental frequencies to estimate the force constants and angle  $\beta$  for the molecule by a least squares technique, then the frequencies for ammonia-D<sub>3</sub> calculated from these parameters agree very well (Table 16) with the experimentally observed values.

As seen from Figures 22 and 23 the intensity of the spectral bands exhibit a marked temperature dependence. The degenerate  $\nu_3$  and  $\nu_4$  vibrations sharpen considerably on cooling as a result of increased restriction of

TABLE 16

Calculated frequencies for liquid ammonia and ammonia-D<sub>3</sub> at room temperature

	<u>Ammonia</u>		<u>Ammonia-D<sub>3</sub></u>	
	Exp. frequencies (cm <sup>-1</sup> )	Calc. frequencies (cm <sup>-1</sup> )	Exp. frequencies (cm <sup>-1</sup> )	Frequencies calc. from NH <sub>3</sub> parameters (cm <sup>-1</sup> )
v <sub>1</sub>	3240 (a)	3251	2344	2325
v <sub>2</sub>	1066	1061	816	805
v <sub>3</sub>	3379	3368	2517	2490
v <sub>4</sub>	1638	1641	1203	1190

---

(a) Corrected for Fermi resonance.

Values calculated from parameters:  $\beta = 71.2^\circ$ ,  $k_1 = 6.088 \text{ m.dynes/\AA}^\circ$ ,  $k_d/l^2 = 0.588 \text{ m.dynes/\AA}^\circ$ .

rotation (98), but the temperature dependence of  $2\nu_4$  and  $\nu_1$  had not been explained previously. The spectra shown here exhibit a small frequency shift with temperature. This would cause the unperturbed  $2\nu_4$  and  $\nu_1$  levels to move apart thereby reducing the Fermi interaction and causing changes in intensity.

The  $\nu_2$  band in all this work, both in the Raman, Figures 22 and 23, and infrared, has been observed as a single broad peak with no sign of any splitting.

A comparison of the force constants of the hydrides and hydride ions of groups IV and V

Having calculated the simple valence force field constants of the geryml ion, Table 14, it was of interest to compare them with the similarly derived force constants of the isoelectronic species germane ( $\text{GeH}_4$ ) and arsine ( $\text{AsH}_3$ ), Table 17. When compared to arsine the GeH bonds in  $\text{GeH}_3^-$  are definitely weaker with both the stretching and bending force constants being significantly smaller in the charged species. When compared to germane, however, the situation is less clear; the stretching force constant of the geryml ion is much smaller but the bending force constant is nearly twice as big. In order to study the problem further the force constants of all the related groups IV and V hydrides and hydride ions were collected and are tabulated in Table 17. As the valence force field used to calculate these force constants gives a good representation of the vibrations for both  $\text{MH}_3$  and  $\text{MH}_4$  molecules (85) it seemed reasonable to suppose that a comparison could be made of the force constants of the two different geometries. The spectra from which these force constants were calculated were recorded in different phases. This leads to a small variation in spectra and hence in

TABLE 17

Force Constants for Hydrides and Hydride Ions of Groups IV and V

Compound	Phase	MH <sub>4</sub>		Compound	Phase	MH <sub>3</sub>	
		Force Constants (a)	Force Constants (a)			Force Constants (a)	Force Constants (a)
		stretching	bending			stretching	bending
CH <sub>4</sub> (85)	gas	5.04	0.46	NH <sub>3</sub> (85)	gas	6.37	0.51
NH <sub>4</sub> <sup>+</sup> (85)	solid	5.46	0.56	NH <sub>3</sub> (b)	liquid	6.09	0.59
SiH <sub>4</sub> (85)	gas	2.84	0.19				
PH <sub>4</sub> <sup>+</sup> (90)	solid	3.19	0.24	PH <sub>3</sub> (85)	gas	3.09	0.33
GeH <sub>4</sub> (90)	gas	2.63	0.13	GeH <sub>3</sub> <sup>-</sup> (b)	solution	1.79	0.22
				AsH <sub>3</sub> (90)	gas	2.62	0.28

(a) Force constants in millidynes/Å calculated from equations on page 70 using a least squares technique for pyramidal molecules. Tetrahedral molecules calculated as in Ref. (85).

(b) Values measured in this work.

the force constants for a given compound because of intermolecular interactions. For example, ammonia is strongly associated in the liquid phase because of hydrogen bonding (26) and this is reflected in the decreased stretching force constant and increased bending force constant of the molecule in the liquid as compared to gas phase. However the variation in force constants between species is considerably greater than the variation from intermolecular interactions and hence a comparison of the data from different phases seems justified.

Several trends are immediately apparent. The force constants diminish as the periodic table is descended,  $\text{CH}_4 > \text{SiH}_4 > \text{GeH}_4$  and  $\text{NH}_3 > \text{PH}_3 > \text{AsH}_3$ ; the decrease in the force constants being related, though not proportional, to the strength of the M-H bond. C-H = 99, SiH = 76 and GeH = 69 kcal/mole (15) and NH = 93, PH = 77 and AsH = 59 kcal/mole (26). There is also a significant difference in the force constants of the ions and the corresponding neutral molecules,  $\text{NH}_4^+ > \text{CH}_4$  and  $\text{PH}_4^+ > \text{SiH}_4$  but  $\text{AsH}_3 > \text{GeH}_3^-$ .

However the most interesting comparison is between the pyramidal and tetrahedral species. With the exception of ammonia and ammonium ion, the pyramidal species have much larger bending force constants than the tetrahedral species while the stretching force constants are marginally smaller. It is suggested that this is due to the increased 'p' character of the bonds in the pyramidal species. A pure 's' bond, being non-directional, would have zero bending force constant but as the 'p' character of the bond increases it becomes more directional and the bending force constant increases. For the two molecules with nitrogen as the central atom, i.e.,  $\text{NH}_4^+$  and  $\text{NH}_3$ , the bond angle is almost the same, H-N-H,  $\text{NH}_4^+ = 109.5$ ;  $\text{NH}_3 = 107.3$  (36), thus the hybridization does not change and the force constants are nearly equal.

## CHAPTER 6

### General Conclusions

The acidity of some aryl germanes has been measured in liquid ammonia relative to each other and to some hydrocarbon indicators. The results confirm a previous observation that germane is much more acidic than triphenyl germane (11), but indicate that the magnitude of the difference is much greater than was previously estimated. Each aryl group reduces the acidity of the germane by approximately 2 orders of magnitude while one alkyl group reduces the acidity by 6 orders of magnitude.

Complete analysis of the NMR spectra of phenyl silane and phenyl germane were carried out. It was shown that the chemical shifts of the compounds could be largely explained by the presence of an electric dipole moment in the molecule. The magnitude of (p-d) $\pi$  bonding was too small to be detected by the NMR method and thus multiple bonding in the acids could not explain the decreased acidity of the aryl germanes over germane. The NMR spectrum of the phenyl germyl anion was unambiguously assigned and partially analysed to show that there is negligible delocalization of the negative charge from the Ge onto the aromatic ring. Therefore aromatic substitution would not be expected to increase the acidity of the germanes as much as for the corresponding carbon compounds where extensive delocalization of charge does occur. Moreover the solvation energy of the anion will be considerably decreased by substitution of bulky aromatic groups for hydrogen and the acidity thereby reduced.

The vibrational spectra of the germyl anion was examined for possible

evidence of strong solute-solvent interaction but none was detected. However a normal coordinate analysis of the data was carried out and the H-Ge-H bond angle estimated. This is the first estimate of the geometry of the germyl ion which has been reported.

As a result of the investigation of the Raman spectrum of the germyl ion in liquid ammonia, the spectrum of the solvent has been re-investigated and the assignment of two bands changed. The Raman spectrum of liquid ammonia-D<sub>3</sub> has been reported for the first time.

## APPENDIX I

### Calculation of Symmetry-allowed NMR Transitions of a Phenyl Group

Under the operations of the  $C_{2v}$  group two pairs of nuclei of a phenyl group interchange. The nuclear wavefunctions for the three types of nuclei present may be classed as symmetric (s) or antisymmetric (a) under these operations. In the absence of spin-spin coupling these wavefunctions are:

	<u>para</u>	<u>meta</u>	<u>ortho</u>
$F_Z(1)$		$F_Z(2)$	$F_Z(3)$
$+ \frac{1}{2}$	$\alpha$ (s)	$+ 1$	$\alpha \alpha$ (s)
$- \frac{1}{2}$	$\beta$ (s)	$0$	$2^{-\frac{1}{2}}(\alpha\beta + \beta\alpha)$ (s)
		$- 1$	$\beta \beta$ (s)
		$0$	$2^{-\frac{1}{2}}(\alpha\beta - \beta\alpha)$ (a)

A complete nuclear wavefunction can be found by multiplying any 3 group wavefunctions. The total  $F_Z$  value is given by adding the corresponding group  $F_Z$  values and the symmetry of the total wavefunction is given by the rules:

$$(s) \times (s) = (s) \quad (a) \times (s) = (a) \quad (a) \times (a) = (s)$$

E.g., a symmetric wavefunction with  $F_Z = \frac{1}{2}$  is:

$$\text{Wavefunction} = \alpha \times \beta\beta \times \alpha\alpha = \alpha\beta\beta\alpha\alpha$$

$$F_Z = (+\frac{1}{2}) + (-1) + (+1) = +\frac{1}{2}$$

$$\text{symmetry} = (s) \times (s) \times (s) = (s)$$

The complete set of wavefunctions can be classified by symmetry and by  $F_Z$  value:

$F_Z$	Symmetric (s) No. of Wavefunctions	Antisymmetric (a) No. of Wavefunctions	No. of Wavefunctions with given $F_Z$
+5/2	1		1
+3/2	3	2	5
+1/2	6	4	10
-1/2	6	4	10
-3/2	3	2	5
-5/2	1		1
Total	20	12	32

A useful check is given by the last column. The total number of wavefunctions for  $n$  spins =  $2^n$  and when divided into groups by  $F_Z$  value give the binomial coefficients of order  $n$ .

The form of the energy level diagram can now be shown:

$F_Z$	Symmetric	Antisymmetric
-5/2	—	
-3/2	— — —	— —
-1/2	— — — — —	— — — —
+1/2	— — — — —	— — — —
+3/2	— — —	— —
+5/2	—	

Using the following two selection rules the maximum possible number of transitions can be calculated.

(1) Only transitions between states of the same symmetry are allowed.

(2)  $\Delta F_Z = \pm 1$ .

$$\begin{array}{rcl}
 \text{Symmetric transitions} & = & (1 \times 3) + (3 \times 6) + (6 \times 6) + (6 \times 3) + (3 \times 1) = 78 \\
 \text{Antisymmetric transitions} & = & (2 \times 4) + (4 \times 4) + (4 \times 2) = 32 \\
 \text{Total transitions} & = & \underline{110}
 \end{array}$$

Included in this total are a number of combination transitions where

$F_Z = +1$  but which correspond to interchange of three spins; these are forbidden, but under the influence of spin-spin coupling states mix and such transitions become weakly allowed.

## APPENDIX 2

### Calculation of Bond Angles from Coupling Constants of Directly Bonded Nuclei

The fraction  $s$  character of the hybrid orbital forming the bond can be calculated from the coupling constant (81), if the Fermi contact mechanism is presumed to predominate for the system considered and the coupling constant of the tetrahedral species is known. The hybrid orbital is considered to be only  $s + p$  hybridized with no  $d$  orbital participation and the bond angle is calculated as follows (104).

$$\text{fraction } s \text{ character of hybrid orbital} = a^2 = \frac{J(M-H)}{4J(MH_4)}$$

The orbitals of atom  $M$  are represented  $\psi_i = \left[ \frac{1}{(1 + \lambda_i^2)^{1/2}} \right] (s + \lambda_i p_i)$  where  $p_i$  is a linear combination of  $p$  orbitals chosen to lie along the axis of the  $i^{\text{th}}$  bond and

$$(a^2)_i = 1/(1 + \lambda_i^2).$$

It can be shown that for  $\psi_i$  and  $\psi_j$  to be orthogonal

$$\lambda_i \lambda_j = -1/\cos\theta_{ij}$$

where  $\theta_{ij}$  is the angle between bonds  $i$  and  $j$ . If all bonds are equivalent this simplifies to

$$\lambda^2 = -1/\cos\theta.$$

Thus the bond angle can be found.

## REFERENCES

1. O. H. Johnson, Chem. Revs. (1951) 48 259.
2. F. Rijkens, 'Organogermanium Compounds', Schotanus and Jens, Utrecht (1960).
3. F. Rijkens and G. J. M. Van der Kerk, 'Organogermanium Chemistry', Schotanus and Jens, Utrecht (1964).
4. F. Glocking, 'The Chemistry of Germanium', Academic Press, London (1969).
5. F. G. A. Stone, 'Hydrogen Compounds of Group IV Elements', Prentice-Hall Inc., Englewood Cliffs, N.J. (1962).
6. P. M. Kuznesof and W. L. Jolly, Inorg. Chem. (1968) 7 2574.
7. S. Craddock, G. A. Gibbon and C. M. van Dyke, Inorg. Chem. (1967) 6 1751.
8. H. J. Emeleus and K. M. MacKay, J. Chem. Soc. (1961) 2676.
9. D. Rustad and W. L. Jolly, Inorg. Chem. (1967) 6 1986.
10. E. Amberger and H. Boeters, Angew. Chem. Int. Ed. (1963) 2 686.
11. T. Birchall and W. L. Jolly, Inorg. Chem. (1966) 5 2177.
12. J. Chatt and A. A. Williams, J. Chem. Soc. (1954) 4403.
13. A. G. Brook, J. Amer. Chem. Soc. (1957) 79 4373.
14. F. Agolini, S. Kemenko, I. G. Csizmadia and K. Yates, Spectrochim. Acta (1968) 24A 169.
15. E. A. V. Ebsworth, 'Volatile Silicon Compounds', Pergamon Press, N.Y. (1963).
16. A. M. Coleman and H. Freiser, J. Amer. Chem. Soc. (1961) 83 4127.
17. V. Vaisarová, J. Hetflejš and V. Chvalousky, J. Organomet. Chem. (1970) 22 395.
18. H. Bock, H. Alt and H. Seidl, J. Amer. Chem. Soc. (1969) 91 355.
19. L. Goodman, A. H. Konstam and L. H. Sommer, J. Amer. Chem. Soc. (1965) 87 1012.
20. J. A. Bedford, J. R. Bolton, A. Carrington and R. H. Prince, Trans. Faraday Soc. (1963) 59 53.

21. A. L. Alred and L. W. Bush, J. Amer. Chem. Soc. (1968) 90 3352.
22. R. W. Taft and J. W. Rakshys, J. Amer. Chem. Soc. (1965) 87 4387.
23. J. M. Wilson, A. G. Briggs, J. E. Sawbridge, P. Tickle and J. J. Zuckerman, J. Chem. Soc. A (1970) 1024.
24. A. Streitwieser and J. H. Hammons, 'Progress in Physical Organic Chemistry', (1965) 3 41, J. Wiley and Sons, N.Y.
25. A. Carrington and A. D. McLauchlan, 'Introduction to Magnetic Resonance', Harper International, N.Y. (1967).
26. F. A. Cotton and G. Wilkinson, 'Advanced Inorganic Chemistry', Second Edition, Interscience, N.Y. 1966.
27. J. A. Pople and D. P. Santry, Mol. Phys. (1964) 8 1.
28. J. A. Pople, J. W. McIver and N. S. Ostlund, J. Chem. Phys. (1968) 49 2960.
29. K. Hayamizu and O. Yamamoto, J. Mol. Spec. (1968) 25 422.
30. M. D. Curtis, J. Amer. Chem. Soc. (1969) 91 6011.
31. C. H. Rochester, Quart. Rev. (1966) 20 511.
32. R. Stewart and J. P. O'Donnell, Can. J. Chem. (1964) 42 1681.
33. E. C. Steiner and J. D. Starkey, J. Amer. Chem. Soc. (1967) 89 2751.
34. T. Birchall and W. L. Jolly, J. Amer. Chem. Soc. (1966) 88 5439.
35. 'The Chemistry of Non-Aqueous Solvents', Edited by J. J. Lagowski, Academic Press, N.Y. (1967).
36. 'The Handbook of Chemistry and Physics', The Chemical Rubber Co., 49th Ed. (1968).
37. J. E. Hofman, A. Schriesheim and D. D. Rosenfeld, J. Amer. Chem. Soc. (1965) 87 2523.
38. M. R. Booth and R. J. Gillespie, Endeavour (1970) 29 89.
39. D. R. Eaton and W. R. McClellan, Inorganic Chem. (1967) 6 2134.
40. J. N. Murrell, S. F. A. Kettle and J. M. Tedder, 'Valence Theory', J. Wiley and Sons, N.Y. (1965).
41. G. Fraenkel, R. E. Carter, A. McLachlan and J. H. Richards, J. Amer. Chem. Soc. (1960) 82 5846.

42. J. Corset, P. V. Huong and J. Lascombe, *Spectrochim. Acta* (1968) 24A 1385.
43. I. V. Demidenkova and L. D. Shcherba, *Izvest. Akad. Nauk. SSSR, Ser. Fiz.* (1959) 22 1122.
44. G. E. Coates, M. L. H. Green and K. Wade, 'Organometallic Compounds', Third Ed., Methuen, London (1967).
45. O. H. Johnson, *Inorg. Synth.* (1961) 5 74.
46. F. Glockling and K. Hooton, *J. Chem. Soc.* (1962) 3509.
47. K. Kuehlen and W. P. Neumann, *Annalen* (1967) 702 17.
48. W. L. Jolly and J. E. Drake, *Inorg. Synth.* (1963) 7 34.
49. A. D. Norman, J. R. Webster and W. L. Jolly, *Inorg. Synth.* (1968) 11 176.
50. L. G. L. Ward, *Inorg. Synth.* (1968) 11 161.
51. A. E. Finholt, A. C. Bond, K. E. Wilzbach and H. I. Schlesinger, *J. Amer. Chem. Soc.* (1947) 69 2692.
52. S. D. Gokhale and W. L. Jolly, *Inorganic Synth.* (1967) 9 56.
53. C. F. Koelsch and P. R. Johnson, *J. Org. Chem.* (1941) 6 534.
54. N. Campbell and K. W. Delahunt, *J. Chem. Soc. C* (1966) 1810.
55. A. D. Buckingham, T. Schaefer and W. G. Schneider, *J. Chem. Phys.* (1960) 32 1227.
56. S. M. Castellano and A. A. Bothner-By, *J. Chem. Phys.* (1964) 41 3863.
57. M. P. Williamson, R. J. Kostelnik and S. M. Castellano, *J. Chem. Phys.* (1968) 49 2218.
58. K. Noack, *Spectrochim. Acta* (1968) 24A 1917.
59. J. W. Smith, *Trans. Faraday Soc.* (1950) 46 394.
60. A. L. McClellan, 'Table of Experimental Dipole Moments', W. H. Freeman and Co., San Francisco (1963).
61. J. A. Pople, W. G. Schneider and H. J. Bernstein, 'High Resolution Nuclear Magnetic Resonance', McGraw-Hill, N.Y. (1959).
62. T. Birchall and W. L. Jolly, *J. Amer. Chem. Soc.* (1965) 87 3007.
63. A. Streitwieser, J. H. Hammons, E. Ciuffarin and J. I. Brauman, *J. Amer. Chem. Soc.* (1967) 89 59.

64. C. D. Ritchie and R. E. Uschold, J. Amer. Chem. Soc. (1968) 90 2821.
65. C. D. Ritchie and R. E. Uschold, J. Amer. Chem. Soc. (1967) 89 2752.
66. R. E. Cutherell, E. C. Fohn and J. J. Lagowski, Inorg. Chem. (1966) 5 111.
67. A. Streitwieser, E. Ciuffarin and J. H. Hammons, J. Amer. Chem. Soc. (1967) 89 63.
68. A. D. Buckingham, Can. J. Chem. (1960) 38 300.
69. J. W. Burley, R. Ife and R. N. Young, Chem. Comm. (1970) 19 1256.
70. M. A. Ring and D. M. Ritter, J. Amer. Chem. Soc. (1961) 83 802.
71. J. J. Daly, J. Chem. Soc. (1964) 3779.
72. F. W. G. Fearson and H. Gilman, J. Organomet. Chem. (1967) 9 403.
73. T. Schaefer and W. G. Schneider, Can. J. Chem. (1963) 41 966.
74. J. C. Shug and J. C. Deck, J. Chem. Phys. (1962) 37 2618.
75. V. R. Sandel and H. H. Freedman, J. Amer. Chem. Soc. (1963) 85 2328.
76. V. O. Reikhsfeld, I. E. Saratov and L. N. Gubanova, Zhur. Obshchei Khim. (1965) 35 2014.
77. H. Spiescke and W. G. Schneider, J. Chem. Phys. (1961) 35 722.
78. G. M. Whitesides, J. G. Selgestad, S. P. Thomas, D. W. Andrews, B. A. Morrison, E. J. Panek and J. San Filippo, J. Organomet. Chem. (1970) 22 365.
79. F. A. Bovey, F. P. Hood, E. Pier and H. E. Weaver, J. Amer. Chem. Soc. (1965) 87 2060.
80. S. Castellano and C. Sun, J. Amer. Chem. Soc. (1966) 88 4741.
81. J. W. Emsley, J. Feeney and L. H. Sutcliffe, 'High Resolution Nuclear Magnetic Resonance Spectroscopy', Pergamon Press, London (1966).
82. G. M. Sheldrick, Trans. Faraday Soc. (1967) 63 1077.
83. G. M. Sheldrick, Trans. Faraday Soc. (1967) 63 1071.
84. J. Bacon, R. J. Gillespie, J. S. Hartman and U. R. K. Rao, Mol. Phys. (1970) 18 561.
85. G. Herzberg, 'Infrared and Raman Spectra of Polyatomic Molecules', Van Nostrand, N.Y. (1945).

86. J. A. Pople and D. P. Santry, *Mol. Phys.* (1964) 8 1.
87. J. D. Roberts, E. A. McElhill and R. Armstrong, *J. Amer. Chem. Soc.* (1949) 71 2923.
88. K. D. Bartle and D. W. Jones, *J. Mol. Structure* (1967) 1 131.
89. D. D. Elleman and S. L. Manatt, *J. Chem. Phys.* (1962) 36 2346.
90. K. Nakamoto, 'Infrared Spectra of Inorganic and Coordination Compounds', J. Wiley and Sons, N.Y. (1963).
91. G. B. B. H. Sutherland, E. Lee and Cheng-Kai Wu, *Trans. Faraday Soc.* (1939) 35 1373.
92. J. R. Durig, C. W. Sink and J. B. Turner, *J. Chem. Phys.* (1968) 49 3422.
93. J. E. Drake, U. S. Atomic Energy Commission Report, UCRL 9709 (1961).
94. P. Royen and C. Rocktaeschel, *Z. Annorg. Chem.* (1966) 346 279.
95. E. Amberger, R. Romer and A. Layer, *J. Organomet. Chem.* (1968) 12 417.
96. J. A. Morrison and M. A. Ring, *Inorg. Chem.* (1967) 6 100.
97. N. A. D. Carey and E. A. V. Ebsworth, *J. Inorg. Nucl. Chem.* (1969) 31 2953.
98. C. A. Plint, R. M. B. Small and H. L. Welsh, *Can. J. Phys.* (1954) 32 653.
99. C. C. Cummings and H. L. Welsh, *J. Chem. Phys.* (1953) 21 1119.
100. S. Kinumaki and K. Aida, *Sci. Reports Res. Inst. Tohoku Univ.* (1954) A6 186.
101. I. V. Demidenkova and L. D. Shcherba, *Izvest. Akad. Nauk. SSSR, Ser. Fiz.* (1959) 22 1122.
102. F. P. Reding and D. F. Hornig, *J. Chem. Phys.* (1951) 19 594.
103. J. Corset, P. V. Huong and J. Lascombe, *Spectrochim. Acta* (1968) 24A 1385.
104. K. Wiberg, 'Physical Organic Chemistry', John Wiley and Sons, N.Y. (1964).
105. M. J. D. Powell, 'VAO4A' Program 60, Quantum Chemistry Program Exchange, Indiana University (1970).